DOCTOR OF PHILOSOPHY

Characterisation of the (H3-H4)2-tetramer and its interaction with histone chaperones

Bowman, Andrew

Award date:
2010

DOCTOR OF PHILOSOPHY

Characterisation of the (H3-H4)2-tetramer and its interaction with histone chaperones

Andrew Bowman

2010

University of Dundee

Characterisation of the $(H3\text{-}H4)_2$-tetramer and its interaction with histone chaperones

Andrew James Bowman

A thesis submitted for the degree of Doctor of Philosophy

University of Dundee

10th September 2010

Table of Contents

List of figures and tables

Abbreviations

Asf1	Anti silencing function 1
ATP	Adenosine tri-phosphate
BMOE	bis-maleimidoethane
CAF1	Chromatin assembly factor 1
CENPA	Centromere protein A
Cse4	Chromosome segregation protein 4
DEER	Double electron-electron resonance
DTT	Dithiothreitol
EDTA	Ethylenediaminetetraacetic acid
EPR	Electron paramagnetic resonance
FACT	Facilitates transcription
GCN5	General control non-derepressible
HAT	Histone acetyl transferase
HDAC	Histone deacetylase
HIRA	Histone regulator A
HFM	Histone fold motif
HFD	Histone fold dimer
HP1	Heterochromatin protein 1
Ino80	Inositol requiring 80
ISWI/1/2	Imitation switch 1/2
M3M	1,3-Propanediyl bismethanethiosulfonate
MCM	Mini chromosome maintenance
MMTV	Mouse mammary tumor virus
MTSL	*S*-(2,2,5,5-tetramethyl-2,5-dihydro-1H-pyrrol-3-yl)methyl methanesulfonothioate
Nap1	Nucleosome assembly protein 1
NCP	Nucleosome core particle
PCNA	Proliferating cell nuclear antigen
PELDOR	Pulsed electron double resonance

PHO5	Phosphate metabolism 5
Pob3	DNA polymerase 1 binding 3
PTM	Post translational modification
RFC	Replication factor C
RPA	Replication protein A
RSC	Remodel the structure of chromatin
Rtt109	Regulator of Ty transposition 109
SDSL	Site directed spin labelling
SET	Suppressor of varigation
Snf	Sucrose non fermenting
Spt16	Suppressor of Ty 16
Swr1	Swi2/Snf2 related
Swi	Switching deficient
TAF1β	Template activating factor 1β
Vps75	Vacuolar protein sorting 75

Abstract

Histones are a major protein component of chromatin, yet mechanisms which control synthesis, post translational modification, deposition and removal of histones are not fully understood. Although atomic resolution structures have been solved for the nucleosome core particle, there is limited information regarding the conformation of the core histones outside of chromatin. Insight into the structure of soluble histones, and the complexes they form, is likely to further our understanding of important nuclear processes such as transcription, chromatin replication and epigenetic inheritance. In this study we employ novel biochemical and biophysical techniques to address two key questions in the field: the structure of the soluble $(H3\text{-}H4)_2$-tetramer, and the conformation of H3 and H4 in complex with histone chaperones.

Firstly, we determined the conformation of histones H3 and H4 when in complex with two histone chaperones from *S. cerevisaie*, Nap1 and Vps75. Within the nucleosome H3 and H4 form a heterotetrameric structure sustained by the interface between two histone H3 proteins. Interestingly, when bound to the histone chaperone Asf1 the H3-H3' interaction is disrupted, thus Asf1 effectively splits the tetramer binding a single H3-H4 dimer. Using targeted protein crosslinking and pulsed EPR we determine that, unlike Asf1, the Nap1 family of histone chaperones can bind H3-H4 in their tetrameric conformation, analogous to that observed within the nucleosome. The ability to bind H3 and H4 as a tetramer has implications in the prevalence of chromatin states during DNA replication and transcription, and may be in part responsible for the alternate *in vivo* functions of these two classes of chaperones.

Secondly, using site direct spin labelling in conjunction with pulsed EPR we probe in detail the structure of the soluble $(H3\text{-}H4)_2$-tetramer. Whilst the core crescent shape of the tetramer surrounding the H3-H3' interface is retained, discrete regions such as the αN helix of H3 are more structurally heterogeneous than in the histone octamer or nucleosome. Such structural heterogeneity in the αN helix of H3 highlights potential roles in the post translational modification of histones and in their binding to histone-chaperones. These new findings reveal possible modes of interaction between a tetramer

of H3-H4 and Nap1 proteins, and highlight the need for further investigation into histone – chaperone complexes.

1. Introduction

1.1 The nucleosome core particle, higher order chromatin structure and the dynamic nature of nucleosomes.

The genomic DNA of eukaryotic cells is packaged into a DNA-protein complex referred to as chromatin. Packaging of genomic DNA is necessary to constrain the physical size of eukaryotic genomes to cellular dimensions, but also in regulating processes that require access to the underlying genetic material. Thus, chromatin is not a static structure, but subject to assembly and disassembly throughout the cell cycle.

1.1.1 Structure of the NCP

Early insights into the underlying structure of chromatin revealed the fundamental repeating unit of chromatin is comprised of a segment of ~200 base pairs of DNA and four core histones, H2A, H2B, H3 and H4 (Kornberg 1974; Kornberg and Thomas 1974; Oudet, Gross-Bellard et al. 1975). This nucleo-protein ensemble was termed the nucleosome. Extensive nuclease treatment yielded a further particle, known as the nucleosome core particle (NCP) [1], which retains its histone content, but sequesters only ~150 base pairs of DNA (Axel 1975; Lohr, Corden et al. 1977; Lohr, Kovacic et al. 1977). Initial characterisation of the NCP using crystallography and neutron scattering demonstrated that the nucleosome adopts a disk-like shape with DNA on the outside and histones in the centre (Hjelm, Kneale et al. 1977; Suau, Kneale et al. 1977; Richmond, Finch et al. 1984). Further crystallographic analysis yielded an atomic resolution structure of the core histone octamer (Arents, Burlingame et al. 1991), and the nucleosome core particle (Luger, Ma?der et al. 1997; Davey, Sargent et al. 2002; Richmond and Davey 2003) (figure1.1A).

The 1.9 Å resolution crystal structure of the NCP allows us to see, with atomic detail, how the core histones coordinate the 147 base pairs of DNA within the

[1] Although strictly speaking the term ‘nucleosome’ corresponds to the NCP plus ~50 base pairs of linker DNA, ‘nucleosome’ and ‘NCP’ are used interchangeably within the literature, and also within this report.

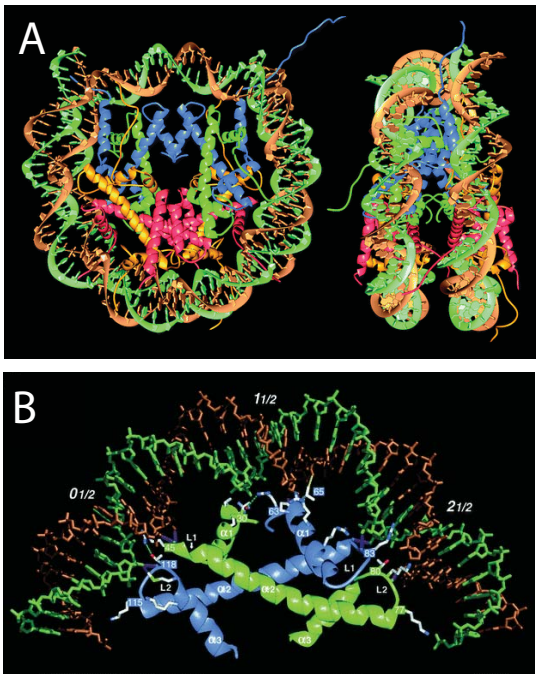

Figure 1.1. The atomic resolution crystal structure of the nucleosome core particle. (A) The NCP displayed in two orientations. Two of each of the histones H2A (orange), H2B (red), H3 (blue) and H4 (green) form the core protein component of the NCP, around which ~147 base pairs of DNA wraps in a left-handed superhelical fasion. (B) A histone fold dimer of H3 (blue) and H4 (green) and its interaction with a segment of DNA within the nucleosome. Note the psuedo 2-fold axis of symmetry running vertically through superhelical location 1½ (taken from Luger *et al.,* 1997. Nature 389, 251-260).

nucleosome. DNA is wound in 1.7 superhelical turns around the histone octamer forming a near symmetrical complex with a two-fold (pseudo) axis of symmetry running through the central nucleotide, known as the dyad. Thus, both the translational and rotational positioning of DNA around the octamer can be defined in terms of its superhelical location (SHL) from the dyad. The highly basic histones are arranged in the octamer so that a positively charged, left-handed superhelical ramp is formed, providing the binding platform for the sugar-phosphate backbone of DNA. The limited contacts made with the bases of DNA demonstrate the ability of the histone octamer to accommodate virtually any sequence variation, a property required for packaging the near infinite sequence variations within eukaryotic genomes. The N-terminal domains of the histones, which can account for up to one third of the protein, exist in a disordered state, protruding out of the NCP between the minor groves of the DNA gyres (figure 1.1A). All except for the H4

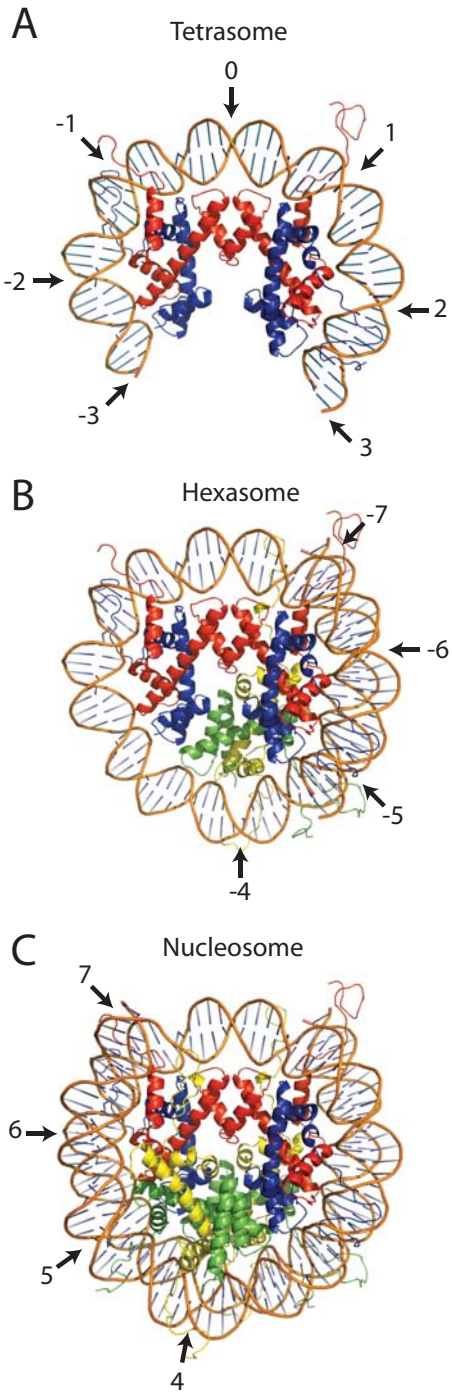

Figure 1.2. The modular nature of nucleosome assembly. (A) The first step in nucleosome assembly is the deposition of H3 and H4 onto DNA. From the nucleosome crystal structure we can see that the (H3-H4)2-tetramer organises the central ~60 base pairs of DNA. This particle has been termed the 'tetrasome'. The superhelical locations from the dyad are indicated. (B) Additon of a single H2A/B dimer to a tetrasome results in a 'hexasome'. The hexasome is a hypothetic intermediate in the formation of the nucleosome, coordinating the perphiral ~40 base pairs of DNA. Superhelical locations of the DNA coordinated by addition of a single dimer are labelled. (C) Additon of a second dimer forms the nucleosome. Superhelical locations of the remainding DNA are labelled. Color scheme: H3, red; H4, blue; H2A, yellow; H2B, green (images created from PDB coordinates 1KX5).

tail, which makes inter-nucleosomal contacts with an acidic patch on the surface of the H2A-H2B dimer (see section 1.1.2).

The atomic resolution crystal structures of the core histone octamer and NCP revealed that H2A-H2B and H3-H4 exist as obligate dimers defining a protein fold known as the histone fold motif (HFM). The HFM consists of three helices (α1, α2 & α3), a long central α-helix (α2) flanked on each side by two smaller α-helices (α1 & α3).

This arrangement results in a cleft between the flanking helices, which can accommodate the central helix of another histone fold motif in an orthogonal fashion, resulting in a histone fold dimer (HFD) (figure 1.1B). Complementary interactions between the histone fold motifs along this interface result in the specific pairing of H3 with H4 and H2A with H2B.

The contacts made between the histones and the DNA predominantly occur at the two loops (L1 and L2) formed between the central (α2) and flanking (α2 & α3) helices of the HFD, as well as the N-termini of the α1 helices (α1α1) (figure 1.1B). DNA is rotationally positioned so that the HFD interacts with the minor groove at each of its three contact points (L1, L2 and α1α1) (figure 1.1B), with a total of three helix turns of

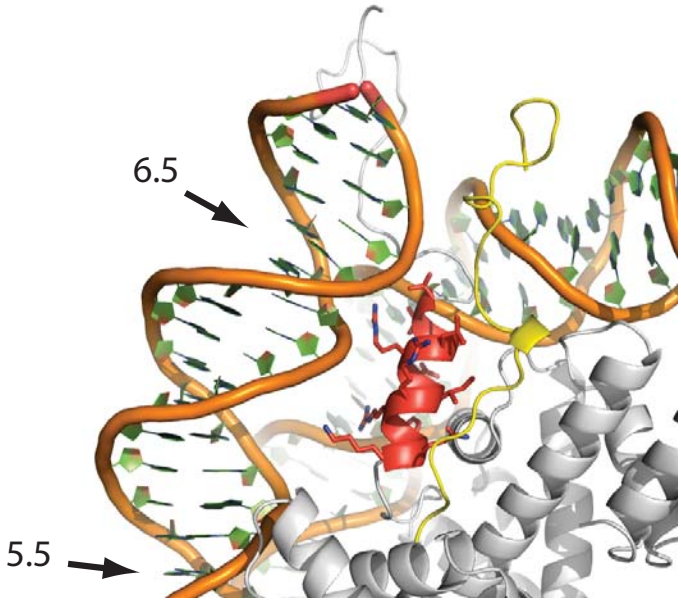

Figure 1.3. The position of the H3 aN helix within the nucleosome. Pinned between the entry/exit gyre of DNA, a portion of the dyad DNA and the C-terminal extension of H2A, the αN helix of H3 resides at a strategic location for regulating intrinsic nucleosome dynamics (image created using PDB coordinates 1KX5). Colour scheme: H3 αN helix, red; H2A C-terminal extension, yellow; other histone content, grey; DNA, orange. Sidechains for the αN helix are represented as sticks. The superhelical locations of the DNA at +5.5 and +6.5 are indicated.

the DNA bound by each HFD (figure 1.1B). H3 and H4 occupy a central location coordinating ~60 base pairs of DNA from SHL -3 to +3 (figure 1.1A, 1.2A). The HFD of H2A and H2B coordinate the flanking ~40 base pairs of DNA from SHL -4 to -7 and +4 to +7 (figure 1.2B & C). Deposition of two H2A-H2B dimers forms the nucleosome proper, bringing the entry and exit points into close proximity, and accounting for the 1.7 superhelical turns of DNA within the nucleosome (figure 1.1A, 1.2C). Structural

elements outside of the HFD, such as the αN helix of H3, the C-terminal extension of H2A and the αC helix of H2B (figure 1.3), make additional contacts with the DNA and play an important role in maintaining the structural integrity of the nucleosome.

1.1.2 Higher order chromatin structure

Assembly of the core histones onto DNA to form nucleosomes is the primary level of chromatin packaging. The secondary level requires the folding of a linear array of nucleosomes into a regular fibre of ~30 nm in diameter, which is assembled into higher order structures of 100-300 nm in diameter, which are then further condensed into meiotic and mitotic chromosomes. Little is known about higher order chromatin structures beyond the 30 nm fibre, mainly due to the complexity in the reconstitution or purification of homogenous material.

Initial insights into the secondary level of chromatin packaging came from electron microscopy where chromatin fibres of 30 nms could be isolated from interphase nuclei (Finch and Klug 1976; Widom and Klug 1985; Williams, Athey et al. 1986), suggesting that this may be the structural form in which most chromatin resides *in vivo*. Further biochemical and biophysical analyses revealed the importance of divalent cations (Schwarz, Felthauser et al. 1996; Huynh, Robinson et al. 2005), linker histones (Carruthers, Bednar et al. 1998; Huynh, Robinson et al. 2005) and histone tails (Allan, Harborne et al. 1982; Garcia-Ramirez, Dong et al. 1992; Schwarz, Felthauser et al. 1996) as important factors in regulating condensation of nucleosomal arrays. Of particular interest was the finding that post translation modification of the H4 N-terminal tail, which participates in internucleosome interactions within the crystal lattice (Luger, Ma?der et al. 1997), can regulate compaction and decompaction of the 30 nm fibre (Shogren-Knaak, Ishii et al. 2006; Lu, Simon et al. 2008; Robinson, An et al. 2008).

With the ability to reconstitute 30 nm fibres *in vitro* (Simpson, Thoma et al. 1985; Huynh, Robinson et al. 2005), further characterisation was possible. The two main models that have so far been put forward are the solenoid (Finch and Klug 1976; Widom nd Klug 1985; Williams, Athey et al. 1986; Robinson, Fairall et al. 2006; Kruithof, Chien et al. 2009) and the two start zigzag (Bednar, Horowitz et al. 1998; Dorigo, Schalch et al. 2004; Schalch, Duda et al. 2005) (figure 1.4). In the solenoid helix the nucleosome are stacked in register, each nucleosome facing its two neighbors to form a single chain that

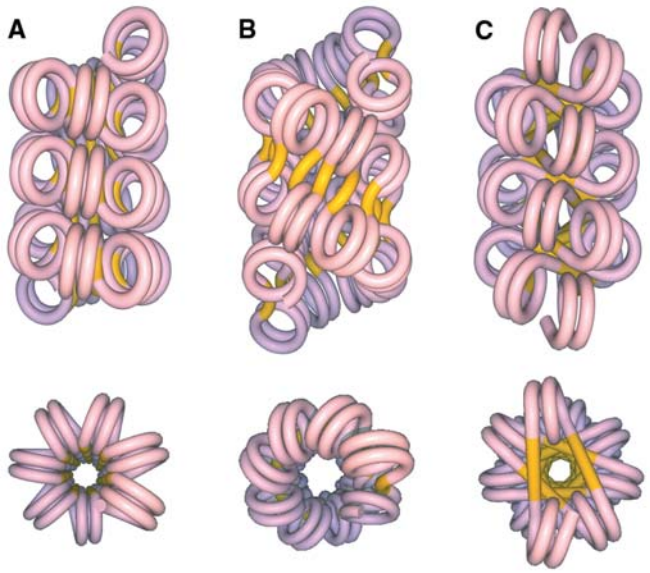

Figure 1.4. Three different models for the arrangement of nucleosomes within the 30 nm fibre. (A) One-start, solenoidal helix. (B) Two-start supercoiled helix. (C) Two-start twisted helix. Nucleosomal DNA is coloured pink, linker DNA is coloured yellow (Taken from Dorigo et al., 2004).

coils around the helical axis of the fibre (figure 1.4A). In the two-start, 'zigzag' model DNA crosses the helical axis of the fibre with each nucleosome making contacts with every other nucleosome in register. Thus, on first inspection the fibre appears to be comprised of two interdigitated arrays (figure 1.4C). Discrepancies between the two models may be due to artifacts derived from the different techniques used for investigation: evidence for a solenoid is derived predominantly from electron microscopy and single molecule force spectroscopy (Finch and Klug 1976; Widom and Klug 1985; Williams, Athey et al. 1986; Robinson, Fairall et al. 2006; Kruithof, Chien et al. 2009), whereas evidence for the two start helix has come from x-ray crystallography and targeted protein crosslinking (Dorigo et al., 2004; Schalch et al., 2005). Discrepancies may also be the result of the alternative methods for *in vitro* fibre preparation (Robinson and Rhodes 2006). However, it has not been proven that the 30 fibre is comprised of only a single structural form *in vivo*. Thus, it is possible that the 30 nm fibre need not conform to a single structural conformer within the cell and that both models are indeed correct.

1.1.3 Non canonical nucleosomes and the dynamic nature of the NCP

Although the high resolution model of the nucleosome has provided key insights into chromatin structure, such crystal structures represent a snapshot of an idealised nucleosome derived from a non-physiological environment that favours crystal packing. Rather, it has become increasingly apparent that nucleosomes are not static entities. Instead they undergo numerous dynamic alterations, including alterations in histone-DNA contacts, translational repositioning and alterations to histone content. Many of these alterations are mediated by factors that have evolved directly for this reason (discussed in sections 1.2 and 1.3), yet such factors generally act to exploit the underlying dynamic properties of nucleosomes which are inherent in its structure.

The crystal structure of the nucleosome would suggest that histones sequester DNA so that it is not available to other DNA binding factors. Multiple studies carried out by Widom and co-workers have shown that this is not the case. Initital work probing the accessibility of nucleosomal DNA using restriction endonucleases found that DNA towards the entry/exit points was more susceptible to digestion than DNA toward the dyad (Polach and Widom 1995). Further studies utilising stopped-flow and FRET based assays demonstrated conclusively that DNA is able to undergo transient unwrapping and rewrapping on the millisecond timescale (Li and Widom 2004; Li, Levitus et al. 2005). The phenomenon has been termed 'site-exposure'[2] as it was hypothesised that such transient unwrapping exposes binding sites that would otherwise be sequestered. This provides a mechanism for allowing access to factors requiring genomic DNA as a substrate without the removal of histones. The αN helix of H3 resides in a strategic location, making contacts with the entry/exit sites of DNA (figure 1.3). Consequently, it was found that mutations with the αN can affect such wrapping and unwrapping of DNA (Ferreira, Somers et al. 2007) and may be regulated by post translational modification of key residues in the αN (Neumann, Hancock et al. 2009).

The idea of transient unwrapping of DNA from the nucleosome agrees well with other observations regarding the stability of H2A-H2B dimers. An H2A-H2B HFD is

[2] Transient unwrapping of DNA from the nucleosome has also been described in the literature as 'DNA breathing'. Both 'site exposure' and 'DNA breathing' refer to the same process of partial, transient wrapping and unwrapping of DNA around the octamer core.

responsible for wrapping the peripheral ~40 base pairs of DNA, and thus site exposure would result in the loss of many of these histone-DNA contacts. Due to the highly basic nature of histones, H2A-H2B experience repulsive forces towards the $(H3\text{-}H4)_2$-tetramer under physiologically ionic conditions. Therefore, loss of the charge compensating interactions with DNA may result in the ejection of an H2A-H2B dimer from the nucleosome. This has been observed *in vitro* (Bruno, Flaus et al. 2003; Ferreira, Somers et al. 2007), and provides a mechanistic insight into the observation that H2A and H2B show a much more rapid turnover than H3 and H4 in living cells (Kimura and Cook 2001; Thiriet and Hayes 2005). Transient unwrapping of DNA and associated dimer loss may also account for nucleosomes being able to invade each others territories (Engeholm, de Jager et al. 2009), although the biological importance of such 'di-nucleosome' particles is still under debate.

A consequence of dimer loss is the formation of a 'tetrasome', that is a $(H3\text{-}H4)_2$-tetramer associated with DNA. Evidence for the formation of such tetrasome particles has been observed upon induction of viral gene promoters. Beato and colleagues have demonstrated that upon induction of the mouse mammary tumour virus (MMTV) promoter H2A and H2B are lost from specific, discretely positioned nucleosomes at the promoter region (Vicent, Nacht et al. 2004). The loss of dimers from promoter nucleosomes is driven by an ATP-dependent nucleosome remodelling complex and is necessary for the binding of transcription factors to their cognate sites, which would otherwise be occluded by a nucleosome containing its full cohort of histones (Eisfeld, Candau et al. 1997; Spangenberg, Eisfeld et al. 1998; Venditti, Di Croce et al. 1998; Vicent, Zaurin et al. 2010). *In vitro* characterisation of the tetrasome has shown that it is a highly dynamic structure. One remarkable observation is its ability to undergo a transition from wrapping DNA with a canonical left-handed chirality to a right-handed chirality (Hamiche, Carot et al. 1996; Bancaud, Wagner et al. 2007). It has been suggested that such chiral transitions may also aid in the release of H2A-H2B dimers from the nucleosome thereby facilitating the passage of polymerases through nucleosomes (Levchenko, Jackson et al. 2005; Wunsch and Jackson 2005). Indeed, there is a wealth of literature that would suggest transcription by RNA polymerase results in depletion of H2A-H2B dimers both *in vitro* an *in vivo* (Studitsky, Clark et al. 1995;

Studitsky, Kassavetis et al. 1997; Kireeva, Walter et al. 2002; Belotserkovskaya, Oh et al. 2003; Schwabish and Struhl 2004; Thiriet and Hayes 2005; Kulaeva, Gaykalova et al. 2007).

1.1.4 Nucleosome positioning and associated free energies of histone-DNA interactions

Nucleosomes purified from nuclei are generally stable in aqueous solution of physiological ionic strength, yet the mixing of purified histones with 147 base pair DNA under identical buffer conditions results in very little nucleosome formation. The proposed reason for this is that non-nucleosomal associations between histones and DNA, which are readily formed upon direct addition, act as a kinetic block for the correct assembly of the NCP. The free energy of nucleosome formation is no doubt negative, although has yet to be determined empirically. This is somewhat surprising when one considers the constraints that are put on DNA to achieve the 1.7 superhelical turns present in the nucleosome. The thermodynamic cost of such bending is offset, in part, by the numerous ionic and hydrogen bonds made with the core histones. Paradoxically, the same ionic properties of the core histones are most likely responsible for the non-nucleosomal associations that form the kinetic block to correct nucleosome folding. *In vivo* this contradiction seems to be solved by the actions of acidic proteins[3], *in vitro* this block is often overcome by modulating the ionic strength of the aqueous environment (Thastrom, Lowary et al. 2004), and has allowed detailed investigations into the rules governing the positioning of the histone octamer on DNA with respects to the underlying DNA sequence.

Early studies showed that purified nucleosomes from chicken erythrocytes displayed DNA sequence motifs that occurred with a ~10 base pair periodicity (Satchwell, Drew et al. 1986). AAA/TTT and AAT/TTA repeats rotationally aligned so that their minor groove faced toward the histone octamer, whereas GGC/CGG and AGC/TCG repeats aligned so that their minor groove face away from the histone octamer. Later studies used purified genomic DNA (Lowary and Widom 1997; Widlund,

[3] Such acidic proteins are known as histone chaperones. The action of histone chaperones in nucleosome assembly is reviewed in detail in section 1.3.

Cao et al. 1997) or synthetic DNA sequences (Cao, Widlund et al. 1998; Lowary and Widom 1998), or both (Thastrom, Lowary et al. 1999), to isolate DNA fragments that displayed a high affinity, or low affinity (Cao, Widlund et al. 1998), for the histone octamer. In good agreement with earlier studies, it was found that AT dinucleotides were favoured at positions where the minor groove contacts the histone octamer, whereas long repeats consisting of TGGA selectively disfavoured nucleosome formation (Cao, Widlund et al. 1998). It can be seen from the nucleosome crystal structure that bending of DNA results in a local compaction at locations where the minor groove interacts with the histone octamer (Richmond and Davey 2003). Thus it appears that AT dinucleotides, by accommodating such distortions, confer a certain bendedness to the DNA template which may favour nucleosome formation. It can also be seen from the high resolution structure of the nucleosome that the DNA contains twist distortions, thus it may also be that the periodicity of AT dinucleotides can accommodate the local helical twists better than other sequences (Thastrom, Lowary et al. 1999; Richmond and Davey 2003). Another interesting observation was that the strongest synthetic DNA sequences had a much higher affinity than the strongest naturally selected sequences (Lowary and Widom 1998; Thastrom, Lowary et al. 1999), leading the authors to conclude that "even the highest-affinity sequence region of eukaryotic genomes are not evolved for the highest affinity or nucleosome positioning power" (Thastrom, Lowary et al. 1999).

The preference of the histone octamer for various DNA sequence motifs is of great interest as, with the onset of the post genomic era, it has been demonstrated that nucleosomes reside at defined locations *in vivo* (Yuan, Liu et al. 2005). The positioning of nucleosomes at discrete locations with the genome would provide a potential mechanism for regulating access to DNA. Indeed, a strong correlation between purified histones positioned on genomic DNA *in vitro* and nucleosome positions determined *in vivo* suggests that the *S. cerevisiae* genome may have evolved nucleosome positioning capabilities (Segal, Fondufe-Mittendorf et al. 2006; Kaplan, Moore et al. 2009). However, the extent to which positioning is determine solely by DNA sequence alone is still not clear, with other studies adopting similar approaches coming to the conclusion that nucleosome positioning *in vivo* in *Saccharomyces cerevisiae* is primarily determined by transcription factors, RNA polymerase, and additional DNA binding factors and not

by intrinsic histone-DNA interactions (Zhang, Moqtaderi et al. 2009). Indeed, many other factors may be responsible for the location of nucleosomes *in vivo* (Segal and Widom 2009).

The positions of nucleosomes assembled onto DNA is no doubt important in regulating access to the genome, however, it has also been discovered that the histone octamer, once deposited, can be repositioned along DNA without its disassembly (Meersseman, Pennings et al. 1992; Whitehouse, Flaus et al. 1999). This implies that a DNA motif which is sequestered within a nucleosome can become available by the 'sliding' of the histone octamer to an alternate location along the chromosome. This phenomenon was first observed *in vitro* using octamers assembled onto the 5S rDNA sequence (Meersseman, Pennings et al. 1991; Pennings, Meersseman et al. 1991; Meersseman, Pennings et al. 1992). Upon thermal incubation, it was found that the nucleosomes repositioned to alternate locations along the DNA template. Further investigations using base pair resolution nucleosome mapping on the MMTV LTR region demonstrated that nucleosomes could move up to 156 base pairs from their initial position, which proceeded via intermediates positioned between 46 and 62 base pairs (Flaus and Owen-Hughes 2003). Thus, it seems that after energy is introduced into the system (in the form of heat) the positions of nucleosomes differ to those favoured during histone deposition. This may reflect differences in sequence preferences between the tetrasome, which is deposited first and directs the positioning of the nucleosome, and the nucleosome (Flaus and Owen-Hughes 2003). *In vivo,* nucleosomes can be repositioned by remodelling motors powered by energy derived from ATP-hydrolysis (discussed in section 1.2.2), providing further evidence for the idea that nucleosome positioning *in vivo* is not solely dependent on free energy minimisation during histone deposition (Segal and Widom 2009).

Alternative models have been proposed for the mechanism of DNA translocation in nucleosome repositioning. In the 'twist diffusion' model DNA translocation is caused by the formation and dissolution of single base pair twist defects (Kulic and Schiessel 2003; van Holde and Yager 2003). Such defects could be propagated around the nucleosome so that the HFD's interactions with the minor groove is only partially and transiently broken. Indeed, one can observe twist defects when comparing crystal

structures of nucleosomes prepared from 146 and 147 base pairs of DNA (Luger, Ma?der et al. 1997; Richmond and Davey 2003). Another model is the bulge/loop propagation model (Kulic and Schiessel 2003; Langst and Becker 2004). In this model a bulge or loop is generated at the entry/exit site of DNA (possibly through the transient wrapping and unwrapping of DNA as described earlier) and rapidly diffuses around the nucleosome so that the histone octamer is translocated to the origin of the bulge/loop. In this model histone-DNA contacts again are transiently broken, but can traverse, in a single step, segments of DNA much larger that those proposed in the twist diffusion model. An additional model recently put forward is the octamer swivel (Bowman 2010). In this model the octamer rotates by ~18° so that the HFDs switch to interacting with the minor groove one SHL away, yet without the need for looping or bulging of the DNA. Such a dramatic switch may not require such a large input of energy, be it thermal or through ATP hydrolysis, as lysine and arginine sidechains, which are responsible for the ionic interaction between the histone core and the octamer, extend enough from the peptide backbone to bridge such a switch (Bowman 2010). Following the octamer's 'swivel' the DNA at the entry/exit points wrap and unwrap accordingly so that the two fold pseudo-symmetry of the nucleosome is re-established.

1.1.5 Summary

In this section current knowledge regarding the structure of chromatin at the primary level of the nucleosome has been reviewed. The ability of histones to form non-canonical nucleosome structures and the transient wrapping and unwrapping of DNA within the NCP has demonstrated that nucleosomes are not static entities, but are amenable to dynamic alterations. The thermodynamic properties governing the positioning of nucleosomes has been discussed with respects DNA sequence and histone-DNA interactions, and additionally the underlying mechanisms by which nucleosomes can be repositioned has been reviewed with emphasis on the dynamic alterations of histone-DNA contacts. In the proceeding section pathways that have evolved for alteration of chromatin structure via the action of trans-acting factors will be described. We will see that such pathways often exploit the inherent dynamism present within the nucleosome.

1.2 Pathways for altering chromatin structure and composition

Access to genetic material sequestered within the nucleosome and the 30 nm fibre is a fundamental necessity for all processes requiring DNA as a substrate. In this section, pathways that have evolved to alter chromatin structure, thereby regulating access to the genome, are discussed with respects to histone modification, ATP-dependent nucleosome mobilisation and histone variants. The actions of histone chaperones are discussed in more detail in section 1.3.

1.2.1 Post translation modification of histones

One pathway which has evolved to alter chromatin structure is the post translational modification of the core histones. Post translational modifications (PTM) on histones were first identified in the 1960's (Allfrey, Faulkner et al. 1964), and since have been the subject of intense investigation. Lysine residues are the predominant and most well characterised carriers of PTMs in the form of acetylation, methylation, sumolation and ubiquitination. Other residues are also subject to PTM, such as arginine (methylation, citrullination, ribosylation), threonine (phosphorylation) and serine (phosphorylation). Sites of modification appear to be clustered within the histone tails (Goll and Bestor 2002; Turner 2002), with the H3 tail containing by far the most. Yet with the onset of modern mass spectrometric analysis numerous sites within the core HFD have also been discovered (Mersfelder and Parthun 2006). Alternate patterns of modification can recruit specific regulatory proteins and affect specific aspects of chromatin stability, leading to the proposal of the 'histone code' hypothesis (Strahl and Allis 2000), in which the post translational modification status of histones coordinates genomic function, is heritable, and can lead to distinct phenotypes and cell lineages. Thus, specific patterns of modification are often found at defined regions of the genome, for example, H3 and H4 lysine acetylation at gene promoters (Liu, Kaplan et al. 2005; Li, Carey et al. 2007; Rando 2007).

Lysine acetylation was one of the first histone PTMs to be discovered (Allfrey, Faulkner et al. 1964). Acetylation is catalysed by a group of enzymes known as histone acetyl transferases (HATs) via the nucleophilic attack on the acetyl group of acetyl-CoA from the primary ε-amine of a lysine residue, which is deprotonated by a conserved

glutamate or aspartate residue (Berndsen and Denu 2008; Smith and Denu 2009). There are currently three main families grouped on their structural and sequence similarities: the MYST family (named after its founding members Ybf2/Sas3, Sas2 and Tip60) the GNAT family (Gcn5 related-N-acetyltransferases), and the p300 family (containing p300 from metazoans and Rtt109 from yeast) (Berndsen and Denu 2008). Interestingly, lysine residues can also be deacetylated by a group of enzymes known as the histone deacetylases (HDACs), through a more complex and not yet fully understood mechanism (Smith and Denu 2009). Thus, histone acetylation, like many other modifications is not a permanent mark, but is subject to dynamic fluctuations both locally and globally (Liu, Kaplan et al. 2005; Kaplan, Liu et al. 2008; Wellen, Hatzivassiliou et al. 2009).

Chemically, acetylation of a lysine residue both increases the bulk of the sidechain and removes its positive charge, and thus can modulate histone-DNA and histone-histone interactions. The most well characterised acetylation sites occur within the tails of histones, yet recently additional sites which reside within the HFD have also been discovered (Mersfelder and Parthun 2006). Some of these sites, such a H3 K56, make ionic contacts with the sugar-phosphate backbone of DNA, their acetylation serving to destabilise nucleosomes (Neumann, Hancock et al. 2009). In addition to altering histone-DNA contacts, acetylation of the H4 tail at lysine 16 has been shown to promote decondensation of the 30 nm fibre, as discussed previously, through the disruption of histone-histone contacts (Shogren-Knaak, Ishii et al. 2006; Robinson, An et al. 2008). Indeed, multiple acetylation marks within the HFD interfaces have recently been discovered (Ye, Ai et al. 2005; Mersfelder and Parthun 2006), suggesting that disruption of histone-histone interactions within the histone octamer may be a more widespread phenomenon.

In addition to affecting electrostatic interactions within the nucleosome acetylation marks also serve as binding platforms for a multitude of regulatory chromatin proteins. Three protein folds have been discovered that have the ability to bind acetylated lysine residues. They are the bromodomain (Dhalluin, Carlson et al. 1999), the double pleckstrin homology (PH-PH) domain (Li, Zhou et al. 2008) and the tandem PHD finger (Zeng, Zhang et al. 2010). The bromodomain and the tandem PHD finger are the only domains whose structure has been solved in complex with an acetylated histone tail

peptide (Owen, Ornaghi et al. 2000; Zeng, Zhang et al. 2010). The bomodomain consists of four parallel α-helices that form a hydrophobic pocket at one end. It is in this pocket that the charge-neutralised acetyl lysine can bind. Interestingly, bromodomains are present in many histone acetyl transferases, such as Gcn5, suggesting a positive feedback loop in histone lysine acetylation (Kuo, Brownell et al. 1996). They are also found in ATP-dependent chromatin remodelers and basal transcription factors (Zeng and Zhou 2002). Bromodomains show specificity in the acetylated lysine they bind. For instance, the bromodomain in Gcn5 interacts preferentially with acetylated H4 lysine 16, with specificity being imparted by interactions formed with flanking residues (Owen, Ornaghi et al. 2000). Bromodomains can also exist in tandem arrays as for the double bromodomain of TAFII250 (Jacobson, Ladurner et al. 2000). Unsurprisingly, such double bromodomains preferentially interact with a diacetylated histone tail peptide (Jacobson, Ladurner et al. 2000), suggesting certain combinations of acetylation marks can be recognised and act to recruit alternate factors than single acetylation marks alone (Jenuwein and Allis 2001). Recently, it was also found that a single bromodomain can interact preferentially with a diacetylated tail peptide, with structural analysis showing that two acetylated lysines cooperate in binding a single pocket (Moriniere, Rousseaux et al. 2009). Interestingly, in contrast to this the structure of the tandem PHD finger reveals that the two intergrated PHD finger domains bind to a single acetylated tail peptide (Zeng, Zhang et al. 2010).

Considering such effects on the stability of chromatin and recruitment of transcriptional regulators, it is not surprising that acetylation of lysines occurs at regions in the genome where access to DNA is required, such as regions of active transcription and during DNA replication and repair (Liu, Kaplan et al. 2005; Li, Carey et al. 2007; Rando 2007; Downs 2008; Hansen, Nyborg et al. 2010). Consequently, many HAT complexes, such as SAGA, NuA4 and Elongator play pivotal roles in transcription initiation and elongation (Huisinga and Pugh 2004; Li, Carey et al. 2007). Whereas others, such as Rtt109, are important in DNA replication (Fillingham and Greenblatt 2008; Fillingham, Recht et al. 2008; Li, Zhou et al. 2008) and repair (Chen, Carson et al. 2008; Downs 2008)

Lysine residues of the core histones can also be modified by methylation, with mono-, di- and tri-methylation varieties being characterised to date (Kouzarides 2007; Smith and Denu 2009). Unlike acetylation, methylation does not remove the charge of the ε-amine, in fact it becomes more polar (Smith and Denu 2009). Methyl groups are transferred by enzymes known as histone methyl transferases, of which two families have currently been characterised: the SET family, and the DOT1 family. Both families utilise a similar mechanism, transferring a methyl group from S-adenosyl-L-methionine to the ζ-amine of the lysine. Methylation of lysines at different sites correlates with gene silencing or activation. For example, H3 K9 methylation promotes heterochromatin formation through recruitment of heterochromatin protein 1 (HP1) (Bannister, Zegerman et al. 2001; Lachner, O'Carroll et al. 2001), and H3 K27 methylation is associated with X-inactivation through the actions of polycomb group proteins (Cao, Wang et al. 2002). However, other methylation sites are found associated with areas of active transcription. For example, H3 K4 tri-methylation is found at the 5' end of actively transcribed genes, whereas H3 K36 di- and tri-methylation are more abundant at the 3' end of actively transcribed genes (Bernstein, Kamal et al. 2005; Pokholok, Harbison et al. 2005; Li, Carey et al. 2007). Indeed, the methyl transferases that are responsible for methylation of H3 K4 and H3 K36, Set1 and Set2, interact with the RNA polymerase II complex during transcription elongation (Krogan, Kim et al. 2003; Ng, Robert et al. 2003).

As with lysine acetylation, lysine methylation serves as a platform for the recruitment of chromatin regulatory proteins through recognition by certain domains (Taverna, Li et al. 2007). The chromodomain, PHD finger and the tudor domain have all been shown to bind to methylated lysines. For example, the second PHD finger of the Nurf remodelling complex BPTF subunit binds specifically to H3 K4 carrying a tri-methylation mark (Wysocka, Swigut et al. 2006), whereas the chromodomain of HP1 has been shown to specifically interact with di-methylated H3 K9, with specificity imparted by the recognition of the proceeding peptide tetrad (Nielsen, Nietlispach et al. 2002).

Lysine methylation draws additional parallels with lysine acetylation in that the PTM is reversible (Smith and Denu 2009). Lysine specific demethylase 1 (LSD1) is a component of many transcriptional repressor complexes and has been found to have lysine demethylase activity (Shi, Lan et al. 2004; Bannister and Kouzarides 2005; Yang,

Gocke et al. 2006; Culhane and Cole 2007). Fitting with its silencing role, it seems to be specific in its targeting of H3 K4 methylation, a methylation mark which corresponds to active transcription. Demethylation of H3 K4 is also carried out by a family of proteins that share the Jumonji C domain (Iwase, Lan et al. 2007). In addition to H3 K4, demethylation by Jumonji C domain containing proteins also occurs at H3 K27 di and tri-methylation (Culhane and Cole 2007), K9 and K36 methylation (Klose, Kallin et al. 2006; Klose, Yamane et al. 2006), pertaining to diverse cellular functions for this protein fold.

In addition to lysine methylation and acetyaltion, other histone residues can be post translationally modified, and lysines can receive other post translational modifications. For example, H3 S10 is found to be phosphorylated during mitosis (Nowak and Corces 2004; Johansen and Johansen 2006), and H2A ubiquitination at K119 is associated with transcriptional repression (Weake and Workman 2008; Zhou, Wang et al. 2009). A detailed description of these modifications is beyond the scope of this report.

1.2.2 ATP-dependent remodelling of chromatin

Chromatin structure can also be altered as a result of the action of ATP-dependent remodelling complexes. These complexes are typified by a catalytic helicase, and consist of multiple subfamilies with sequence homology to yeast Snf2 protein (Eisen, Sweder et al. 1995; Flaus, Martin et al. 2006). Structural insight into the Snf2 helicases has revealed tandem RecA-like domains, where the conserved motifs that define individual subfamilies are aligned at the domain interface (Subramanya, Bird et al. 1996; Caruthers and McKay 2002; Durr, Korner et al. 2005).

Unlike archetypal helicases, most Snf2 subfamily members do not unwind DNA or RNA duplexes in strand displacement assays. However, certain members are able to exert superhelical torsion on nucleosomal substrates (Havas, Flaus et al. 2000), and ATP-dependent DNA translocation has been observed directly using single molecule experiments (Lia, Praly et al. 2006; Zhang, Smith et al. 2006). Indeed, an atomic resolution structure of an archeal Snf2 helicase in complex with DNA supports a model of chromatin reorganization through DNA distortion driven by DNA duplex translocation rather than helical unwinding (Durr, Korner et al. 2005).

The Snf2 subfamily of the Snf2 helicases (Flaus, Martin et al. 2006) includes the catalytic subunits of both the Swi/Snf and RSC complexes in budding yeast. Snf2-like remodeling complexes are often associated with disruption, removal or relocation of histones from DNA. For example, Swi/Snf can facilitate nucleosome sliding on mono-nucleosomal templates (Whitehouse, Flaus et al. 1999), and the RSC complex can facilitate in the removal and exchange of H2A/H2B dimers (Bruno, Flaus et al. 2003). Indeed, some reports suggest that whole histone octamers can be transferred to acceptor DNA (Lorch, Zhang et al. 1999) possibly through complete nucleosome disassembly (Lorch, Maier-Davis et al. 2006). Insight into how these large multi-subunit complexes remodel nucleosomes has come from electron microscopy, where the complex is seen to form a large central cavity (Leschziner, Saha et al. 2007; Chaban, Ezeokonkwo et al. 2008) within which a nucleosome can bind (Chaban, Ezeokonkwo et al. 2008). Within this binding pocket extensive interaction between RSC subunits and both the histone octamer and DNA are made. It is these interactions that are thought to aid in the translocation of DNA around the nucleosome driven by superhelical torsion generated by the ATP driven helicase domain by stabilizing translocation intermediates (Chaban, Ezeokonkwo et al. 2008; Lorch, Maier-Davis et al. 2010).

Another subfamily member of the Snf2-like proteins is Iswi. There are two Iswi homologues in budding yeast, Isw1 and Isw2 (Tsukiyama, Palmer et al. 1999), and numerous homologues in higher eukaryotes (Flaus, Martin et al. 2006). Similar to Swi/Snf and RSC Iswi is often found in multimeric remodeling complexes, but in contrast to the nucleosome disrupting activities of Snf2 homologues, Iswi containing complexes tend to reorganize nucleosome into well ordered arrays (Ito, Bulger et al. 1996; Tsukiyama, Palmer et al. 1999). Biochemical and single molecule characterization of Iswi containing complexes have shown that they function as dimeric motors (Strohner, Wachsmuth et al. 2005; Racki, Yang et al. 2009). Whereas the RSC complex can envelop a complete nucleosome within it central cavity, it is thought that the Iswi complexes specifically interact with DNA close to the dyad and additionally to flanking DNA (Kagalwala, Glaus et al. 2004). Generation of superhelical torsion at these locations results in the translocation of DNA around the nucleosome (Schwanbeck, Xiao et al. 2004; Zofall, Persinger et al. 2006), with single molecule studies demonstrating that these

translocations occur in discrete 3 and 7 base pair steps (Blosser, Yang et al. 2009). Interaction with the flanking DNA through dedicated DNA binding domains, coupled with the dimeric nature of Iswi complexes, would allow sampling of linker length either side of the nucleosome, allowing the complex to space nucleosomes into regular arrays (Racki and Narlikar 2008).

Additional subfamilies of the Snf2 family exhibit further diversity. For example, the Swr1-like proteins Swr1 and Ino80 act to specifically exchange the histone variant H2A.Z in an ATP-dependent fashion [reviewed by (Morrison and Shen 2009)]. However, a detail description of these classes of ATP-dependent chromatin remodelers is beyond the scope of this report.

1.2.3 Histone variants

Another pathway for altering chromatin structure is the exchange of canonical histones for histone variants. Histone variants are proteins that share a sequence and structural homology with the core histones, but often contain functional differences. Incorporation of histone variants is highly regulated and usually occurs at specific loci within the genome. Drawing parallels with histone post translational modifications, histone variants have been proposed to regulate the epigenetic landscape of the genome (Talbert and Henikoff 2010). True to this idea, histone variants often function in specific nuclear processes, such as DNA damage and repair, transcriptional regulation and centromere demarcation. Of the four core histones, variants relating to H3 and H2A are the most abundant.

In higher eukaryotes there are three highly similar forms of H3: H3.1, H3.2 and H3.3 (Malik and Henikoff 2003). Despite being virtually identical in primary sequence (with a substitution of 4 residues between H3.1 and H3.3, and 1 residue between H3.1 and H3.2), they are incorporated into the genome at different times and locations during the cell cycle. H3.2 and H3.1 are the major type of H3 which are mainly incorporated during S-phase throughout the genome, whereas H3.3 is incorporated at sites of active transcription throughout the cell cycle (Tagami, Ray-Gallet et al. 2004). Consistent with this division, in HeLa cells soluble H3.1 is found in complex with CAF1, whereas soluble H3.3 is found in complex with HIRA (Tagami, Ray-Gallet et al. 2004) and more recently in complex with the putative histone chaperone Daxx (Drane, Ouararhni et al. 2010;

Lewis, Elsaesser et al. 2010). A recent study using tagged endogenous H3.3 suggests it has an additional function in telomeric silencing in embryonic stem cells and neuronal precursors, a function which is dependent on Daxx and not HIRA (Goldberg, Banaszynski et al. 2010).

Another histone H3 variant is the CENtromeric Protein A (CENPA) in humans, and Chromosome Segregation Protein 4 (Cse4) in yeast, but commonly referred to across species as CenH3 (Allshire and Karpen 2008; Black and Bassett 2008). The CenH3 variant replaces canonical H3 in centromeric nucleosomes and are thought to provide the basic scaffold for attachment of the kinetochore during mitosis. Biophysical analysis has shown that CENPA containing tetramers are more rigid than canonical tetramers, with chimeric CENPA/H3 constructs defining a region of CENPA, known as the CENPA targeting domain (CTAD), which is responsible for its localisation to the centromere (Black, Foliz et al. 2004). Interestingly, it has been suggested that the nucleosome formed by CenH3 variants does not wrap DNA in a left-handed superhelix, as in the canonical nucleosome, but has a reversed chirality (Dalal, Wang et al. 2007; Furuyama and Henikoff 2009). This has been proposed to occur through the formation of two heterotetramers, each containing an H2A/H2B/H4/CenH3, termed the 'hemisome' (Furuyama and Henikoff 2009), although direct evidence for such a radical structure is still lacking.

Similar to the H3 family, H2A also contains numerous variants including H2A.Z, H2A.X, macro H2A and H2A.bdb [reviewed by (Talbert and Henikoff 2010)]. Of these four variants two are conserved throughout eukaryotes, H2A.Z and H2A.X (Malik and Henikoff 2003). H2A.Z contains ~60% homology to wildtype H2A and appears to have diverse functions within the genome, centred around both transcription activation and heterochromatin silencing [reviewed by (Zlatanova and Thakar 2008)]. The H2A.Z variant in yeast, Htz1, is found in complex with two histone chaperone complexes, Nap1 and Chz1 (Mizuguchi, Shen et al. 2004; Luk, Vu et al. 2007) which are responsible for its nuclear import and delivery to the Swr1 complex (Mizuguchi, Shen et al. 2004; Straube, Blackwell et al. 2010) which is responsible for its incorporation into chromatin (Krogan, Keogh et al. 2003; Kobor, Venkatasubrahmanyam et al. 2004; Mizuguchi, Shen et al. 2004). Although the crystal structure of a H2A.Z containing nucleosome is virtually

identical to that of the canonical nucleosome (Suto, Clarkson et al. 2000), H2A.Z has been suggested to function through altering higher order chromatin structure, regulating the folding of nucleosomes into 30 nm fibres (Fan, Gordon et al. 2002), possibly mediated through HP1α (Fan, Rangasamy et al. 2004). H2A.X is another H2A variant that has been implicated in DNA damage and repair. Although the HFM of H2A and H2A.X are highly similar, H2A.X contains a S-Q-E/D motif on its C-terminus that is subject to phosphorylation upon double strand breaks (van Attikum and Gasser 2009). Phosphorylated H2A.X then helps to recruit DNA repair proteins to the sites of DNA damage (Pinto and Flaus 2010).

1.3 Histone chaperones in the regulation of chromatin

1.3.1 The structure of histone chaperones and their interaction with core histones

In the late 1970s Laskey and co-workers demonstrated that nucleosomes are assembled through the interaction of histones with an acidic protein (Laskey, Honda et al. 1978). The term 'molecular chaperone' was coined as they protected the highly basic histones from unscrupulous interaction with other proteins[4], thus promoting proper nucleosome formation. In the proceeding three decades multiple factors containing histone chaperoning ability have been identified and their individual functions are currently being dissected.

A feature which is common to all chaperones is the presence of an intrinsically unstructured acidic domain, usually found at the C-terminus. In addition, histone chaperones usually contain a globular domain, or domains, that specifically interact with histones. The protein folds of a number of these globular domains have been determined at atomic resolution, and can be grouped into seven families (figure 1.5) (Das, Tyler et al. 2010). The structural diversity within histone chaperones suggests that the mode of interaction between alternate classes of chaperone and their histone cargo differs, and is most likely responsible for the diverse role of histone chaperones in regulating chromatin

[4] Subsequently, the term 'molecular chaperone' has been used to describe factors involved in protein folding. Thus, molecular chaperones that are involved in chaperoning histones have more recently been termed 'histone chaperones'.

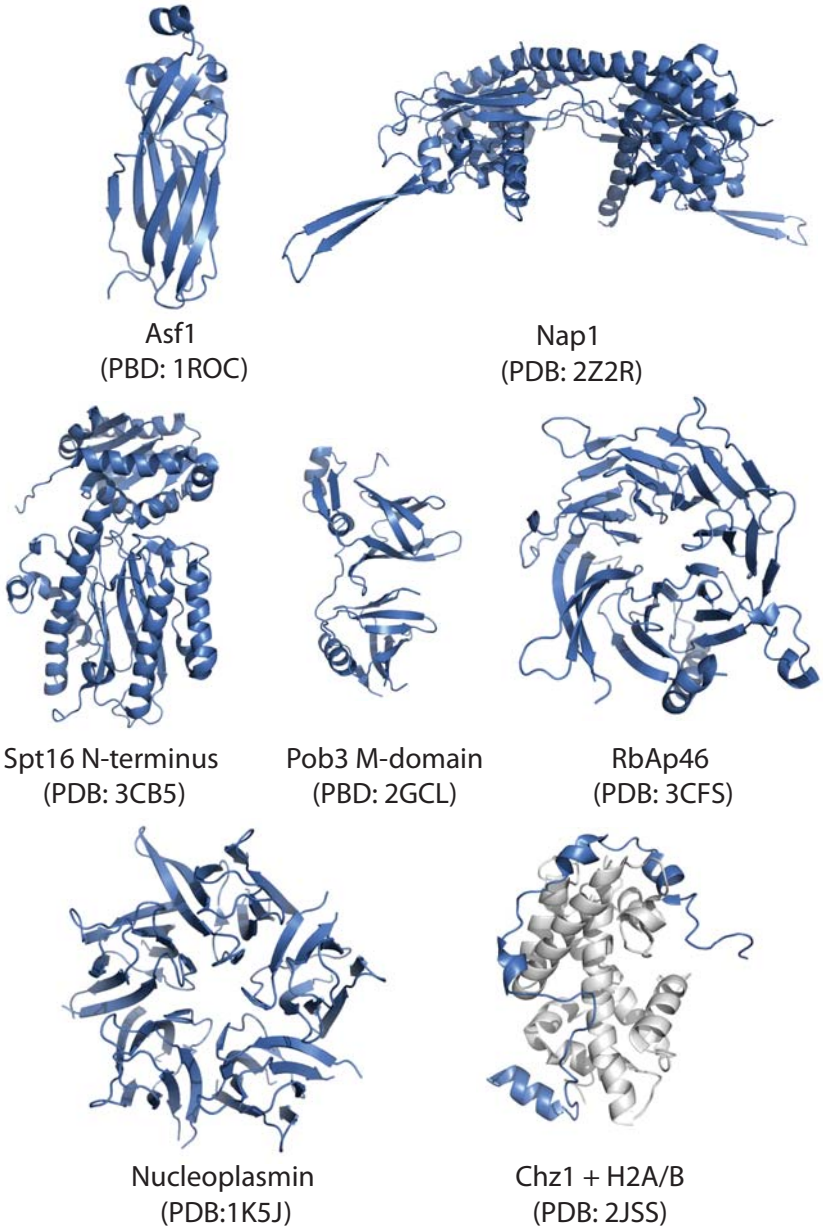

Figure 1.5. Structural diversity within histone chaperones. A representative member for each of the seven families of histone chaperone folds known to date displayed in a cartoon format. The name of the chaperone and its PDB accession number are indicated. Note, Chz1 adopts an irregular structure that forms only in the presence of an H2A/B dimer (Chz1 shown in blue, H2A/B shown in grey).

fluidity. Indeed, most chaperones are discerning with respect to the type of core histone with which they interact: some chaperones binding H2A-H2B (e.g. Chz1 & Nucleoplasmin), whereas others interacting specifically with H3-H4 (e.g. Asf1, RbAp46, Caf1 & Hira). Others are less discerning, interacting with both H2A-H2B and H3-H4 (e.g. Nap1 & Nasp).

Asf1 is a ubiquitous histone chaperone, conserved from yeast to humans, whose N-terminal domain adopts an immunoglobulin-like β-sandwich fold that selectively interacts with H3 and H4 (figure 1.5) (Daganzo, Erzberger et al. 2003). Additionally, it is the only chaperone to date whose co-crystal structure with its histone substrate has been solved (figure 1.6A) (Mousson, Lautrette et al. 2005; English, Adkins et al. 2006; Natsume, Eitoku et al. 2007). The co-crystal structure revealed that Asf1 binds a dimer of H3-H4 through its interaction with the H3 C-terminal interface, supporting previous biochemical characterisation (English, Maluf et al. 2005). Thus, Asf1 effectively acts to split the tetramer of H3-H4. The YEATS domain from Yaf9, a component of both the NuA4 and Swr1 complex (Le Masson, Yu et al. 2003; Zhang, Richardson et al. 2004), also adopts a β-sandwich fold and interacts specifically with H3 and H4, yet conservation of primary sequence is very low (Wang, Schulze et al. 2009), and it is not yet know if Yaf9 binds H3-H4 in an analogous fashion to Asf1. The YEATS domain also occurs in two other proteins in yeast, Taf14 and Sas5, both of which are components of multiple chromatin regulating complexes (Schulze, Wang et al. 2009). Indeed, Asf1 has also been shown to interact genetically with ATP-dependent chromatin remodelers (Gkikopoulos, Havas et al. 2009; Takahata, Yu et al. 2009) and histone acetyl transferases (Han, Zhou et al. 2007; Fillingham, Recht et al. 2008; Williams, Truong et al. 2008). Thus it seems that the β-sandwich fold may have evolved as a basic scaffold for mediating interactions with H3 and H4.

Nucleosome assembly protein 1 (Nap1) from yeast was identified as a protein that directed proper assembly of nucleosomes *in vitro* (Ishimi and Kikuchi 1991; Fujii-Nakata, Ishimi et al. 1992). Nap1 exists as an obligate homodimer via a non-coiled coil interaction (Park and Luger 2006), which is capped by two globular domains (one per monomer) (figure 1.5). The overall structure resembles that of a pair of headphones, and thus the unique fold that Nap1 adopts was termed the ‘headphone fold’. A cavity is formed between the two globular domains that form the ‘earmuffs’ of the headphone (figure 1.5). This cavity is predominantly acidic in nature, and thus Nap1 contains a discrete surface charge distribution, with the interaction between Nap1 and H2A-H2B being mediated by ionic strength of the environment (Park and Luger 2006) (figure 4.10). Nap1 proteins are found throughout the eukaryotes, with crystal structures solved for

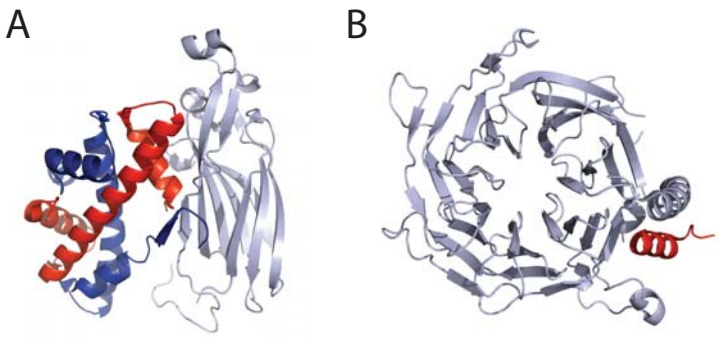

Figure 1.6. Structural insights into the conformation of histones H3 and H4 outside of chromatin. (A) The co-crystal structure of Asf1-H3-H4 revealled that Asf1 competes for the H3-H3' interface observed in the nucleosome, effectively disrupting the (H3-H4)2 -tetramer (PDB code: 1HUE). Colour scheme: Asf1, grey; H3; red; H4; blue. (B) Co-crystal structure of human RbAp46 in complex with an H4 peptide. The H4 peptide, corresponding to the α1 helix of H4, sits within a groove on the side of the β-propeller fold. (PDB code: 3CFS). Colour scheme: RbAp46, grey; H4 peptide, red.

both plasmodium (Gill, Yogavel et al. 2009; Gill, Kumar et al. 2010) and human Nap1 homologues (Muto, Senda et al. 2007), as well as other Nap1 paralogues, such as Vps75 in yeast (Berndsen, Tsubota et al. 2008; Park, Sudhoff et al. 2008; Tang, Meeth et al. 2008). Nap1 proteins have diverse functions related to chromatin metabolism including nuclear import of H2A-H2B dimers (Mosammaparast, Ewart et al. 2002), nucleosome assembly (Ishimi and Kikuchi 1991; Fujii-Nakata, Ishimi et al. 1992; Del Rosario and Pemberton 2008; Andrews, Chen et al. 2010), disassembly in conjunction with chromatin remodelers (Lorch, Maier-Davis et al. 2006; Selth, Lorch et al. 2009) and mediation of histone lysine acetylation (Han, Zhou et al. 2007; Tsubota, Berndsen et al. 2007; Fillingham, Recht et al. 2008). Unlike Asf1, Nap1 proteins are able to interact with both H2A-H2B dimers and H3-H4 *in vitro* and *in vivo* (Krogan, Cagney et al. 2006), but often individual homologues show a preference for one or the other (Selth and Svejstrup 2007). The thermodynamic interactions between yeast Nap1 and the four core histones has been studied extensively (Andrews, Downing et al. 2008; Andrews, Chen et al. 2010). It has been shown that Nap1 has a low nanomolar affinity for both H2A-H2B and H3-H4, and that per chaperone dimer two histone fold dimers can bind (Andrews, Downing et al. 2008). Yeast Nap1 also has the tendency to homomultimerise through a short β-hairpin motif, to form higher molecular weight assemblies (Toth, Mazurkiewicz et al. 2005; Park,

McBryant et al. 2008). The biological role of such higher order associations are not yet clear as mutations that inhibit such oligomerisation do not affect the nucleosome assembly activity of Nap1 (Park, McBryant et al. 2008).

Alternative protein folds containing histone chaperoning ability are encoded in the FACT (facilitates transcription) complex. FACT is a heterodimer of Spt16 and Pob3, in yeast, and Spt16 and SSRP1 in humans. Spt16 contains multiple domains. The N-terminal domain of yeast Spt16 adopts a 'pita-bread' fold and shows structural similarity to a number of amino peptidases (figure 1.5) (Stuwe, Hothorn et al. 2008; VanDemark, Xin et al. 2008). This fold has lost its peptidase activity, but can bind to histone H3 and H4 tails, both with and without modifications (Stuwe, Hothorn et al. 2008). Indeed, the N-terminus of Spt16 seems to be selective in binding H3 and H4 over H2A-H2B (Stuwe, Hothorn et al. 2008). The C-terminus of Spt16 contains an acidic domain, similar to other histone chaperones, and also a putative double pleckstrin homology domain, but its structure has yet to be solved. Pob3 contains a double pleckstrin homology domain (PH-PH) that interacts with replication protein A (RPA) (figure 1.5) (VanDemark, Blanksma et al. 2006). A direct interaction between Pob3 and histone has yet to be shown. A PH-PH domain is also present in the histone chaperone Rtt106 (Liu, Huang et al. 2010). Rtt106 functions downstream of Asf1, possibly in concert with other chaperone complexes, and has been implicated in binding to H3 acetylated on lysine 56 (Li, Zhou et al. 2008). Rtt106 also interacts directly with DNA, with residues important in histone and DNA binding occupying discrete locations within the PH-PH domain (Liu, Huang et al. 2010).

RbAp46/48 and p55 represent WD40 repeat proteins that contain histone chaperoning ability (figure 1.5) (Murzina, Pei et al. 2008; Song, Garlick et al. 2008). Both proteins adopt a seven bladed beta-propeller structure and have been co-crystalised with an H4 α1 peptide bound to a shallow groove on the lateral surface of the beta-propeller (figure 1.6B) (Murzina, Pei et al. 2008; Song, Garlick et al. 2008). Interestingly, the α1 helix of H4 is buried within the HFD, thus a significant structural rearrangement would be required to bind H3-H4 in this manner (Murzina, Pei et al. 2008). WD40 repeat proteins are often found to act as scaffolds, each WD40 repeat interacting with different complex components. True to this function, RbAp46/48, and the related p55, are found in

multiple complexes involved in chromatin metabolism, including the HAT1 complex (Verreault, Kaufman et al. 1998), the NuRD complex (Zhang, Ng et al. 1999) and CAF1 complex (Verreault, Kaufman et al. 1996).

Nucleoplasmin is the founding member of the acidic histone chaperones (Laskey, Honda et al. 1978) and is representative of the pentameric β-barrel fold (figure 1.5) (Dutta, Akey et al. 2001) shared by N038 (Namboodiri, Akey et al. 2004). The monomer of nucleoplasmin forms a β-barrel fold consisting of 8 β-strands arragned in an anti-parallel conformation. Five β-barrel folds come together to form a pentameric ring with a width of ~6 nm, which may further dimerise to form a decameric complex (figure 1.5) (Dutta, Akey et al. 2001). Nucleoplasmin can interact with all four core hsitones, but preferentially interacts with H2A and H2B dimers (Dutta, Akey et al. 2001; Frehlick, Eirin-Lopez et al. 2007; Taneva, Banuelos et al. 2009). Small angle X-ray scattering and isothermal titration calorimetry have show that five H2A-H2B dimers can bind per pentamer, interacting via the lateral surface of the pentameric ring (Taneva, Banuelos et al. 2009), reflecting on its proposed role of histone storage and transport typified within the nuclei of *Xenopus* oocytes (Dilworth, Black et al. 1987; Kleinschmidt, Seiter et al. 1990).

Chz1 is also an H2A-H2B chaperone, but is unique in that it adopts an irregular structure in solution only becoming structured when in complex with its histone cargo (figure 1.5) (Zhou, Feng et al. 2008). Also, Chz1 preferentially interacts with a HFD that contains the variant H2A.Z in place of canonical H2A (Luk, Vu et al. 2007). Chz1 forms three helices connected by two loops in complex with H2A.Z-H2B and effectively wraps around the HFD contacting the α1 and α3 helices of H2B and the α2 helix of H2A.Z (figure 1.5) (Zhou, Feng et al. 2008). . The predominant interactions between the HFD and chaperone are through charged residues (Luk, Vu et al. 2007), thus the acidic Chz1 may stabilise H2A-H2B outside of chromatin through charge compensation of the HFD, a function that may be related to its role in histone variant exchange in conjunction with the Swr1 complex (Luk, Vu et al. 2007).

1.3.2 Histone chaperones in chromatin replication

Each cell division requires duplication of the genome. Chromatin has to be disassembled to allow DNA replication to occur, and then reassembled in its wake as to sustain the correct chromatin state of individual loci. One of the major tasks during S-phase is the production, trafficking and incorporation of new histones into chromatin at sites of DNA replication, as well as disruption and reassembly of parental nucleosomes. In this section the function of histone chaperones involved in chromatin replication are discussed.

Anti silencing function 1 (Asf1) was originally identified as a protein whose over expression resulted in transcription from silenced telomeric regions (Singer, Kahana et al. 1998), and has subsequently also been shown to associate with newly synthesised histones during S-phase, directing incorporation into DNA at the replication fork (Tagami, Ray-Gallet et al. 2004; Groth, Ray-Gallet et al. 2005; Groth, Corpet et al. 2007). This is achieved most likely through its interactions with key replication fork components, such as the PCNA clamp loader RFC (Franco, Lam et al. 2005) and the MCM helicase (Groth, Corpet et al. 2007). It has also been reported to interact with parental histones, possibly having roles in the shuttling of histones across the replication fork (Groth, Corpet et al. 2007; Jasencakova, Scharf et al. 2010). Interestingly, Asf1 doesn't seem to be directly responsible for the deposition of histones onto DNA during replication. Instead histones appear to be passed onto the chaperone complex CAF1 or Rtt106, which are responsible for their deposition (Li, Zhou et al. 2008). The handover of histones is potentially driven by the PTM status of H3 and H4 (Li, Zhou et al. 2008), with newly synthesised histones being highly acetylated whilst in transit to chromatin (Parthun, Widom et al. 1996; Fillingham, Recht et al. 2008). These acetylation marks occur predominantly on tails of the histones, but also, at least in yeast, on lysine 56 of H3 (Ozdemir, Spicuglia et al. 2005; Recht, Tsubota et al. 2006). Asf1 is absolutely required for the acetylation of H3 K56 by the histone acetyl transferase Rtt109 (Adkins, Carson et al. 2007; Han, Zhou et al. 2007; Tsubota, Berndsen et al. 2007), and it is thought that this acetylation mark provides the switch for the histone handover between chaperones (Li, Zhou et al. 2008).

Chromatin assembly factor 1 (CAF1) functions downstream of Asf1 in histone deposition during S-phase and is responsible for the direct depositon of H3 and H4 onto

DNA (Stillman 1986; Smith and Stillman 1989). The complex is a heterotrimer, consisting of Cac1, Cac2 and Cac3 in yeast. In higher eukaryotes CAF1 selectively associates with the major histone isoform H3.1, but not with the variant H3.3 (Tagami, Ray-Gallet et al. 2004), highlighting it role in replication dependent histone deposition. Structural insight into how the CAF1 complex interacts with histones comes from the drosophila homologue of Cac3, p55, and the related human proteins RbAp46/48, which have both been cocrystalised with a peptide fragment of H4 (figure 1.6B) (Murzina, Pei et al. 2008; Song, Garlick et al. 2008). Interaction appears to be mediated, at least in part, through the binding of the H4 α1 helix to a shallow groove on the side of the chaperone. This region is far from the H3-H3' interaction interface, providing the possibility that CAF1 interacts with H3 and H4 in their tetrameric conformation. However, structural alignment of nucleosomal H3-H4 onto the α1 peptide from the p55/RbAp46/ RbAp48 co-crystal structures reveals that major rearrangements of the HFD are required if they are to bind in this fashion (Murzina, Pei et al. 2008). This being said, Cac1/p55/RbAp46 is the smallest of the three CAF1 subunits. Elucidation of the structure of the whole complex should spread light on how it associates with H3 and H4, and how acetylation of H3 K56 mediates the handover of histones from Asf1.

The chaperone Rtt106 has also recently been shown to be involved in replication coupled nucleosome assembly (Li, Zhou et al. 2008), with additional roles in heterochromatin silencing (Huang, Zhou et al. 2005; Huang, Zhou et al. 2007). Analysis of the primary sequence revealed that Rtt106 conatins a double pleckstrin homology (PH) domain. Structural and biochemical analysis of this domain revealed two functional sites: one which can bind selectively to histones H3-H4, and another that binds DNA (Liu, Huang et al. 2010). Both of these sites appeared to affect heterochromatin silencing at telomers, but their effect of DNA replication was not addressed (Liu, Huang et al. 2010).

Another histone chaperone complex which is present at the replication fork is FACT. Originally identified as a chaperone involved in transcription (Orphanides, LeRoy et al. 1998; Belotserkovskaya, Oh et al. 2003), FACT has been shown to have additional roles in chaperoning histones during replication (Okuhara, Ohta et al. 1999). FACT is comprised of two subunits in human, Spt16 and SSRP1, whereas in yeast the domain homologues of SSRP1 are found in two separate proteins, Pob3 and Nhp6 (figure 1.5).

As with Asf1, FACT is found associated with many components of the replication machinery, such as the single stranded DNA binding protein RPA (VanDemark, Blanksma et al. 2006), the MCM complex (Tan, Chien et al. 2006) and DNA polymerase α (Wittmeyer and Formosa 1997; Wittmeyer, Joss et al. 1999), but interacts with both H2A-H2B and H3-H4. These interactions are mediated by different domains, with the N-terminus of Spt16 containing an amino peptidase-like fold which binds H3-H4 (Stuwe, Hothorn et al. 2008; VanDemark, Xin et al. 2008), and the C-terminal domain of Spt16 responsible for interacting with H2A-H2B. The precise role of FACT in histone chaperoning during DNA replication is unclear. The ability of FACT to be able to alter chromatin structure, without the requirement for ATP (Rhoades, Ruone et al. 2004; Formosa 2008; Xin, Takahata et al. 2009), and promote unwinding of DNA by the MCM helicase *in vitro* (Tan, Chien et al. 2006) suggests that it may be important in nucleosome disruption ahead of the replication fork.

1.3.3 The role of histone chaperones in transcription

Histone chaperones also play key roles in regulating gene expression, most notably at the level of transcription (Hansen, Nyborg et al. 2010). The actions of chaperones during transcription can roughly be separated into two groups, those which have roles in promoter remodelling and transcription initiation, and those which associate with RNA pol II and effect transcription elongation.

Asf1 and FACT have both been implicated to have roles in remodelling promoter nucleosomes during transcription initiation. It has been shown that Asf1 is required for efficient histone removal at position spanning 1800 base pairs upstream of the transcription start site of the HO promoter in yeast (Gkikopoulos, Havas et al. 2009). Binding of Asf1 to these positions assists in the removal by Swi/Snf (Gkikopoulos, Havas et al. 2009) and recruits additional co-activators such as SAGA and Mediator (Takahata, Yu et al. 2009), linking the actions of histone chaperones, histone modifiers and ATP-dependent chromatin remodelers. FACT has also been found to be recruited to the promoter regions of genes prior to transcription (Biswas, Yu et al. 2005; Takahata, Yu et al. 2009), but has a more established role in transcription elongation.

Interestingly, whereas Asf1 functions to promote transcription initiation through nucleosome disassembly, other chaperones have been identified that act to silence

transcription. The chaperone complex Hir (HIRA in metazoans) from budding yeast was identified as a corepressor in core histone gene silencing during the cell cycle (Spector, Raff et al. 1997; Fillingham, Kainth et al. 2009) and has a similar function in fission yeast (Anderson, Wardle et al. 2009). Its histone chaperoning ability is directed towards the replication independent variant H3.3 in humans (Tagami, Ray-Gallet et al. 2004), functioning downstream of Asf1 in depositing H3.3/H4 outside of S-phase in *Xenopus* eggs extracts (Ray-Gallet, Quivy et al. 2007). H3.3 deposition is decoupled to replication and occurs at sites of active transcription *in vivo*. Thus, the propensity of HIRA for chromatin reassembly at nucleosome depleted regions of promoters agrees with its role as a corepressor. Indeed, nucleosomes reassembled by the yeast Hir complex are more resistant to remodelling by the Swi/Snf machinery (Prochasson, Florens et al. 2005). In addition to HIRA, the budding yeast chaperone Rtt106 has been identified through genetic screens as a regulator of gene silencing (Huang, Zhou et al. 2005; Fillingham, Kainth et al. 2009). Although Rtt106 displays nucleosome assembly *in vitro*, the current mechanism of how it promotes silencing is unclear, although it does appear to involve both its DNA binding and H3-H4 interaction sites (Liu, Huang et al. 2010).

The FACT complex is another histone chaperone that has dual roles in both DNA replication and transcription. FACT was originally identified as a chaperone involved in transcription elongation (Orphanides, LeRoy et al. 1998), and has been shown to associate with elongating RNA polymerase I, II and III (Belotserkovskaya, Oh et al. 2003; Birch, Tan et al. 2009) where it appears to alter nucleosome structure to aid in the passage of the polymerase (Rhoades, Ruone et al. 2004; Formosa 2008; Xin, Takahata et al. 2009). It may also function in the deposition of the original H3-H4 behind the elongating polymerase (Jamai, Puglisi et al. 2009).

The two Nap proteins in budding yeast, Vps75 and Nap1, have also been shown to have functions in transcription elongation. Both proteins interact genetically with factors involved RNA polymerase progression (Kong, Kobor et al. 2005; Selth, Lorch et al. 2009). Genome wide analysis of Vps75 has shown that it is enriched in open reading frames (Selth, Lorch et al. 2009), whereas deletion of Nap1 affects the expression of ~10% of the yeast genome (Ohkuni, Shirahige et al. 2003). Additionally, Nap1 is recruited to the coding region of the PHO5 gene during transcription activation in yeast,

and a ΔNap1 strain show sensitivity to 6-azauracil, a transcription elongation inhibitor (Del Rosario and Pemberton 2008). Nap1 and Vps75 both appear to have a role in histone acetylation, a role which is most likely linked to their function in chaperoning histones. *In vivo*, Vps75 is found in complex with Rtt109 (Krogan, Cagney et al. 2006), where it mediates acetylation of sites within the H3 tail (Tsubota, Berndsen et al. 2007; Berndsen, Tsubota et al. 2008; Fillingham, Recht et al. 2008). Interestingly, Asf1 also binds Rtt109, but directs acetylation of the H3 core at lysine 56 (Han, Zhou et al. 2007; Tsubota, Berndsen et al. 2007). Lysine 56 acetylation has been shown to be prevalent outside of S-phase, occurring at sites of high histone turnover, such as gene promoters (Rufiange, Jacques et al. 2007), and thus localises to regions of Asf1 activity as would be expected. The redundancy between acetyl transferases in acetylation of the H3 tail makes it difficult to draw similar comparisons for Vps75 (Burgess, Zhou et al.; Fillingham, Recht et al. 2008). However, an interesting studying looking at the rate of histone turnover between ΔAsf1 and ΔVps75 strains in budding yeast demonstrated that Asf1 functions mainly to disassemble chromatin whereas Vps75 promotes chromatin stability (Kaplan, Liu et al. 2008). Whether these alternate functions correlate with the discrete acetylation patterns mediated by the two chaperones, or whether alternative modes of interaction with H3-H4 are responsible, or both, has yet to be determined.

Interestingly, the action of Nap1, and its homologues, in humans has also been linked to histone acetylation. Nap1, Nap2 and TAF1β/SET appear to directly interact with the coactivator and histone acetyl transferase CBP/p300 (Shikama, Chan et al. 2000; Asahara, Tartare-Deckert et al. 2002). However, in this case it seems that Nap1 cooperates in the activation of CBP/p300 target genes by the removal of acetylated histones, but not in mediating acetylation itself (Sharma and Nyborg 2008). Genetic analysis of yeast ΔNap1 strains has shown that they are synthetic lethal with three subunits of the Elongator complex, including the acetyl transferase domain Elp3 (Kong, Kobor et al. 2005), providing an additional link to histone acetylation. The Elongator complex has been shown to associate with elongating RNA polymerase II, and is thought to facilitate the passage through chromatin by acetylation of lysine residues on H3 and H4 (Kristjuhan and Svejstrup 2004). The synthetic lethality with Nap1 is difficult to

interpret due to the lack of biochemical data, however, it is clear that both complexes play important roles in the mechanism of transcription elongation.

1.3.4 The role of histones in DNA damage and repair

As well as having roles in DNA replication, Asf1 and CAF1 are also a key regulators of DNA repair (Mello, Sillje et al. 2002). During DNA repair, as with DNA replication, nucleosomes have to be disassembled to allow access to the repair machinery, and then reassembled after repair is complete. It is thus unsurprising that many of the factors required for nucleosome assembly during DNA replication have also been implicated in chromatin reformation after DNA repair (Ransom, Dennehey et al. 2010). Asf1 and CAF1 have been shown to associated with regions of DNA repair and to play key roles in nucleosome assembly once repair is complete (Mello, Sillje et al. 2002). Actylation of histones is also critical in nucleosome reformation after repair, with the phenotypes of ΔRtt109 yeast strains showing sensitivity to DNA damaging agents (Han, Zhou et al. 2007; Tsubota, Berndsen et al. 2007; Chen, Carson et al. 2008; Fillingham, Recht et al. 2008; Li, Zhou et al. 2008). Interestingly, ΔAsf1 and H3 K56R mutations display similar phenotypes (Han, Zhou et al. 2007; Fillingham, Recht et al. 2008; Erkmann and Kaufman 2009), thus it seems that the ability of Asf1 to promote acetylation of H3 K56 by Rtt109 is key to both DNA replication and DNA repair coupled nucleosome assembly (Chen, Carson et al. 2008; Fillingham and Greenblatt 2008; Li, Zhou et al. 2008). The role of Asf1, therefore, seems to be in the generating the correct PTM pattern of histones in the form of acetylation, whereas CAF1 is possibly responsible for the direct deposition of H3 and H4 onto DNA after repair has occurred. The ability of Asf1 to promote removal during transcription (Rufiange, Jacques et al. 2007; Gkikopoulos, Havas et al. 2009; Takahata, Yu et al. 2009) would suggest that it may also play a histone removal function during DNA resection. However, such a role for Asf1 in DNA repair has yet to be proven (Ransom, Dennehey et al. 2010).

1.4 Aims and objectives

The primary goal of this research was to investigate the structure of soluble H3 and H4, both on their own and in complex with histone chaperones, to further our understanding of the dynamic nature of chromatin regulation. This has been approached through the

blending of traditional biochemical characterisation with more novel biochemical and biophysical techniques. In particular, pulsed electron paramagnetic resonance and site-direct spin labelling have been applied for the first time to study chromatin proteins, yielding insights into the structure of the soluble histone tetramer and the conformation of H3 and H4 when in complex with the Nap1 family of histone chaperones. Thus, this study has provided a small, but significant step into the understanding of how histones behave outside of chromatin and how they interact with their chaperones. It is hoped that the techniques implemented in this research provide useful tools, complimenting more traditional techniques, for the further analysis of chaperone-histone interactions, the conformation of histones and their variants outside of chromatin, and in the study of alternative aspects of chromatin biology.

2. Materials and Methods

2.1 Protein expression and purification

2.1.1 Expression of recombinant histones

Site directed mutagenesis was used to introduce cysteine residues at strategic locations on *Xenopus laevis* histone H3C110A and H4 wild-type, aided by the crystal structure of the histone octamer (1TZY.pdb) using standard cloning procedures. Recombinant *Xenopus* histones were purified from *E. coli* (strain BL21(DE3) pLysS, Stratagene) grown is 2YT media as described previously (Luger, Rechsteiner et al. 1997), dialysed into H_2O and stored as lyophilates.

2.1.2 Expression and purification of deuterated histones

The four core histones, H2A, H2B, H3 and H4, were expressed in Rosetta 2 cells (Novagen) from pET3d expression vectors. Histone H3 contained the mutations C110A and Q76C for site directed spin labelling. Freshly transformed cells were grown to stationary phase in 4 ml of 2YT media containing ampicillin and chloramphenicol for selection. The cells were then pelleted, washed once with deuterated media (Spectra9, Cambridge Isoptope Laboratories), pelleted again and used to inoculate a 250 ml culture. Cell growth was markedly slower in spectra9 than in 2YT media, with a doubling time in the order of 60-90 mins compared to ~25 mins for cells growing in 2YT. Protein expression was induced by the addition of 1 mM IPTG when the optical density at 600 nm reached 0.6. Induction was carried out at 37 °C for 14 hours.

The cultures were spun down and resuspended in 2 ml of wash buffer (100 mM NaCl, 20 mM HEPES-KOH pH 7.5, 1 mM EDTA, 1 % Triton X-100, 1 mM DTT) and lysed by sonication. Histones were present in the insoluble fraction, which was further washed once in Wash Buffer and twice in Wash Buffer without Triton X-100. The insoluble histones were dissolved in 4 ml of unfolding buffer (7 M Guanidinium-HCL, 20 mM HEPES-KOH pH 7.5, 1 mM EDTA, 1 mM DTT) and dialysed into SAU200 Buffer (20 mM sodium acetate pH 5.2, 200 mM NaCl, 1 mM EDTA, 5 mM β-mercaptoethanol). 0.5 ml of cation exchange resin (SP FF, GE Healthcare) was equilibrated with SAU200

buffer in 10 mL dispoable chromatography columns (Bio-Rad). Dialysed histones were bound to the resin, washed twice with 2 mL of SAU200, once with 2 mL of SAU400 (400 mM NaCl), and eluted in 2 mL of SAU800 (800 mM NaCl). Fractions were analysed by SDS-PAGE to assess purity (figure 4.9A). Eluted histones were dialysed into H_2O + 5 mM β-mercaptoethanol and stored as lyophilates. The yields from Spectra9 medium varied from 3-10 mg/L culture, which is comparable to expression of histones in non-deuterated media.

2.1.3 Refolding of histone octamer and tetramer

lyophilised histones were dissolved in unfolding buffer, quantified by absorbance at 280 nm and mixed in equimolar amounts. The octamer complex was refolded by dialysis into refolding buffer, and purified from misfolded aggregates by gel filtration on a GL 10/300 column packed with Superdex™ S200 (GE Healthcare). If the samples were to be labelled on a cysteine residue, 20 mM DTT was added to the sample and incubated at 25 °C for 30 minutes before gel filtration to insure complete reduction of labelling sites. Gel filtration was carried out in refolding buffer without β-mercaptoethanol additionally serveing as a desalting step to remove reducing agent before spin labelling. If samples were not to be labelled gel filtration was carried out with complete refolding buffer.

2.1.4 Expression and purification of recombinant histone-chaperones

S. cerevisiae Vps75 and Asf1 open reading frames were amplified from yeast genomic DNA by PCR and ligated into a modified pET15b vector (Novagen) containing a 6-histidine N-terminal tag with a precision protease cleavage site. The intron in Vps75 was removed by quickchange PCR (Stratagene). Cloned *S. cerevisiae* Nap1 (a kind gift from Karolin Luger, Colorado State University) was amplified and ligated into pET15b. Nap1, Vps75 and Asf1 were expressed and purified by the same method. Expression was in BL21 (DE3) pLysS cells (Stratagene) grown in 2YT media until an OD600nm of 0.8 was reached, at which point 0.5 mM isopropyl β-D-1-thiogalactopyranoside was added. Expression was allowed to proceed for 16 hours at 30 °C. Cells were resuspended in Buffer A with the addition of protease inhibitors E64, pepstatin, ABSF and apoprotin, freeze-thawed and sonicated to lyse. Lysates were centrifuged at 40,000 g to remove cell debris and the soluble fraction passed over HisPur cobalt resin (Thermo Scientific). The

resin was washed extensively in buffer A supplemented with 10 mM imidazole and the protein eluted with buffer A supplemented with 200 mM imidazole. Eluted protein was loaded onto a 5 ml HiTrap Q anion exchange column (GE Healthcare) and eluted with a linear gradient of 0.1 M to 1.0 M NaCl in buffer A with 2 mM DTT. Fractions containing Nap1/Vps75/Asf1 were pooled, concentrated and subjected to gel filtration chromatography on a 16/60 S200 column (GE Healthcare) in buffer B. Fractions containing Nap1/Vps75/Asf1 were pooled, concentrated on an Amicon Ultra centrifugal concentrator (Millipore) and aliquots stored at -80 °C. Cysteine to alanine mutants of Nap1, Vps75 and Asf1 were generated by quickchange PCR mutagenesis (Stratagene) and purified in the same way. Cysteine null mutants were found to behave identically to wild type protein, consistent with previous reports (Andrews et al., 2010; Andrews et al., 2008; Park et al., 2008).

For co-expression of Vps75 and Rtt109, the open reading frame of Vps75 was ligated into a pET30a derived vector using the restriction sites BamHI and NotI. Rtt109 cloned into a pGEX 6P vector (GE Healthcare) was a kind gift from John Rouse (Univeristy of Dundee, UK). The vectors pGEX 6P and pET30a can be sustained in tandem due to their alternate selection markers and origins of replication. Vps75 and Rtt109 were co expressed as in BL21 (DE3) cells (Stratagene) after induction at OD600nm of 0.8 with 0.5 mM isopropyl β-D-1-thiogalactopyranoside. After 12 hours expression at 30 °C cells were resuspended in buffer A supplemented with the aforementioned protease inhibitors, lysed by sonication and sequentially purified on HisPur cobalt resin (Thermo Fisher) and SuperGlu glutathione resin (Generon). The eluate from the glutathione elution was cleaved with precision protease at 4 °C for 16 hours to remove the GST tag. The complex was purified away from the GST by cation exchange chromatography using a 5 mL Heparin HP column (GE Healthcare) with a linear salt gradient of 0.1 – 1 M sodium chloride in 20 mM HEPES-KOH pH 7.5. Fractions containing the complex in a 2:1 molar ratio, Vps75:Rtt109, were pooled and dialysed into buffer C, concentrated and stored at -80 °C. Rtt109 was expressed on its own from a pET28a derived vector, a kind gift from Paul Kaufman (University of Massachusetts Medical School, USA). The N-terminal 6xhis tagged Rtt109 was purified

essentially the same way as Nap1/Vps75/Asf1 except a Heparin HP column was used for ion exchange chromatography (GE Healthcare).

2.1.5 Sequential affinity purification for single labelling a dimer

Coexpression of GST and six-histidine tagged Vps75 followed a similar strategy to coexpresssion of Vps75 and Rtt109. The open reading frame of Vps75 was ligated into vetors pET30a and pGEX 6P1 using restriction sites BamHI and NotI. Plasmids were co-transfected into BL21 (DE3) cells (Stratagene) and selected for by both ampicillin and kanamycin resistance. Expression was in 2YT media until an OD600 nm of 0.8 was reached, upon which IPTG was added to a concentration of 0.5 mM and expression allowed to proceed for 16 hours at 30 °C. Cells were resuspended in Buffer A with the addition of protease inhibitors E64, pepstatin, ABSF, apoprotin, and 0.1 mg/ml lysozyme, freeze-thawed and sonicated to lyse. The soluble fraction was isolated by centrifugation and passed over HisPur cobalt chelating resin (Thermo Scientific). After washing in the same buffer, bound protein was eluted in Buffer A with the addition of 200 mM imidazole. The eluate was then loaded on to SuperGlu glutathione affinity resin (Generon). After washing in Buffer A, proteins were eluted in Buffer A with the addition of 10 mM reduced glutathione (with the pH readjusted to 7.5 using concentrated sodium hydroxide). The affinity tags were cleaved by precision (GST) and TEV (six-histidine) proteases in the same buffer with the addition of 5 mM EDTA, 5 mM EGTA and 5 mM DTT. The Vps75 dimer was separated from the cleaved affinity tags and proteases by anion exchange chromatography using a HiTrap Q 5 mL column (GE Healthcare) with a linear salt gradient of 0.1-1.0 M sodium chloride in buffer A. Fractions contained Vps75 were pooled and dialysed into buffer B before storage at -80 °C.

2.2 Spin labelling of proteins

2.2.1 Labelling of histones

Immediately after gel filtration, fractions containing the correctly folded histone octamer or tetramer were concentrated, using an Amicon® Ultra-4 centrifugal concentrator (Millipore) with a molecular weight cut off of 10,000, to approximately 25 μM and spin labelled with a ten fold excess of *S*-(2,2,5,5-tetramethyl-2,5-dihydro-1H-pyrrol-3-yl)methyl methanesulfonothioate (MTSL) at 25 °C for 3 hours. The effect of protein

concentration on labeling efficiency, monitored by MALDI-TOF, was minimal in the range of 10-100 μM (data not shown). Excess MTSL was removed by dialysis verses 2 L of refolding buffer without reducing agents at 4 °C for 16 hours.

2.2.2 Labelling of Asf1

Asf1 carrying a labelling site at position K41C was labelled in essentially the same way as the histone octamer and tetramer. Purified recombinant Asf1 was reduced with 20 mM DTT for 30 minutes at 25°C, after which it was subjected to gel filtration chromatography on a 16/60 column packed with Superdex S200 (GE Healthcare) in buffer B. Immediately after gel filtration fractions containing Asf1 K41C were pooled, concentrated and labeled with a 10 fold molar excess of MTSL for three hours at 25 °C. Excess MTSL was removed by dialysis versus one liter of buffer D.

2.3 Preparation of proteins for EPR

2.3.1 Preparation of histone octamer and tetramer

Labeled octamer was combined with a 1 fold excess of H2A-H2B dimers, refolded and purified separately, as previous work had shown that an excess of dimer stabilises the octamer complex (data not shown). Water in the refolding buffer was exchanged for deuterium oxide by four rounds of sequential concentration and dilution using Amicon® Ultra-4 centrifugal concentrators (Millipore), achieving a 99.8 % exchange. The spin labeled samples were finally concentrated to a concentration of 100-200 μM and diluted 1:1 with D8-glycerol (Cambridge Isotope Laboratories), giving a final spin pair concentration of 50-100 μM, and stored at 4 °C until EPR measurements were made.

2.3.2 Preparation of labelled H3 in complex with Asf1 K41R1

After dialysis to remove free MTSL, Asf1 K41R1 was transferred into buffer D, made up with deuterium oxide in exchange for water, by multiple rounds of concentration and dilution using centrifugal concentrators (Amicon® Ultra-4, Millipore), as described above. The labeled chaperone was finally concentrated to 400 μM. At this point it could be stored, flash frozen in liquid nitrogen, at -80 °C. Histone tetramer carrying spin labels at position L65 or R49 of H3 was also exchanged into buffer D with water substituted for deuterium oxide, and concentrated to 200 μM tetramer. 25 μL of 400 μM Asf1 K41R1

was combined with 25 μL of 200 μM H3 L65R1 or H3 R49R1 tetramer to achieve a 1:1 ratio of H3-H4 dimer to Asf1 monomer in a concentration of 1 M sodium chloride. This was diluted with 50 μL of D_8-glycerol (Cambridge Isotope Laboratories) to yield a final concentration of 100 μM spin pairs in 0.5 M sodium chloride.

2.3.3 Preparation of labelled histones in complex with unlabelled chaperones

For Asf1, preparation was identical to the procedure detailed in section 2.3.2, except for the altered locations of label on the histone tetramer (H4 R45R1 and H3 Q125R1) and the lack of spin label on Asf1 resulting in a final spin pair concentration of 50 μM. For Vps75 and Nap1, histones (H4 R45R1 and H3 Q125R1 tetramer) and histone-chaperones were buffer exchanged into buffer E made up with deuterium oxide in the place of water and concentrated to 200 μM histone tetramer or chaperone dimer. 25 μL of histone tetramer was mixed with 25 μL of chaperone dimer and 50 μL of D_8-glycerol resulting in a final spin pair concentration of 50 μM and a final sodium chloride concentration of 0.4 M sodium chloride. The samples were stored at -80 °C until EPR measurements were made.

2.4 Analytical gel filtration

Analytical gel filtration chromatography was carried out using a Superdex S200 PC 3.2/30 column attached to a SMART® System (Pharmacia Biotech).

2.4.1 Histones in complex with chaperones

Nap1, Vps75 and Asf1 were mixed with histones to a final concentration of 50 μM complex (with respects to the histone fold dimer) and a final volume of 20 μL and subject to gel filtration in 20 μM HEPES-KOH pH 7.5, 1 mM EDTA, 30% glycerol, 2 mM DTT with differing sodium chloride concentrations as stated in the text. Fractions spanning the void (~1.2 mL) to the bed volume (~2.5 mL) were taken and 10 μL analysed by SDS-PAGE electrophoresis. Direct mixing of histones and chaperones at sodium chloride concentrations below 0.4 M resulted in precipitation of both proteins. To achieve soluble complexes at 0.2 M, mixing was carried out at 1 M sodium chloride and slowly equilibrated, through two successive dialysis membranes, to a concentration of 0.2 M.

This method worked well for Nap1-H3-H4, Nap1-H2A-H2B and Asf1-H3-H4; however, precipitation still occurred with Vps75-H3-H4. Thus it was deemed that Vps75-H3-H4 complex is not stable at lower salt concentrations.

Gel filtration of histone tetramer crosslinked at H3 K115C in complex with Nap1 and Vps75 was subject to gel filtration chromatography under the following conditions: 20 μM HEPES-KOH pH 7.5, 1 mM EDTA, 30% glycerol and 0.2 (Nap1) or 0.4 M (Vps75) sodium chloride.

2.4.2 Histone tetramer

Gel filtration of histone tetramer and histone tetramer crosslinked at H3 K115C was essentially the same as in section 2.4.1, but in the presence of 1 M sodium chloride and without reducing agent.

2.5 Protein crosslinking

2.5.1 Site directed sulfydryl reactive crosslinking

For probing the conformation of H3 and H4 when in complex with Asf1, Vps75 and Nap1 the H3 K115C tetramer-chaperone complexes (cysteine null chaperones) were made up in 20 mM HEPES-KOH pH 7.5, 0.2 M sodium chloride, 1 mM EDTA at a concentration of 1 μM, with respects to the histone tetramer. It should be noted that at the lowered protein concentration of 1 μM directing mixing of histones and chaperones did not result in precipitation as was the case at 25 μM (see section 2.4.1). Additionally, the Vps75-H3-H4 appeared to be stable in 0.2 M sodium chloride when kept at 1 μM tetramer or below (see section 2.4.1). 1,3-Propanediyl bismethanethiosulfonate (M3M) (Toronto Research Chemicals) was made up in dimethyl sulfoxide (DMSO) to a concentration of 25 μM. 48 μL of the complex was added to 2 μL of crosslinker to achieve a 1:1 ratio of crosslinker to histone tetramer, and the crosslinking reaction allowed to proceed for 3 minutes, at which point MTSL was added to a concentration of 200 μM to quench any unreacted cysteine residues. Quenching proceeded for one minute before samples were subjected to non-reducing SDS-PAGE. 20 μL at 1 μM provided a sufficient quantity for detection by coomaisse staining whilst remaining in the linear region for quantitation.

To look at binding of Asf1g to the crosslinked tetramer, Asf1g was mixed at 20 μM with an equal stoichiometry of pre-crosslinked tetramer (10 μM) in a total volume of 30 μL in buffer B. Binding was allowed to take place for 1 hour at 25 °C and complexes separated by filtration chromatography using a Superdex S200 PC 3.2/30 column attached to a SMART® System (Pharmacia Biotech) in the same buffer. Fractions were taken from the void to bed volume, and 20 μL of each loaded on an SDS-PAGE gel. Quantification of the bands was carried out using the software AIDA (Raytest).

For the tetrasome assembly reactions, aliquots of reduced histone tetramer containing the H3 K115C mutation were thawed, diluted with buffer D to 15 μM (tetramer) and crosslinked with a 1:1 stoichiometry of bis-maleimidoethane (BMOE) (Thermo Fisher) that had been dissolved in DMSO. At this higher concentration of tetramer the reaction was more efficient resulting in ~80% crosslinking. The final concentration of dimethyl sulfoxide was kept below 4 % total volume. BMOE was used instead of M3M as it forms a thioether, rather than a disulphide, and is thus cannot be reduced by DTT. Crosslinking proceeded for 3 minutes and was quenched with 10 mM DTT. Crosslinked tetramer was used directly in tetrasome assembly.

For acetyl transferase assays, aliquots of reduced histone tetramer containing the H3 K115C mutation were thawed, diluted with buffer D to 1 μM tetramer and crosslinked with an equimolar ratio of BMOE. Crosslinking reactions were quenched with DTT at regular intervals and the time point which corresponded to an equimolar ratio of crosslinked to non-crosslinked H3 was chosen for the competition assay, as analysed by SDS-PAGE.

2.5.2 Amine reactive crosslinking

Vps75 and H3-H4 were combined in 0.4 M sodium chloride, 20 mM HEPES-KOH pH 7.5, 1 mM EDTA, 2 mM DTT at a concentration of 5 μM, with respects to the histone tetramer or Vps75 dimer, in a volume of 20 μL. Equlibration was allowed to take place at 25 °C for one hour after which Bis(Sulfosuccinimidyl) glutarate (BS2G), dissolved at 50 mM in DMSO, was added to separate samples to give final concentrations of 0.031, 0.063, 0.125, 0.25, 0.5, 1.0 and 2.0 mM. Crosslinking was allowed to proceed for 30 minutes at 25 °C before quenching with 50 mM Tris-HCl pH 8.5. Crosslinked species

were separated by SDS-PAGE electrophoresis on both 4-12% Bis-Tris and 3-8% Tris-acetate precast NuPAGE® gels (Invitrogen), and visualized by staining with coomassie.

2.6 *In vitro* tetrasome reconstitution and template preparation

2.6.1 Amplification of tetrasomal templates by PCR

All templates used for tetrasome reconstitution were derived from the high affinity 601 sequence (Thastrom, Lowary et al. 1999). For analysis of sequence length on tetrasome reconstitution, fragments of length 61, 71, 81, 91, 101, 111 and 147 base pairs were amplified by PCR. In each case the dyad nucleotide was in the centre of the fragment with an equal number of nucleotides each side. For each template length 5 mL of PCR reaction was used comprising of 16 mM $(NH_4)_2SO_4$, 67 mM Tris-Cl pH 8.8, 0.01 % (v/v) Tween-20, 10 μM of each primer, 0.2 mM dNTPs, 1.5 mM $MgCl_2$, 100 ng 601 plasmid template, 40 μL recombinant Taq polymerase. Recombinant Taq polymerase was made by previous members of the laboratory. The 5 mL of PCR reaction was distributed in a 96 well PCR plate (Thermo fisher) and subject to 20 amplification cycles. The amplified DNA was ethanol precipitated and purified by anion exchange chromatography using POROS HQ 50 μm resin (Applied Biosystems) packed into a 2 mL PEEK column with a linear gradient of 0.1-1.0 M sodium chloride in 20 mM Tris-HCl pH 8.5 and 5 mM EDTA. Fractions containing the tetrasomal template were concentrated by ethanol precipitation and stored at -20 °C.

2.6.2 Cloning of a 601 tetrasomal array construct

The method of repeat doubling was used to clone multiple copies of a tetrasomal length 601 template into a plasmid vector for large scale production (Richmond, Searles et al. 1988). A repeating unit was constructed consisting of the following restriction sites, HindIII-BglII-BsaAI-EcoRV-HpyCH4V-71bp 601 sequence-HpyCH4V-EcoRV-BsaAI-BamHI. The restriction sites BsaAI, EcoRV and HpyCH4V were positioned so that digestion with the corresponding endonuclease would result in a 91, 81 and 71 base pair fragment, respectively. A PCR amplified copy of the repeat was cloned into a pUC19 vector using restricution sites HindIII and BamHI. The restriction site BamHI and BglII have identical overhangs allowing a second copy, digested with HindIII-BamHI, to be

cloned into the HindIII-BglII sites of the first. The two copies of the tetrasomal template were released with HindIII-BamHI and ligated into the same vector digested with HindIII-BglII to create a tetra-601 tetrasomal array construct. Doubling the repeat number of the tetrasomal fragment was continued in this fashion until 16 repeats were created. Sustaining more repeats during growth of *E. coli* proved problematic as even growth in recombinase deficient strains resulted in loss of repeat number (data not shown).

2.6.3 Reconstitution by salt dialysis

Equimolar ratios of purified histone tetramer and tetrasomal template were mixed in refolding buffer to a final concentration of 5 μM in a volume of 30 μL. The double-dialysis technique for reconstitution of nucleosomes was used for its reproducibility (Thastrom, Lowary et al. 2004). Briefly, samples were transferred to the lid of a 200 μL PCR tube and capped with a section of dialysis membrane to form a dialysis button. The buttons were then placed in a dialysis bag containing refolding buffer. The dialysis bag was subjected to two rounds of equilibration in 1 L of buffer A with the addition of 1 mM EDTA. Reconstituted tetrasomes were recovered, centrifuged to remove precipitated material and quantified by absorbance at 260 nm. Samples were then analysed by electrophoresis at 4 °C on a 6.5 % polyacrylamide gel in 0.2x TBE with buffer recirculation. Migration of the bands relative to a molecular weight marker was analysed using the software AIDA (Raytest).

2.6.4 Reconstitution by Nap1

A DNA template derived from the 601 sequence (Thastrom, Lowary et al. 1999) comprising 45 bp each side of the dyad nucleotide was generated by PCR amplification resulting in a 91 bp fragment and purified by anion exchange chromatography (see section 2.6.1). 20 μL reactions containing 1 μM crosslinked tetramer (see section 2.5.1), 1 μM template, 10 mM DTT, 0.2 M sodium chloride, 20 mM HEPES-KOH pH 7.5 and 1 mM EDTA were made. To these reactions Nap1 was added to a final concentration of 0, 0.1, 0.25, 0.5 and 1 μM dimer. Assembly was allowed to proceed for 2 hours at 25 °C at which point glycerol was added to a final concentration of 5%. Tetrasomes were resolved from free DNA on a 6.5 % polyacrylamide gel in 0.5x TBE. After staining with ethidium

bromide the tetrasome bands were excised, soaked in 50 mM β-mercaptoethanol, 0.1 % sodium dodecyl sulphate for 10 minutes and cast within an SDS-PAGE gel. This step insured that the crosslinked histone tetramer was derived from only the BMOE crosslinked fraction, and not from H3 K115C that had disulphide bonded during native gel electrophoresis. Crosslinked tetramer was separated from non crosslinked tetramer and probed by western blotting with an anti-H3 antibody (ab1791, Abcam).

2.7 Acetyl transferase assay

BMOE crosslinked tetramer on H3 K115C (see section 2.5.1) was analysed by SDS-PAGE and coomassie staining. Acetyltransferase reactions were performed in 50 mM Tris HCl pH 7.5 and 100 mM NaCl using 1mM acetyl CoA. The 10 μL reactions contained 0.5 μM BMOE treated tetramer with Rtt109 and associated chaperone at concentrations stated in the text. Reactions were incubated for 2 hours at 37°C and the reactions stopped by the addition of SDS-PAGE loading buffer. Crosslinked and non-crosslinked H3 were separated by SDS-PAGE and the histone acetyl transferase activity of Rtt109 analysed by immunblotting using an anti-acetyl-histone H3 (Lys56) antibody (Upstate).

2.8 Circular dichroism

All circular dichroism experiments were carried out by Dr Sharon Kelly, Joseph Black Building, University of Glasgow, Glasgow, G12 8QQ, United Kingdom.

2.9 Electron paramagnetic resonance & molecular dynamics simulations

All pulsed EPR measurements, associated data processing and molecular dynamic simulations were performed by Dr Richard Ward and Dr David Norman, College of Life Sciences, University of Dundee, 5 Dow Street, Dundee, DD1 5EH, United Kingdom.

Experiments were performed on a Bruker ELEXSYS E580 operating at X-band with a Brucker 400U second microwave source. A dielectric resonator was used with a sample chamber of 100 μL allowing for maximum echo intensity, giving a Q-factor of approximately 100. The video bandwidth was set at 20 MHz.

A four pulse, dead-time free, sequence was implemented with a pump pulse frequency placed at the centre of the nitroxide spectrum and the observer pulse positioned at +80 MHz relative to this to insure minimal cross excitation between coupled spins. The pump pulse was set at 16 ns, whereas the observer sequence was typically set at 32 ns.

An averaging rate (or Shot Repetition Time – SRT) of 4 ms was used. Although this typically did not allow for full spin-lattice relaxation of the sample, the increased repetition within the given time frame increased the signal to noise ratio relative to a longer SRT. A total number of scans to achieve sufficient resolution spectra were carried out. At sample concentrations of 50-100 μM spin-pairs this was typically 400-600, with 50 shots sat each time-point. The length of time required was dependent on the distance between the coupled spins: distances less than 4 nm generally took less than 7 hours while distances up to 7.5 nm took close to 16 hours.

Obtaining the strongest echo with respects to temperature is a trade-off between spin-lattice relaxation time (defined by T1 relaxation), which increases averaging time at low temperatures, and transverse relaxation time which decreases at higher temperatures. For doubly MTSL-labelled protein samples a window of 50-80 K is generally appropriate. In experiments detailed in this report a temperature of 50 K was typically used.

Spectra obtained from PELDOR experiments were analysed using the software package DeerAnalysis2006 (detailed in section 4.2.3).

2.10 Buffers and reagents

The following are a list of buffers and reagents used in this study.

- Unfolding buffer: 7 M Guanidinium-HCL, 20 mM HEPES-KOH pH 7.5, 1 mM EDTA, 1 mM DTT.
- Refolding buffer: 2 M sodium chloride, 20 mM HEPES-KOH pH 7.5 or 20 mM Tris-HCl pH 7.5, 1 mM EDTA, 5 mM β-mercaptoethanol.
- Wash buffer: 150 mM sodium chloride, 50 mM Tris-HCl pH 7.5, 1 mM EDTA, 5 mM β-mercaptoethanol.

- SAU200, 400, 600, 800: 0.2, 0.4, 0.6, 0.8 M sodium chloride (respectively), 30 mM sodium acetate pH 5.2, 1 mM EDTA, 5 mM β-mercaptoethanol.
- Buffer A: 20 mM HEPES-KOH pH7.5, 0.1 M NaCl.
- Buffer B: 20 mM HEPES-KOH pH 7.5, 0.5 M NaCl, 1 mM EDTA.
- Buffer C: 20 mM HEPES-KOH pH 7.5, 0.3 M sodium chloride, 1 mM EDTA.
- Buffer D: 20 mM HEPES-KOH pH 7.5, 1.0 M sodium chloride, 1 mM EDTA.
- Buffer E: 20 mM HEPES-KOH pH 7.5, 0.8 M sodium chloride, 1 mM EDTA.
- 2YT media: 10g yeast extract, 16g tryptone, 5g sodium chloride, pH 7.4.
- TBE: 10.8g Tris base, 5.5g boric acid, 9.3g EDTA.

3. Characterising the interaction between the core histones and their chaperones Nap1, Vps75 and Asf1

3.1 Introduction

Multiple pathways have evolved for reconfiguring chromatin structure, promoting or impeding access to the underlying genetic material. Histone chaperones are a class of proteins that have been grouped on their ability to bind the core histones and alter chromatin structure without chemically modifying histones or using energy in the form of ATP to alter nucleosome structure or positioning (De Koning, Corpet et al. 2007; Park and Luger 2008; Das, Tyler et al. 2010). They are therefore distinct from ATP-dependent chromatin remodelling enzymes, such as Swi/Snf family members, and histone modifying enzymes, such as the histone acetyl transferases. The term 'histone chaperone' was coined as they were initially thought to prevent improper interactions of the highly basic histones and thus promoting proper nucleosome assembly (Laskey, Honda et al. 1978). In more recent years, histone chaperones have been found to play important roles in nearly all process that require access to the genome, such as transcription, DNA replication, recombination and DNA repair, and often act in concert with histone modifiers and ATP-dependent chromatin remodelers as multi subunit complexes (Lorch, Maier-Davis et al. 2006; Han, Zhou et al. 2007; Fillingham, Recht et al. 2008; Li, Zhou et al. 2008; Gkikopoulos, Havas et al. 2009; Takahata, Yu et al. 2009).

Crystallographic analysis of individual histone chaperones reveals limited structural conservation, with multiple protein folds containing histone chaperoning ability (figure 1.2). Thus, it is likely that different classes of histone chaperone have different modes of interaction with histones. The only detailed mechanism of a chaperone's interaction with its histone cargo is that of Asf1 with histones H3 and H4. This heterotrimeric complex consists of a chaperone monomer with a single H3-H4 dimer, and is mediated by the disruption of the H3-H3' interface by a concave groove on a beta sheet face of Asf1 (English, Adkins et al. 2006; Natsume, Eitoku et al. 2007).

The Nap family of histone chaperones adopt an alternative structure (Park and Luger 2006; Muto, Senda et al. 2007; Berndsen, Tsubota et al. 2008; Park, Sudhoff et al. 2008; Tang, Meeth et al. 2008; Gill, Yogavel et al. 2009), and thus it is conceivable that their interaction with histones differs from that of Asf1. Interestingly, Nap chaperones exist as obligate dimers and have been shown to interact with two histone fold dimers in solution (Andrews, Downing et al. 2008; Andrews, Chen et al. 2010). Here we investigated the content of histones in association with the two yeast Nap protein, Nap1 and Vps75, and compare this to the interaction of histones with Asf1.

3.2 Results

3.2.1 Gel filtration analysis of Nap1 with core histones

Histones are highly basic proteins, with nearly a quarter of residues being arginine or lysine. In contrast, histone chaperones are renowned for their acidic nature. Therefore, it seems likely that the interaction between histones and their chaperones is mediated, at least in part, by ionic interactions. To investigate this further, refolded H3-H4 or H2A-H2B were incubated with Nap1 at increasing sodium chloride concentrations. The complexes were allowed to equilibrate and fractionated by size using gel filtration chromatography (figure 3.1). At 0.2 M and 0.4 M sodium chloride both H3-H4 and H2A-H2B coelute with Nap1 as a higher molecular weight complex (figure 3.1A and B, top two panels). Increasing the ionic strength to 0.6 M, Nap1-H3-H4 eluted as a complex, but in later fractions, whereas Nap1-H2A-H2B only partially coelute, with a large proportion of H2A-H2B eluting in a separate fraction. At 1 M sodium chloride Nap1, H3-H4 and H2A-H2B all elute in their separate fractions.

From these experiments we can conclude three properties of Nap1-histone interactions. Firstly, Nap1-histone complexes exist in higher order structures whose oligomeric state is determined by ionic strength. Secondly, Nap1-H3-H4 is a more stable complex, with regards to ionic strength, than Nap1-H2A-H2B. Thirdly, both H3-H4 and H2A-H2B dissociate from Nap1 at high ionic strengths. Thus, it appears that ionic strength affects both the oligomeric state of Nap1, but also its histone binding ability. To deconvolute these two aspects of Nap1 binding it is first necessary to review what is currently known about the self associative behavior of Nap1.

The self associative nature of Nap1, both alone and in complex with the four core histones, has been extensively studied by other laboratories. An extensive study using analytical ultracentrifugation (Toth, Mazurkiewicz et al. 2005) has shown that there is an equilibrium between dimer, octamer and hexadecamer states of Nap1 at 100 mM potassium chloride. A complex equilibrium state is also shown for Nap1 in

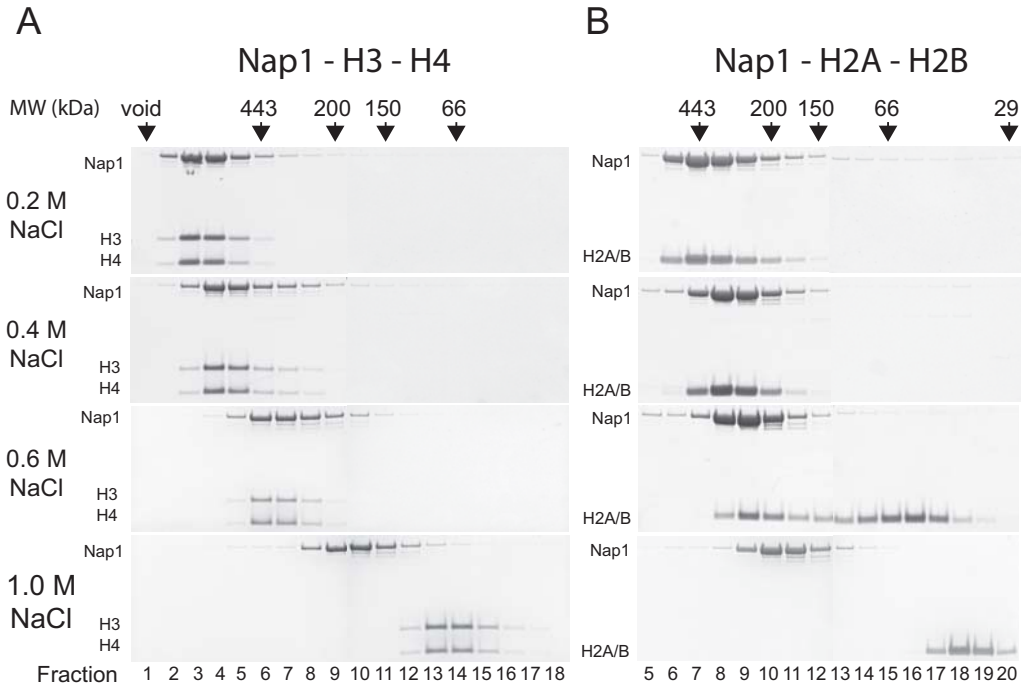

Figure 3.1. The effect of ionic strength on Nap1's interaction with histones H3 and H4. (A) The association of Nap1 and H3-H4 under varying sodium chloride concentrations monitored by gel filtration chromatography. Concentrations are stated to the right. At low ionic strength Nap1 and H3-H4 elute together as a high order complex (fractions 2-4). Increasing the ionic strength first affects the self associative nature of the complex (0.4 M NaCl fractions 3-5, 0.6 M NaCl fractions 6-8), until at 1 M sodium chloride where the proteins elute in there separate fractions (Bottom panel, Nap1 fractions 9-11, H3H4 fractions 13-15). (B) Association of Nap1 with H2A-H2B under varying ionic strength conditions. Nap1's association with H2A-H2B displays a similar trend, except the complex elutes later (0.2 M NaCl fractions 6-8, 0.4 M NaCl fractions 7-9) compared to H3H4. The Nap1-N2A-H2B complex is also more sensitive to ionic strength, partially dissociating at 0.6 M sodium chloride, whereas at the same salt concentration Nap1-H3-H4 was stable.

complex with histones, however, detailed analysis of these states was skewed by incorrect binding stoichiometries determined for H3-H4 and H2A-H2B. Nonetheless, assemblies with a molecular weight in excess of 0.5 MDa were observed for both Nap1-H3-H4 and Nap1-H2A-H2B, in agreement with the elution volumes observed in this study.

Insight into the self associative behaviour of Nap1 has come from its crystallisation. The original structure of Nap1 was derived from crystals grown in a proton rich buffer (Park and Luger 2006). Under these conditions crystal contacts did not give an insight into the oligomeric nature of Nap1. Subsequent crystallographic analysis employing more physiological conditions yielded an alternative mode of

crystal packing implicating a beta-hairpin protruding from the earmuff domain as important in the self association of Nap1 (Park, McBryant et al. 2008). Indeed, mutation of key residues within this region to proline inhibited Nap1 oligomers forming (Park, McBryant et al. 2008). Thus, it would appear that Nap1 oligomerisation is governed by the formation of a secondary structural element. Low pH and high salt concentrations appear to prevent oligomerisation thereby favouring a dimer of Nap1, the lowest of its oligomeric states in solution. These documented properties of Nap1 correlate well with what we observe during gel filtration. Indeed, at 0.6 M sodium chloride Nap1 and H3-H4 still elute as a complex, but the complex elutes considerably later than at 0.2 M sodium chloride (figure 3.1A, fractions 3-5 at 0.2 M compared to fractions 9-11 at 0.6 M). The complex at 0.6 M sodium chloride therefore is likely a Nap1 dimer associated with either two H3-H4 dimers or one $(H3\text{-}H4)_2$-tetramer.

An additional observation concerning the associative behaviour of Nap1-histone complexes from these gel filtration analyses is the discrepancy between the elution profiles of Nap1-H3-H4 and Nap1-H2A-H2B at the lower salt concentrations. At 0.2 M sodium chloride Nap1-H3-H4 can be seen to elute close to the void in fractions 3-5 (figure 3.1A). By comparison, Nap1-H2A-H2B elute later, in fractions 6-8 (figure 3.1B). The stoichiometry of Nap1 binding to H3-H4 and H2A-H2B is the same (Andrews, Downing et al. 2008; Andrews, Chen et al. 2010), and the molecular weight of each histone fold dimer is comparable. Thus, the discrepancy observed may be due to histones differentially affecting the oligomeric nature of Nap1. Further experimentation would be required to see if this is the case. Interestingly, the self association of Nap1 via a beta-hairpin draws parallels with the interaction between H3-H4 and H2A-H2B in the nucleosome where a short beta strand from H4 forms an anti parallel sheet with a short beta strand from H2A, an interaction that has been previously implicated in histone chaperone binding (English, Adkins et al. 2006; Natsume, Eitoku et al. 2007).

Another interesting observation from these experiments is the differing sensitivity of the Nap1-H2A-H2B and Nap1-H3-H4 interaction to ionic strength. This binding event is likely independent of the oligomerisation of Nap1 as it has been shown that mutations within the beta-hairpin motif that mediates self association do not affect binding of Nap1 to histones (Park, McBryant et al. 2008). At 0.6 M sodium chloride all H3-H4 remains associated with Nap1 (figure 3.1A, fractions 6-8). In

contrast, at 0.6 M sodium chloride the Nap1-H2A-H2B complex appears to be at equilibrium with free Nap1 and free H2A-H2B dimmer (figure 3.1B). This is shown by two populations of H2A-H2B: one population eluting with Nap1 (figure 3.1B, fractions 8-10) and another eluting on its own (fractions 15-17). The unbound population elutes a few fractions earlier compared to free H2A-H2B (compared with fractions 17-20 of 1 M NaCl, where Nap1 and H2A-H2B do not interact, figure 3.1B). Interaction with Nap1 during the course of the chromatography would account for this, and suggests a more dynamic interaction between Nap1 and H2A-H2B at this salt concentration.

The difference in the sensitivities of the interaction of H2A-H2B versus H3-H4 with Nap1 is interesting as it mirrors the salt sensitivity of histones within the nucleosome. Early biochemical analysis of the nucleosome structure revealed histone H3 and H4 are more resistant to salt extraction than H2A-H2B (Jorcano and Ruiz-Carrillo 1979). Dissociation of H2A-H2B dimers from the nucleosome occurs at ~0.6 M sodium chloride and at ~ 0.3 M from DNA, whereas H3 and H4 remain associated with DNA until ~1.4 M sodium chloride. The increased stability of the H3 and H4 for DNA is primarily due to its tetramerisation. Tetramerisation effectively doubles the surface contact with DNA, and thus a higher concentration of salt is required to disrupt the increased number of ionic interactions. One could make the tentative suggestion that the increased stability of H3-H4 over H2A-H2B provides the possibility that H3 and H4 are in their tetrameric state when bound to Nap1.

The third, and final, observation made from these experiments is the complete dissociation of the Nap1-H3-H4 and Nap1-H2A-H2B complexes at high sodium chloride concentrations. At 1 M sodium chloride H3-H4, H2A-H2B and Nap1 elute in their separate fractions (figure 3.1, Nap1 – fractions 9-11, H3-H4 – fractions 13-15, H2A-H2-B – fractions 17-20). The ability to completely dissociate histones from Nap1 with a high salt concentration suggests that the mode of interaction between histones and Nap1 is mediated largely by electrostatic interactions, similar to interactions made between the DNA and histones within the nucleosome.

3.2.2 Gel filtration analysis of Vps75 and Asf1 with H3 and H4.

The association of H3 and H4 with histone chaperones Vps75 and Asf1 was also investigated. Vps75 is a Nap1-like chaperone that has been shown to bind preferentially to H3-H4 (Selth and Svejstrup 2007; Tsubota, Berndsen et al. 2007).

Asf1 is also an H3-H4 chaperone whose co-crystal structure with H3 and H4 has been determined (English, Adkins et al. 2006; Natsume, Eitoku et al. 2007). As with Nap1, association was monitored over a range of sodium chloride concentrations using gel filtration chromatography to analyse the hydrodynamic radius of the complexes formed (figure 3.2A and B).

The association of Vps75 with H3-H4 under varying salt concentrations follows a similar trend to Nap1 in that dissociation of the complex occurs at increasing sodium chloride concentrations. The complex at 0.2 M sodium chloride was unstable, precipitating out of solution. At 0.4 M sodium chloride the complex was soluble and eluted with an apparent molecular weight between 443 and 200 kDa (figure 3.2A, fractions 7-9). Increasing the sodium chloride concentration to 0.6 M caused the complex to dissociate, shown by Vps75 and H3-H4 eluting in their separate fractions (figure 3.2A, fractions 13-15 for both proteins). Thus, the basic property of Nap1 and Vps75's interaction with histones H3 and H4 is similar, however, the Vps75-H3-H4 complex is more sensitive to ionic strength than Nap1-H3-H4.

Although Vps75 is a Nap1-like protein there is little known about its tendency to self associate, if indeed it does. To address the composition of the complex formed between Vps75-H3-H4 at 0.4 M sodium chloride amine reactive protein crosslinking was employed. Crosslinking of the complex at 0.4 M sodium chloride with increasing concentrations of BS2G resulted in three major species when analysed by SDS-PAGE (figure 3.2C and D, numbered as 1, 2 and 3). Species 1 migrates close to the molecular weight of a 2(Vps75):2(H3H4) complex (115 kDa) when compared to molecular weight markers (figure 3.2C). To better resolve species 2 and 3 a lower percentage of acrylamide and an alternative buffer system was used for SDS-PAGE. Species 2 represents the major crosslinked species judged by the intensity of staining, and migrated with an apparent molecular weight of ~260 kDa. This is close to the theoretical mass of a 2(2(Vps75):2(H3H4)) complex of 230 kDa. Species 3 migrates further up the gel still, and most likely represents a 3(2(Vps75):2(H3H4)) complex. Therefore, it appears that similar to Nap1, Vps75 also has the ability to self associate to form higher order oligomeric states. However, Vps75 does not contain a beta-hairpin motif analogous to that of Nap1, suggesting an alternative mechanism of oligomerisation.

Asf1 adopts a different fold to Nap1 and Vps75 and exists as a monomer rather than a dimer. Its interaction with H3-H4 has been extensively studied by other laboratories, and a co crystal structure with H3 and H4 has been solved (English, Maluf et al. 2005; English, Adkins et al. 2006; Natsume, Eitoku et al. 2007). From

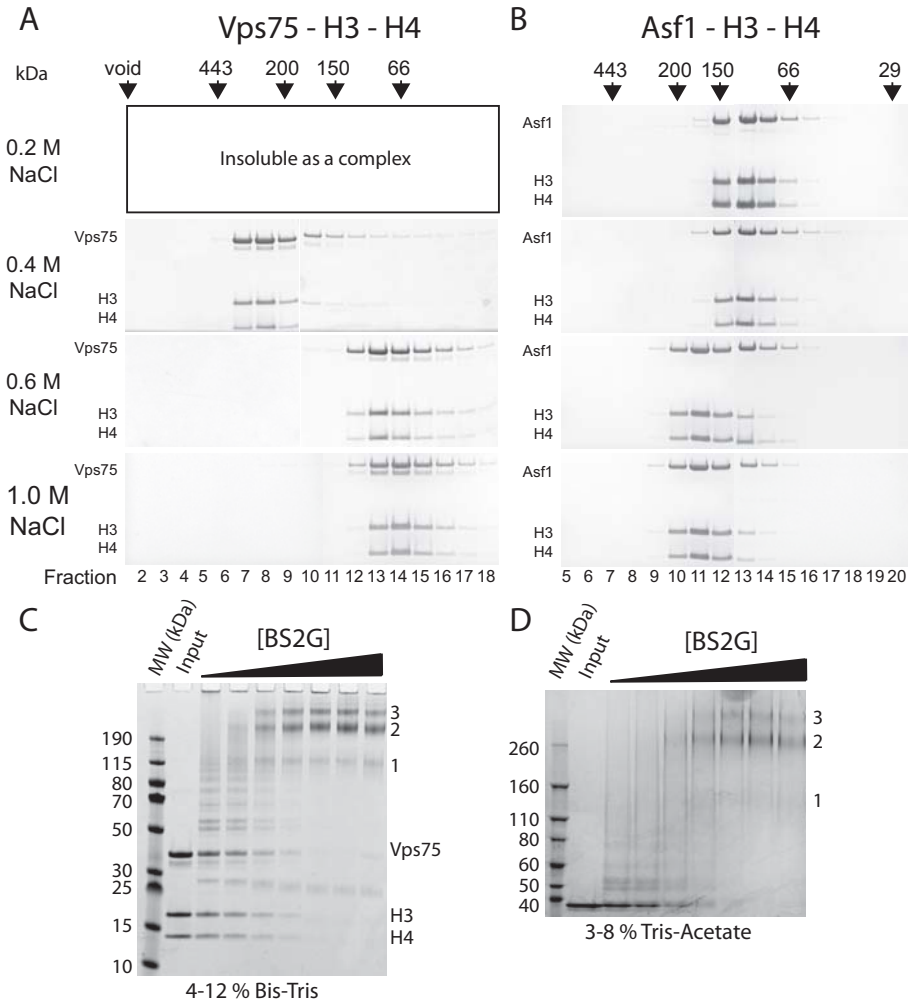

Figure 3.2. The effect of ionic strength on the association of H3-H4 with Vps75 and Asf1. (A) Vps75 shows a similar trend to Nap1 in binding H3-H4 with respects to sensitivity to ionic strength. At 0.2 M sodium chloride the complex was not stable and precipitated out of solution. At 0.4 M sodium chloride Vps75 and H3-H4 elute as a higher molecular weight species (fractions 7-9). However, at 0.6 M and 1.0 M sodium chloride Vps75 and H3-H4 elute in their separate fractions (fractions 13-15 for both proteins). (B) Contrary to Nap1 and Vps75, the apparent molecular weight of the Asf1 and H3-H4 complex increases with ionic strength. At 0.2 and 0.4 M sodium chloride Asf1 and H3-H4 elute in fractions 12-14 (note an Asf1-H3H4 dimer has a similar molecular weight to an H3-H4 tetramer). At 0.6 and 1.0 M sodium chloride Asf1 and H3-H4 elute at an apparently higher molecular weight corresponding to fractions 10-12. (C) The complex formed between H3-H4 and Vps75 at 0.4 M sodium chloride was probed by protein crosslinking using the amine reactive crosslinker BS2G. Titration of crosslinker against a constant concentration of complex shows three major crosslinked products, labelled 1-3, when resolved on an SDS, Bis-Tris buffered, 4-12% polyacrylamide gel. (D) To better resolve the crosslinked products 1-3 the same titration points were run on an SDS, Tris-acetate, 3-8 % polyacrylamide gel.

this structure, one can see the interaction between Asf1 and an H3-H4 dimer is predominantly mediated by hydrophobic interactions with the C-terminus of H3, with the basic surface of the H3-H4 dimer being solvent exposed. It has been hypothesised, guided by homology modelling utilising the beta-sheet face in the earmuff domain of *Plasmodium* NapL, that Nap1-like proteins interact with H3-H4 in a similar manner to

Asf1 (Gill, Yogavel et al. 2009). To test this hypothesis Asf1 in complex with H3 and H4 was subjected to gel filtration chromatography under identical conditions to that of Nap1 and Vps75.

If the interaction between Nap1/Vps75 and H3-H4 was mediated in a similar way to that of Asf1 one would imagine that the properties of the interaction, with respects to ionic strength, would also be similar. At 0.2 M sodium chloride Asf1 and H3-H4 co elute as a slightly super shifted peak (figure 3.2B, fractions 12-14) compared to that of the H3-H4 and Asf1 alone (fractions 13-15, H3-H4; fractions 14-15, Asf1 – data not shown). Asf1 has a similar molecular weight to a H3-H4 dimer, thus the Asf1-H3-H4 heterotrimer elutes close to the $(H3\text{-}H4)_2$-tetramer. Interestingly, as the ionic strength of the buffer is increased to 0.6 and 1 M sodium chloride the Asf1-H3-H4 complex does not dissociate, but elutes with a higher apparent molecular weight (figure 3.2B, fractions 10-12). This decrease in elution volume may be due to stabilisation of the interface between Asf1 and H3-H4, the appearance of secondary or tertiary structure induced at higher ionic strengths, or partial aggregation occurring between Asf1-H3-H4 complexes. Whatever the case may be, it is evident that the interaction between Asf1 and H3-H4 has different properties to that of Nap1 and Vps75. These properties most likely relate to the hydrophobic nature of the Asf1-H3-H4 interaction, yielding resistance to high salt concentrations. This is in stark contrast to the interaction between both Nap1 and Vps75 with H3-H4, which displays sensitivity to ionic strength.

Assuming the interaction between Nap1/Vps75 and histones is predominantly ionic in nature, the most likely surfaces involved would be the basic ramp of H3-H4 and the acidic cavity of Nap1/Vps75. An interaction that is mediated by the basic surface of the H3-H4 complex would also allow for the binding of H3 and H4 in their tetrameric form, analogous to their conformation within the nucleosome. Thus, it is proposed that the differing dependencies on ionic strength between Asf1 and the two Nap proteins reports on fundamental differences in the way in which these alternate classes of chaperone interact with their histone cargo.

3.2.3 A directed crosslinking reporter assay for probing tetramerisation of H3-H4

To investigate the conformation of H3 and H4 when in complex with Nap1 and Vps75 a site directed crosslinking assay was developed. The structure of the (H3-

H4)$_2$-tetramer was surveyed for residues which come into close proximity to the same residue in their partner histone fold dimer. The two lysines at position 115 on H3 were idenfied as being within 9 Å of each other based on their coordinates within the nucleosome crystal structure (Davey, Sargent et al. 2002) (figure 3.3A). A cysteine residue engineered at this position was found to efficiently crosslink in the presence of 1,3-Propanediyl bismethanethiosulfonate (M3M), a homobifunctional thiol reactive crosslinker (the chemical structure of M3M is shown in figure 3.3A). Crosslinking was analysed by SDS-PAGE and visualised by coomassie staining (figure 3.3B). H3 crosslinked at K115C (H3-H3') is twice the molecular weight of non-crosslinked H3, and thus is easily separable by SDS-PAGE. A time course was carried out to investigate the kinetics of crosslinking by M3M towards an H3 K115C tetramer. Figure 3.2B shows the reaction occurs within seconds of adding the crosslinking reagent. Quantifying the intensity of the coomassie stained bands, the ratio of H3 to H3-H3' can be determined, which acts as a measure of crosslinking efficiency. Plotting the ratio of crosslinking efficiency versus time we see that the reaction is virtually complete after 60 seconds, resulting in ~56% of H3 crosslinked (data not shown).

An important control in the development of this assay was to show that the H3-H3' species is derived from intra-tetramer and not inter-tetramer crosslinking. To address this problem the crosslinked tetramer was subjected to gel filtration chromatography. Gel filtration chromatography separates protein complexes by their hydrodynamic radius. The hydrodynamic radius of an intra-tetrameric crosslink at position H3 K115C would be identical to that of non-crosslinked tetramer, and thus both complexes should elute in the same fractions. Indeed, this is exactly what we see. H3-H3' crosslinked at position K115C elutes in the exact same fractions (13-15) as the native tetramer (compare figure 3.3C middle panel: H3 K115C, with the top panel: native tetramer). This assumes that the elution of H3 and H4 derived from an inter-tetrameric crosslink would elute anomalously. To prove this is the case, inter-tetrameric crosslinks were forced by moving the cysteine residue to a position that is out of reach of the crosslinker arm length. H4 R45 residues are greater than 30 Å apart in the nucleosome crystal structure, and have been shown to retain their distance when in solution (Bowman, Ward et al. 2010). Crosslinking at this position yielded an H4-H4' species when analysed by SDS-PAGE, which considering the constraints of the histone tetramer, must be derived from inter-tetrameric crosslinking. Upon gel

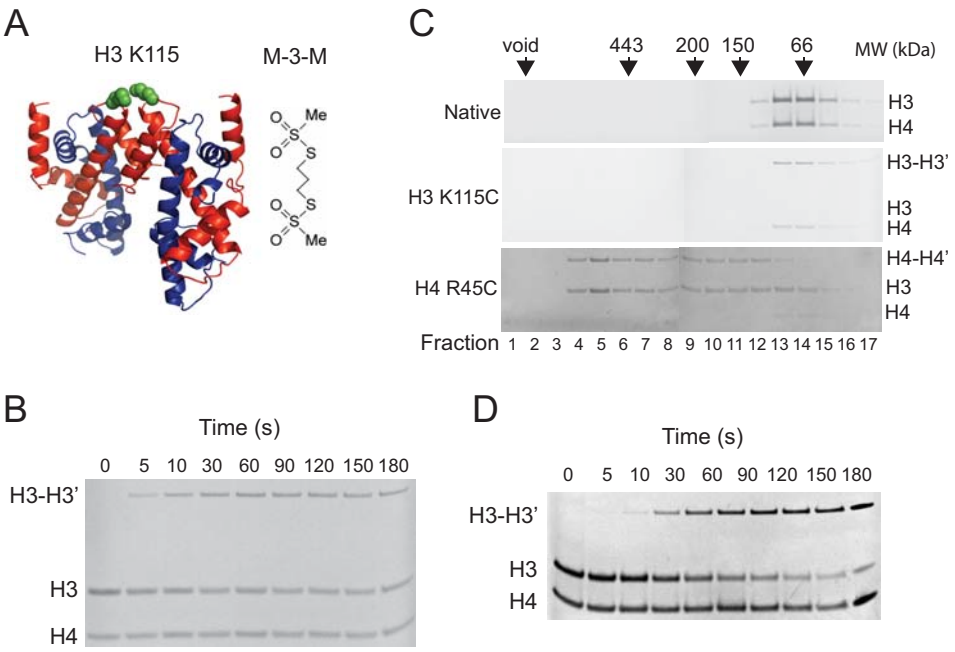

Figure 3.3. Developing a directed crosslinking reporter assay for probing tetramerisation of H3 and H4. (A) Position of H3 K115 on the histone tetramer (green spheres) in its nucleosomal conformation (Taken from PDB 1KX5). Chemical structure of the crosslinker M-3-M. (B) Kinetic analysis of crosslinking at H3 K115C analysed by separation of H3 and H3-H3' by SDS-PAGE. At 1 uM H3-H4 tetramer crosslinking occurs in a matter of seconds and the reactions is all but complete after one minute. (C) Tetramer crosslinked at H3 K115C, but not H4 R45C, elutes as a tetramer. To demonstrate that crosslinking at H3 K115C was occurring specifically across the dyad axis, and not inter-tetramerly, M-3-M crosslinked tetramer was sized on an S200 gel filtration column. Comparing H3 K115C crosslinked (middle panel) with non-crosslinked tetramer (lower panel), one can see they elute in the same volume (fractions 13-15). Crosslinking of the tetramer at a site known to be out of reach of the crosslinker (H4 R45C) results in higher order molecular weight species (top panel) consisting of multiple H3H4 tetramers, demonstating that crosslinking can occur at other sites on the tetramer, but at these sites crosslinking is not tetramer specific. (D) Maleimide crosslinkers are also efficient at crosslinking H3 K115C. Kinetic analysis of the bis maleimide crosslinker BMOE.

filtration chromatography the elution of the crosslinked H4 R45C tetramer was shifted to earlier eluting fractions: fractions 4-13 compared to fractions 13-15 for the native tetramer. Taken together these data show that crosslinking at position K115C on histone H3 results in a tetramer specific covalent linkage. The crosslink therefore acts as a probe of the tetrameric conformation of H3-H4 and can be used as such to probe this conformation when H3 and H4 are in complex with other proteins.

Thus far, crosslinking was generated using the chemistry of a methanothiosulfonate group (figure 3.3A). This results in a disulphide linkage with the thiol of the cysteine, a bond that is cleavable by reducing agents such as DTT. In certain occasions it may be desirable to form a crosslinked product which is non-reducible, for instance when one needs to distinguish between an unwanted disulphide crosslink and an introduced chemical crosslink. An alternate class of thiol reactive crosslinker are the maleimides, whose thioether linkage is resistance to reducing agents. The efficiency of the compound bis-maleimidoethane (BMOE) was tested in

the same kinetic assay used for M3M. Quenching of the crosslinking reaction, this time using DTT, was performed over a series of time points and the crosslinking efficiency analysed by SDS-PAGE. Figure 3.3D shows that BMOE crosslinks H3 K115C with a comparable efficiency to M3M, but the time required for crosslinking is slightly increased to a matter of minutes rather than seconds.

3.2.4 Probing the conformation of H3-H4 when in complex with Nap1, Vps75 and Asf1

The site directed protein crosslinking approach detailed above was employed to probe the tetramerisation status of H3 and H4 when bound to the chaperones Vps75, Nap1 and Asf1. Intensive investigation into the interaction of Asf1 with histone H3 and H4 has shown that Asf1 disrupts the $(H3\text{-}H4)_2$-tetramer, binding a single H3-H4 dimer (English, Maluf et al. 2005; English, Adkins et al. 2006; Natsume, Eitoku et al. 2007). Thus, the Asf1-H3-H4 complex provides a valuable control for the splitting of the $(H3\text{-}H4)_2$-tetramer. Accordingly, when Asf1 was titrated against H3 K115C tetramer the crosslinked H3-H3' band disappeared and the H3 band increased in intensity (figure 3.4A, left panel), further validating this simple approach as a powerful probe of H3-H4 conformation.

The same experiment was carried out using Nap1 and Vps75 in place of Asf1. In contrast with Asf1, the H3-H3' species prevailed in the presence of both Nap1 (figure 3.4A, middle panel) and Vps75 (figure 3.4A, right panel). This suggests that Nap1 and Vps75, unlike Asf1, do not have the ability to disrupt the $(H3\text{-}H4)_2$-tetramer, supporting the hypothesis derived from the gel filtration analysis that H3 and H4 reside in their tetrameric conformation when in complex with the Nap proteins from yeast. The buffer conditions chosen for the crosslinking assays were conditions under which Nap1 and Vps75 were known to interact with H3-H4 (figure 3.1A and 3.2A). However, to be certain that H3-H4 are in complex with the chaperones under the experimental conditions used the final titration points from the two crosslinking experiments were subjected to gel filtration chromatography. Crosslinked (H3-H3') and uncrosslinked (H3) tetramer eluted in complex with the chaperones for both Nap1 (figure 3.4B) and Vps75 (data not shown), showing that an H3 K115C crosslinked tetramer can stably associate with Nap1 and Vps75.

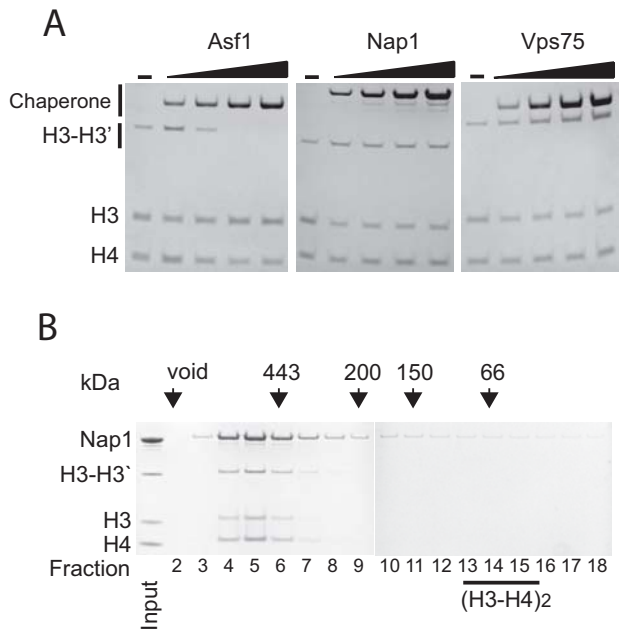

Figure 3.4. Probing tetramerisation of H3 and H4 when bound to chaperones Nap1, Vps75 and Asf1 probed by site directed crosslinking. (A) Nap1, Vps75 and Asf1 were titrated against histone tetramer containing the mutation H3 K115C. After allowing to the complex to equilibrate, crosslinking was carried out using the crosslinker M-3-M, and components separated by SDS-PAGE. The disappearance of the H3-H3' band upon increasing concentrations of Asf1 indicates that Asf1 is disrupting the dyad interface of the H3-H4 tetramer (left panel). The persistence of the H3-H3' band upon increasing concentrations of Nap1 (centre panel) and Vps75 (right panel) suggests that H3 and H4 retain their tetrameric conformation when bound to these chaperones. (B) H3-H4 remain associated with Nap1 under the conditions used for crosslinking. The last titration point of the crosslinking reaction was subject to gel filtration chromatography. Coelution of chaperone and histone was observed indicating the crosslinked tetramer is in complex with the chaperone. Elution volume of H3-H4 tetramer is indicated for comparison (fractions 13-15).

3.2.5 Long range distance extraction from labelled histones in complex with Nap1, Vps75 and Asf1

In the following section all pulsed EPR experiments and data processing were carried out by Dr Richard Ward and Dr David Norman, College of Life Sciences, 5 Dow Street, University of Dundee, Dundee, DD3 5EH, United Kingdom.

The findings from site direct crosslinking suggests that H3 and H4 are in their tetrameric conformation when bound to Nap1 and Vps75. However, one could imagine a scenario where H3 and H4 are bound in an alternate conformation in which the crosslinking site (H3 K115C) is still within reach of the crosslinker arm length. In order to discount this possibility long range distances were extracted from the tetramer in complex with Nap1 and Vps75 using the approach of site directed spin labelling (SDSL) in conjunction with pulsed electron paramagnetic resonance (EPR).

SDSL combined with pulsed EPR is a powerful tool which allows extraction of macromolecular scale distances from labels placed at strategic locations within the

macromolecule of interest. SDSL in proteins is carried out by using the unique reactivity of the thiol side chain of cysteine. By exploiting the lack of cysteine residues within H3 and H4, unique labelling sites can be strategically placed on the tetramer. This allows for a detailed analysis of the conformation of H3 and H4 when in complex with chaperones. To this end, two labelling sites, one on H3 and one on H4, were chosen based on the quality of their EPR signals (Bowman, Ward et al. 2010). The position of H4 R45 and Q125 on the $(H3\text{-}H4)_2$-tetramer taken from the nucleosome are shown in figure 3.5A.

One can imagine three possibilities for the conformation of H3 and H4 when bound to Vps75 or Nap1. Firstly, the chaperones may split the tetramer binding to a single H3-H4 dimer. This mode of binding seems unlikely due to the stoichiometry of binding (Park, Sudhoff et al. 2008; Andrews, Chen et al. 2010) and in light of the results from site directed crosslinking (section 3.2.4). Secondly, the chaperones could bind two H3-H4 dimers, but in an alternative conformation to that seen in the nucleosome. If this were the case an altered distance distribution should result compared to that of the free tetramer. Thirdly, the chaperones could bind H3-H4 in the tetrameric conformation, analogous to that seen in the nucleosome. If this were the case, one would expect the distance distributions extracted from the complex to be comparable to the distances extracted from free tetramer.

To control for tetramer splitting pulsed EPR was carried out on labelled histones in complex with Asf1. Figure 3.5B shows the background corrected spectra (dipolar evolution) and distance distributions for Asf1 in complex with H3 and H4 labelled on H4 R45 (left – H4 R45R1) and H3 Q125 (right – H3 Q125R1). The dipolar evolution and the distance distribution for both labelling sites from free tetramer are plotted on the same axis for comparison (black traces). Splitting of the tetramer by Asf1 has a dramatic effect on the dipolar evolution: dipolar coupling is completely ablated leaving only the exponential background decay, which gives a meaningless distance distribution (figure 3.5B, top). This is seen for both H4 R45R1 and H3 Q125R1.

The conformation of the tetramer was then probed in complex with Nap1 and Vps75. The background corrected data for site H4 R45R1 appears very similar for both free tetramer (black trace) and in complex with Nap1 and Vps75 (red traces) (figure 3.5B). The initial drop and frequency of oscillations are comparable to that of the tetramer, and indeed result in a very similar distance distribution after Tikhonov

regularisation. The spectra are not as discrete as the free tetramer, resulting in a number of minor peaks in the distance distribution. However, it is clear the major population of H3 and H4 are residing a tetrameric conformation. The background corrected data for the site H3 Q125R1 follows a similar trend in that the initial drop is very similar to what we see in the free tetramer, suggesting a major distribution centred around a similar distance. Indeed, that is what we see in the Tikhonov regularised distributions, however, the dampening of the oscillations compared to what we see in the free tetramer results in a much broader distribution, containing multiple subsidiary peaks. This is more evident in data from Vps75. The reason for this is most likely due to the self associative nature of Vps75 and Nap1 as described in section 3.2.1. Indeed, the number of spins interacting in the H3 Q125R1 is slightly increased in the Nap1 and Vps75 samples, evidenced by the increased depth of the dipolar evolution. Why this effect is not as pronounce at position H4 R45R1 is not known. It could be that labels in the multimeric structure of 2(Nap1/Vps75):2(H3H4) are positioned so that they are less prone to inter-tetramer interactions for position H4 R45R1. The increased strength of the dipolar coupling between H4 R45R1 residues compared to H3 Q125R1 may also have an effect. Nonetheless, it is apparent from both labelling sites that the major distance distribution is in very close agreement with that obtained from the free tetramer. Nap1 and Vps75 therefore, unlike Asf1, bind to H3 and H4 in their tetrameric conformation, a conformation that is analogous to that seen in the nucleosome.

3.2.6 Nap1 and Vps75 can utilise H3 and H4 trapped in their tetrameric conformation

The ability of Nap1 and Vps75 to bind H3 and H4 in their tetrameric conformation may be linked to their cellular function. Thus, it would be desirable to see if Nap1 and Vps75 can utilise H3 and H4, trapped as a tetramer, for their biological activity assayed *in vitro*. Crosslinking across the dyad interface of the tetramer provides an opportunity to do this. It is likely that the crosslink at H3 K115C stabilises the tetramer so that it is unable to go through a dimeric intermediate. To test the stability that the crosslink confers to the tetramer, Asf1 binding to H3 K115C crosslinked tetramer was analysed using gel filtration chromatography.

The affinity of Asf1 for H3 and H4 is in the low nanomolar range (Park, Sudhoff et al. 2008), whereas the affinity of H3-H4 dimers for each other is in the

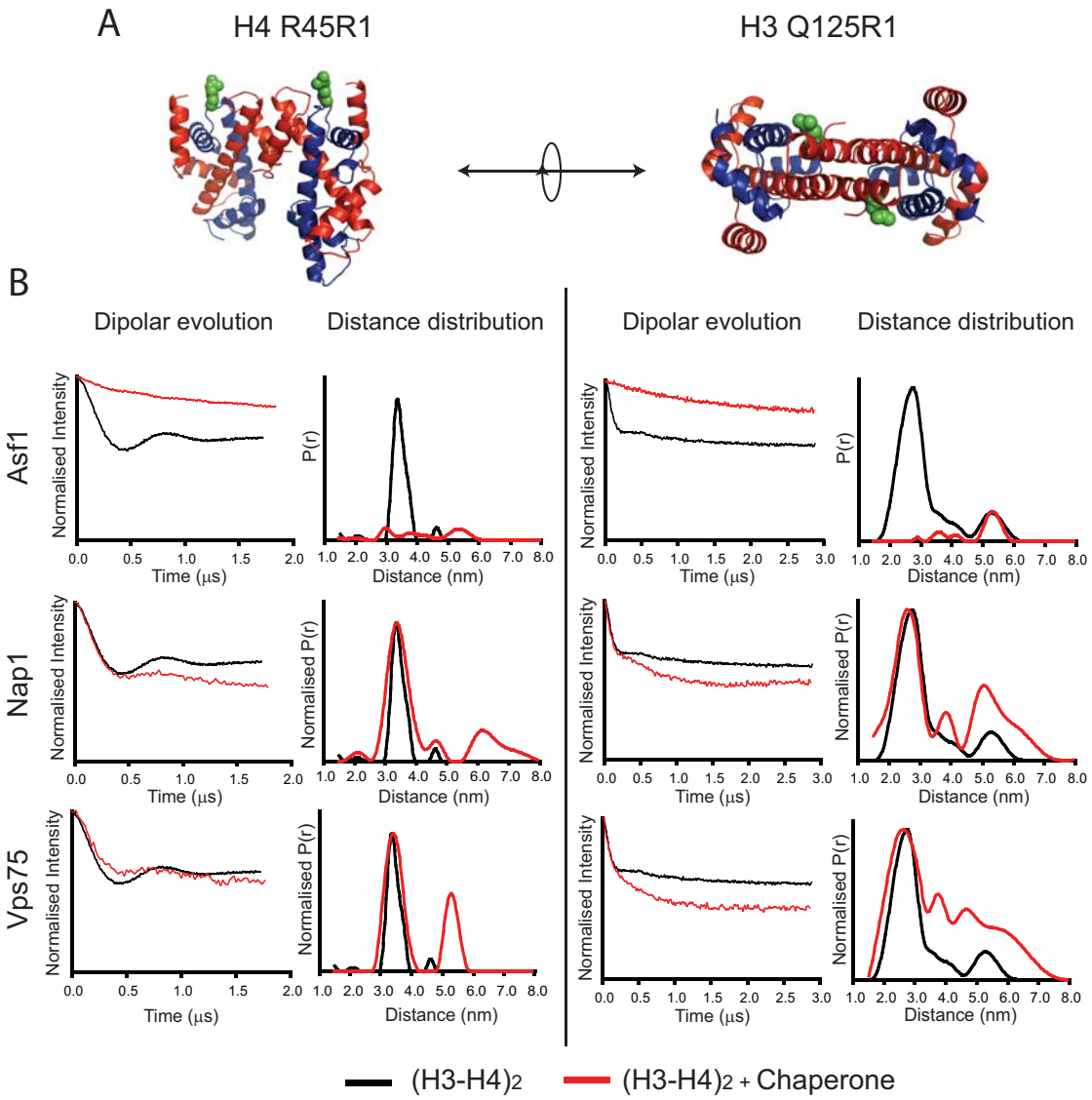

Figure 3.5. Long range distance extraction using pulsed EPR technology shows H3H4 are in their tetrameric state when in complex with Nap1 and Vps75, but not Asf1. (A) Positions of H4 R45 and H3 Q125 (green spheres) on the histone tetramer (coordinates taken from PDB 1KX5) (B) Distance extractions from Nap1/Asf1/Vps75 in complex with spin labelled tetramer (red trace). The left panel shows data from position H4 R45R1, the right panel from position H3 Q125R1. The background corrected spectra (dipolar evolution) along with the Tikhonov regularisation (distance distribution). For comparison the data extracted from the tetramer alone are plotted on the same axis (black trace).

micromolar range (Baxevanis, Godfrey et al. 1991). It was therefore reasoned that if a crosslink at position H3 K115C could inhibit the binding of Asf1 it must confer low or very low nanomolar affinity upon for the tetrameric state of H3 and H4. As Asf1, $(H3\text{-}H4)_2$-tetramer and Asf1-H3-H4 all elute in similar fractions a truncated form of Asf1, missing its acidic C-terminus, was used to ease analysis. This globular form of Asf1 (Asf1g) contains all of the histone binding contacts, and is therefore thought to retain the same affinity for histone H3 and H4. Asf1g, as expected, elutes later than full length Asf1, eluting in fractions 19-21 (figure 3.6A, top panel). When mixed with a stoichiometric amount of H3-H4 dimer a heterotrimeric Asf1-H3-H4 complex

forms, with all proteins coeluting in fractions 14-16 (figure 3.6A, middle panel). However, when mixed with H3-H4 that has been crosslinked across the dyad interface at H3 K115C, the majority of Asf1g now elutes as a monomer (fractions 19-21) with crosslinked H3-H4 tetramer eluting in the tetrameric fractions (13-15). Two other minor populations also exist: an Asf1-H3-H4 heterotrimer comprised of residual non-crosslinked H3 (fractions 14-16), and Asf1-$(H3\text{-}H4)_2$ heteropentamer (or a heterohexamer, depending on whether one or two Asf1 are bound) (fractions 12-13). To ease in the interpretation of the three Asf1 containing species the intensity of the Asf1 band in each fraction was quantified and plotted as shown in figure 3.6B. Although only semi-quantitative, it can be seen that the vast majority of Asf1 elutes as monomer or in complex with residual non-crosslinked H3-H4, with only a small proportion eluting with crosslinked H3. This demonstrates that the crosslink at position H3 K115C in the histone tetramer not only acts as a sensitive probe of tetramerisation, but also must confer a low nanomolar affinity to the dimer-dimer interaction, effectively stabilising the tetramer.

Nap1 has been shown to be an efficient regulator of nucleosome assembly *in vitro* (Ishimi and Kikuchi 1991; Fujii-Nakata, Ishimi et al. 1992) stimulating correct nucleosome formation by regulating the sequential deposition of H3-H4 and H2A-H2B (Andrews, Chen et al. 2010). Assembly of nucleosomes is modular with H3 and H4 being deposited first, providing a high affinity platform for H2A-H2B dimers to bind. To isolate this first stage in nucleosome assembly a 91 bp fragment of DNA, a length which allows deposition of only a single tetramer, was used as a template for deposition. The so called ‘tetrasome’ which results from the association of an $(H3\text{-}H4)_2$-tetramer with DNA can be easily assigned as a single supershifted band after native PAGE.

Tetramer crosslinked at H3 K115C was used as a substrate for Nap1 mediated tetrasome formation. Without Nap1 tetrasome formation was inefficient (figure 3.6C, lane1). Tetrasome formation was increased by the addition of increasing amounts of Nap1, reported by the increased amount of DNA shifted to the slower migrating band when stained with ethidium bromide (figure 3.6C, lanes 2-5), suggesting that Nap1 can indeed use H3 and H4 trapped in their tetrameric conformation as a substrate. However, as the efficiency of tetrasome formation never reached one hundred percent there is a possibility that the population deposited by Nap1 is derived from the residual non-crosslinked pool of histones. To address this possibility, the tetrasome

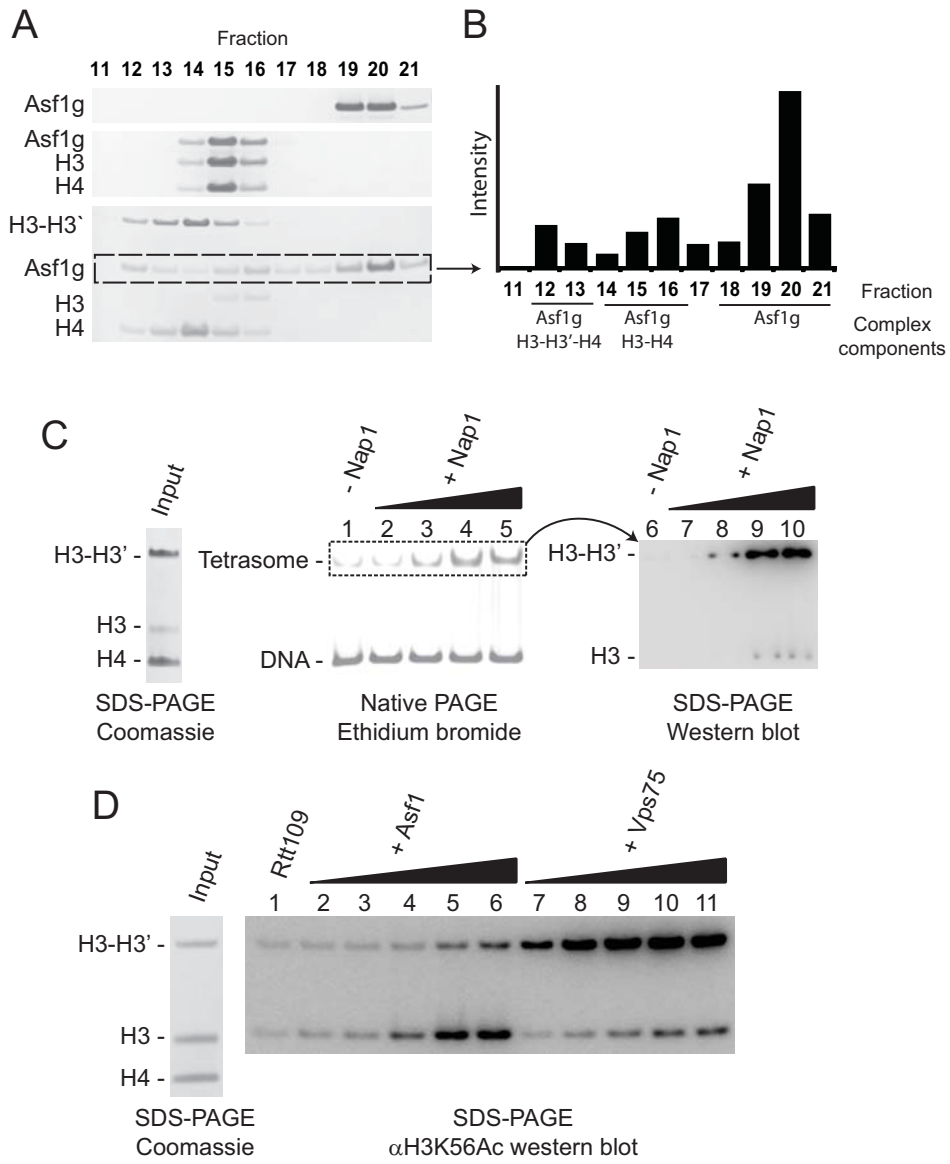

Figure 3.6. Nap1 and Vps75 can use H3H4 trapped in their tetrameric conformation as a substrate for the biological activities *in vitro*. (A) The crosslink at H3 K115 efficiently stabilises the H3H4 tetramer. The low nanomolar binding of Asf1g to H3-H4 is severely impaired by the presence of the chemical crosslink at H3 K115C. Top panel: elution profile of Asf1g alone. Centre panel: elution of Asf1g in complex with non-crosslinked H3 K115C tetramer. Bottom panel: elution of Asf1g and tetramer crosslinked at H3 K115C. (B) To help visualise the stability imposed on the tetramer by the crosslink at H3 K115C the densiometry of Asf1g bands was quantified in each fraction. The major species spans fractions 18-21, and correlates with free Asf1g (A, top panel). A second species spanning fractions 14-16 relates to residual non-crosslinked tetramer in complex with Asf1g (A, centre panel). A third species spanning frations 12 and 13 coelutes with tetramer crosslinked at H3 K115C (A, bottom panel), representing a small fraction of crosslinked tetramer that can be bound by Asf1. (D) Nap1 can deposit a tetramer crosslinked at H3 K115 onto DNA. Left panel: input. Centre panel: tetrasomes where separated from free DNA by native gel electrophoresis and visualised by ethidium bromide staining. Right panel: the tetrasomal band, excised as shown, was cast within an SDS gel and subject to electrophoresis to separate H3 from H3-H3'. The H3 species were visualised by immunoblotting using an antibody specific to H3. (D) Vps75 directs the HAT activity of Rtt109 towards a tetramer of H3H4, whereas Asf1 stimulates acetylation of an H3H4 dimer. Left panel: equimolar amounts of crosslinked to non-crosslinked H3 K115C tetramer was used as an input. Right panel: lane1, Rtt109 140 nM. Lanes 2-6: 60, 80, 100, 120 and 140 mM each of Rtt109 and Asf1, respectively. Lanes 7-11: 10, 15, 20, 25 and 30 nM of Vps75-Rtt109 complex, respectively.

band was excised from the native PAGE gel, soaked in reducing agent (to remove any non-specific disulphide crosslinking), and cast within an SDS-PAGE gel. The

crosslinked and non-crosslinked H3 were then separated by electrophoresis. The major population found when probed by western blotting for H3 was indeed the crosslinked form (figure 3.6C, lanes 6-10), suggesting that Nap1 can indeed incorporate H3 and H4 into chromatin without the requirement to go through a dimeric intermediate.

Unlike Nap1, Vps75 has not been implicated directly in nucleosome deposition, but has been shown to have an important role in chaperone mediated lysine acetylation on H3 of soluble histones (Han, Zhou et al. 2007; Tsubota, Berndsen et al. 2007; Berndsen, Tsubota et al. 2008; Fillingham, Recht et al. 2008; Tang, Holbert et al. 2008; Tang, Meeth et al. 2008). Indeed, Vps75 is found to co-purify with the acetyl transferase Rtt109 from yeast cells (Krogan, Cagney et al. 2006; Selth and Svejstrup 2007), and acts to increase the efficiency of histone acetylation by this enzyme (Tsubota, Berndsen et al. 2007; Berndsen, Tsubota et al. 2008). Interestingly, Asf1 is also implicated in mediating H3 lysine acetylation by Rtt109 both during replication coupled nucleosome deposition and following repair of DNA damage (Han, Zhou et al. 2007; Tsubota, Berndsen et al. 2007; Chen, Carson et al. 2008; Li, Zhou et al. 2008). An assay was therefore developed to see if Vps75 and Asf1 show a preference for dimeric or tetrameric H3-H4 in chaperone mediated histone acetylation.

Crosslinking of H3 K115C tetramer was monitored over time by SDS-PAGE. The time point at which crosslinked to non-crosslinked tetramer was equal was used as an input for a competition assay (figure 3.6D, input lane). Rtt109 on its own showed very poor acetyl tranferase activity towards H3 (probed by anti-H3 K56Ac), as was expected, and showed no preference for crosslinked over non-crosslinked H3-H4. Addition of Asf1 to the reaction increased the activity of Rtt109, which was directed predominantly towards the non-crosslinked tetramer (figure 3.6D, lanes 2-6), further validating our crosslinking approach as a method for stabilising the histone tetramer. Similarly, addition of Vps75 to the reaction resulted in an increase in activity of Rtt109, but in contrast to Asf1, Vps75 directed acetylation predominantly towards crosslinked tetramer (figure 3.6D, lanes 7-11). At first glance the increase in acetylation directed towards the crosslinked tetramer seems a little strange, as if Vps75 could accommodate a tetramer of H3 and H4 one would expect there to be no preference. However, at the physiological ionic concentration that these acetylation reactions were carried out H3 and H4 exist in a dimer-tetramer equilibrium

(Baxevanis, Godfrey et al. 1991). The crosslink at H3 K115C would serve to drive tetramerisation of H3 and H4 in the crosslinked population, which likely accounts for the preference in acetylation that we observe. It was therefore concluded that the ability of Nap1 and Vps75 to bind a tetramer of H3-H4 is mirrored in their ability to use H3-H4 trapped in their tetrameric conformation as a substrate for their biological activity.

3.2.7 Strategies for singly labelling a dimer

SDSL and pulsed EPR is a powerful tool that, as well as reporting on conformational states, can also be used to 'jigsaw' molecular structures together. It is often the case that high resolution crystal or NMR structures of individual subunits of a complex can be solved, yet determining the structure of the biologically relevant complex is much more complicated. Determining multiple distances between discrete locations on two or more proteins and using docking algorithms to piece them together provides an alternative avenue for complex structure determination. However, this avenue is often blocked by homomultimerisation within the complex leading to multiple spin labels being incorporated per labelling site introduced into the primary sequence. The resulting spectrum is highly convoluted, and therefore hard to interpret with any level of accuracy. To combat this problem, especially with regards to Nap1-like proteins and the complexes they form with histones, two avenues for singly labelling dimeric proteins were pursued.

The first avenue was based on the coexpression of alternatively tagged monomers. The rationale was to use two alternative affinity tagged forms of the monomer with a single labelling site on only one of the constructs. Coexpression of both tagged monomers within the same cell would allow for dimerisation of the labelled monomer with the unlabelled monomer, forming a complex containing a single labelling site. Obviously populations of doubly labelled and non-labelled dimer would also be present, however, sequential purification using the alternate affinity tags allows for isolation of the singly labelled form, as depicted in figure 3.7A.

For the purposes of this study, Vps75 was chosen as a candidate protein. Two expression constructs were made, one fused to an N-terminal 6-histidine tag, and the other fused to an N-terminal glutathione S-transferase (GST) tag. The expression constructs also contained different selection makers (ampicilin and kanamycin, respectively) and alternative origins of replications. Thus, both plasmids carrying the

expression cassettes could be sustained with the same bacterial cell, and only bacteria containing both expression cassettes could be selected for. Transcription was driven from a T7 promoter and protein expression was induced accordingly. The results from the co-expression and subsequent sequential affinity purification are shown in figure 3.7B. Lane 1, 2 and 3 are the insoluble, soluble/input and flow through fractions from purification on a cobalt chelating resin, respectively. Lanes 4 and 5 are the eluate from the cobalt chelating resin and the flow through from the glutathione affinity resin, respectively. Loading of these two lanes was normalised to total volume. Lane 6 is the eluate from the glutathione affinity resin, and thus contains both 6-histidine tagged Vps75 and GST tagged Vps75 in equal stoichiometries.

What is immediately apparent from the co-expression is the huge over expression of 6-histindine tagged Vps75 compared to the very moderate expression of the GST tagged form leading to a reduced yield after sequential affinity purification. One may expect that if the two constructs were expressed equally, and associated together in the cell at random, then the population of singly labelled dimers would be close to a third of the total. However, due to the unequal expression, in reality a yield of around one thirtieth is achieved. Yet this diminished yield still provides quantities of protein applicable for pulsed EPR. Typically ~3 nmoles per litre of bacterial culture of singly labelled dimer could be recovered, with ~10 nmoles being required for a single pulsed EPR experiment. It is also necessary to remove the affinity tags before labelling, especially the GST tag as it contains cysteine residues and exists as a dimer. This was easily done using a protease cleavage site present in the linker peptide (figure 3.7B, lanes 7 and 8, before and after cleavage respectively). The affinity tags can then be removed either by passing the sample back over the affinity resin, or in this case by anion exchange chromatography which also serves as a final polishing step in the protein purification (figure 3.7B, lanes 9-15).

The second approach for singly labelling a dimer for pulsed EPR makes use of a commercially available homobifunctional thiol reactive crosslinking spin label. The compound 3,4-Bis-(methanethiosulfonylmethyl)-2,2,5,5-tetramethyl-2,5-dihydro-1H-pyrrol-1-yloxy (abbreviated to 3,4-Bis MTSL) incorporates two methanethiosulfonate groups that conjugate to the thiol group of a cyesteine residue via a disulphide linkage, and a stable nitroxide which is EPR active (figure 3.7C). It has been shown in section 3.2.3 that two cysteine residues in close proximity to reach other can be readily crosslinked with a methanothiosulfonate based crosslinker. And indeed, when

M3M is substituted for 3,4-Bis MTSL crosslinking at H3 K115C on the histone tetramer is equally efficient and specific (data not shown). The same strategy was implemented for labelling the Vps75 dimer.

The crystal structure of the Vps75 dimer (Park, Sudhoff et al. 2008) was surveyed for residues that are within a few angstroms of each other. The only region that comes into close proximity is the alpha helical dimerisation domain. Along this helix the tyrosines at position 35 have a Cβ-Cβ distance of 6.5 Å and are exposed to the solvent (figure 3.7C). A Vps75 C>A Y35C mutant was expressed and purified as was the wild type and subjected to spin label crosslinking at a 1:1 ratio of Vps75 dimer to 3,4-Bis MTSL. As with the crosslinked tetramer, crosslinked Vps75 was subject to gel filtration chromatography and shown to elute in the same fractions (data not shown), demonstrating that crosslinking occurs across the dimerisation interface. The efficiency of crosslinking was determined by separating the crosslinked and non crosslinked species by SDS-PAGE, staining with coomassie and quantifying the proportion of crosslinked to non crosslinked protein both before and after crosslinking (figure 3.7D, dilutions were made to make sure the quantification of staining was in the linear region). Analysis of labelling by this method gave a labelling efficiency of 86 %. Generally, labelling efficiencies in the range of 90% are acceptable for analysis by pulsed EPR, therefore this approach provides a real possibility for simplifying pulsed EPR in multimeric protein assemblies.

3.3 Discussion

3.3.1 Summary

The structural diversity of histone chaperones suggests there is no underlying theme for their interaction with core histones (Das, Tyler et al. 2010; Hansen, Nyborg et al. 2010; Ransom, Dennehey et al. 2010). It is likely that the function of histone chaperones within the cell is closely linked to their mode of interaction with histones. Elucidation of these interactions may therefore provide key insights into the molecular mechanism of chromatin regulation. The ubiquitous chaperone Asf1 and its interaction with H3 and H4 has received much investigation. Remarkably, this chaperone interacts with a dimer of H3 and H4, effectively competing with the tetrameric interaction observed in the nucleosome (English, Maluf et al. 2005; Mousson, Lautrette et al. 2005; English, Adkins et al. 2006; Natsume, Eitoku et al.

2007). Nap proteins show a similar level of sequence and structural conservation, but adopt a different fold to Asf1 (Park and Luger 2006; Muto, Senda et al. 2007; Berndsen, Tsubota et al. 2008; Park, Sudhoff et al. 2008; Tang, Meeth et al. 2008; Gill, Yogavel et al. 2009). Thus, it is possible that the mode of interaction between Nap proteins and their histone cargo differs to that of Asf1. Characterisation of the interaction of Nap proteins with histones has not been studied in as much detail as has been possible for Asf1.

To address this, a study into the mode of interaction of Nap proteins with core histones was undertaken, focusing on the conformation of H3 and H4. Using the two Nap proteins from yeast, Nap1 and Vps75, as model members of this class of chaperone four independent lines of investigation were pursued. Evidence from gel filtration chromatography, site directed crosslinking, long range distance measurements and *in vitro* biological assays all agree with a tetrameric conformation of H3 and H4 when in complex with Nap1 and Vps75. Therefore, it seems that some chaperones, such as Asf1, interact with a dimer of H3-H4, whereas others, such as the Nap family of chaperones, interact with a tetramer of H3-H4. The biological implications of these interactions are discussed with respects to replication dependent and independent chromatin reconfiguration.

3.3.2 Implications in replication dependent chromatin reconfiguration

It has long been known that during chromatin replication parental H3 and H4 are incorporated into newly synthesised chromatin in a conserved fashion with regards to the $(H3\text{-}H4)_2$-tetramer. That is, H3-H4 dimers from parental nucleosomes do not mix with newly synthesised H3-H4 dimers (Seale 1976; Weintraub 1976; Cremisi, Chestier et al. 1978; Prior, Cantor et al. 1980; Sogo, Stahl et al. 1986; Jackson 1990; Annunziato 2005). More recently the inheritance of H3 and H4 has come under closer scrutiny making use of modern proteomic approaches (Xu, Long et al. 2010). Again, it was observed that the $(H3\text{-}H4)_2$-tetramer is conserved during replication with respects to the replication dependent isoform H3.1, whereas the replication independent isoform, H3.3, was more liable to mixing. It is hard to imagine that during the passage of the replication machinery nucleosomes remain bound to DNA at all times. Indeed it has been suggested that a nucleosome free region in the order of 200-600 base pairs exists on the leading and lagging strands (Sogo, Stahl et al. 1986; Lucchini, Wellinger et al. 2001). This would suggest that the $(H3\text{-}H4)_2$-tetramer may

have to pass through a soluble intermediate in its passage from parental to newly synthesised DNA, implicating a histone chaperone that recognises, binds and stabilises the parental tetramer.

Current evidence would implicate the chaperones Asf1 and CAF1 as being the major players in replication coupled nucleosome deposition (Tagami, Ray-Gallet et al. 2004; Groth, Ray-Gallet et al. 2005; Groth, Corpet et al. 2007; Li, Zhou et al. 2008; Jasencakova, Scharf et al. 2010). The property of tetramer splitting conferred by Asf1 seems to be at odds with the established literature. Nonetheless, Asf1 has been found to associate with old and new histones alike (Groth, Ray-Gallet et al. 2005; Groth, Corpet et al. 2007). However, one must bear in mind these lines of evidence are based on enrichment of 'parental' post translational modification of histones under conditions of replication stress, a scenario that may cause unnatural associations between parental histones and chaperones. A definitive model reconciling the established literature on tetramer conservation with the recent characterisation of histone-chaperone interactions has yet to come forward.

There is no evidence to date for a role of Nap1 in chromatin replication, and a tenuous link for Vps75 via its association with Rtt109, a protein that is important in replisome integrity (Li, Zhou et al. 2008). That being said, the passage of a parental tetramer across the replication fork is mostly likely a very transient process, and difficult to purify biochemically. Using a proteomics based approach in conjunction with pulsed labelling, as in Xu *et al*. (2010), but applied to a yeast system, would provide an avenue for analysing the effect of selected chaperone knock-outs on parental tetramer stability, and offers an potential avenue for future investigations addressing the biological significance of the $(H3\text{-}H4)_2$-tetramer particle.

It is also possible that tetramer conservation at the replication fork may not require a tetramer specific chaperone. It is conceivable that conservation of the parental tetramer may be a property of replication kinetics. For example, a higher local concentration of parental histones existing around replication factories may drive 'parental' nucleosome formation irrespective of whether H3 and H4 are processed through a dimeric intermediate or not. Although being transiently detached from DNA, it may be that the parental histones never go through a truly soluble state, staying in constant contact with the replication machinery until their deposition onto newly synthesised DNA. Thereby, incorporation of parental histones into daughter DNA would occur before newly synthesised histones arrive on the scene. Indeed, in

support of this idea most chaperones implicated in DNA replication are found associated with components of the replication fork: Asf1 associates with the Mcm2-7 replicative helicase via an H4 linkage (Groth, Corpet et al. 2007), CAF1 interacts directly with the processivity factor PCNA (proliferating cell nuclear antigen) (Gerard, Koundrioukoff et al. 2006; Ben-Shahar, Castillo et al. 2009) and an additional chaperone complex FACT (facilitates chromatin transcription) has been shown to interact with DNA polymerase α (Wittmeyer and Formosa 1997; Wittmeyer, Joss et al. 1999), the single strand DNA binding protein RPA (replication protein A) and the MCM helicase (VanDemark, Blanksma et al. 2006). Thus, parental histones may be shuttled from chaperone to chaperone, traversing the replication fork to become incorporated into newly synthesised DNA without ever becoming detached from the replication machinery.

Additionally, a recent study has demonstrated the affinity of histones acetylated on lysine 56 of H3, a mark present on newly synthesis histones, for DNA is lower than non-acetyated histones (Andrews, Chen et al. 2010). Therefore, differing affinities between newly synthesised and parental histones for DNA may also aid in a kinetic based mechanism for histone segregation at the replication fork, the high affinity of the parental histones driving their incorporation at a higher rate than the newly synthesised histones carrying acetylation marks.

3.3.3 Implications in replication independent chromatin reconfiguration

This work has demonstrated that Nap proteins and Asf1 differ in their interaction with H3 and H4. Do these two alternative modes of binding relate to different biological functions with respects to replication independent chromatin dynamics? At a very simple level one could hypothesise that a tetramer disrupting activity results in nucleosome disassembly, whereas a tetramer binding activity promotes nucleosome assembly.

This is difficult to test, at least in a cellular environment due to the close association of nucleosome assembly and disassembly. Despite this, it has been shown in *Xenopus* egg extracts that depletion of Asf1, and associated chaperone HIRA, inhibits turnover of the replication independent H3 isoform H3.3 (Ray-Gallet, Quivy et al. 2007). Addition of HIRA, but not Asf1, to these depleted extracts rescues H3.3 depostion. This suggests that Asf1 alone does not have the ability to assemble nucleosomes, requiring passage of its cargo to an alternative chaperone for deposition.

This makes sense as the addition of two H3-H4 dimers to DNA, independent of each other, is not likely to result in productive nucleosome formation.

Additional evidence for nucleosome disassembly comes from Asf1's ability to remove histones from gene promoter regions, in concert with the Swi/Snf complex (Gkikopoulos, Havas et al. 2009; Takahata, Yu et al. 2009). Promoter regions of genes have been shown to be regions of high histone turnover (Lee, Shibata et al. 2004; Dion, Kaplan et al. 2007; Jamai, Imoberdorf et al. 2007), a possible direct consequence of nucleosome disassembly. High turnover is also associated, at least in budding yeast, with H3 K56Ac levels (Rufiange, Jacques et al. 2007; Williams, Truong et al. 2008). Asf1 is crucial for mediating this actelyation mark, a mark that is delivered excusively to soluble histones (Recht, Tsubota et al. 2006; Tsubota, Berndsen et al. 2007; Fillingham, Recht et al. 2008; Li, Zhou et al. 2008). Interestingly, a recent thermodynamic study has shown that H3 K56Ac modified histones have a markedly reduced affinity for DNA (Andrews, Chen et al. 2010). Thus, in addition to functioning in removal nucleosomes from promoter regions, acetylation of specific lysines on H3 by Asf1 may help in keeping promoter regions clear of nucleosomes or aiding in their efficient removal. Nucleosome depleted regions being a characteristic of active transcription at gene promoters in yeast (Lee, Shibata et al. 2004; Lee, Tillo et al. 2007; Hartley and Madhani 2009). Thus, there is both in vitro and in vivo evidence linking Asf1 specifically to removal of histones from chromatin.

Similar to Asf1, the question arises: can the model of histone binding to Nap1 and Vps75, proposed in this study, be reconciled with evidence for their *in vivo* function? The ability to bind H3-H4 in their nucleosomal conformation would suggest that Nap proteins function to assemble nucleosomes. Alternatively, stabilising H3-H4 in their nucleosomal conformation when transiently detached from DNA, so efficient reassembly can take place, may also be a function of an $(H3\text{-}H4)_2$-tetramer binding chaperone. Whereas, Asf1 has been mainly implicated at the promoter remodelling level, Vps75 and Nap1 have been implicated in transcription elongation.

Vps75 and Nap1 genetically interact with the Elongator complex and have been shown to be enriched within open reading frames of genes (Kong, Kobor et al. 2005; Del Rosario and Pemberton 2008; Selth, Lorch et al. 2009). Additionally, Nap1 co-purifies with Elongator subunits (data not shown), and both Vps75 and Nap1 have been shown to work *in vitro* with ATP-dependent remodelling enzymes that aid in

RNA polymerase II progression (Lorch, Maier-Davis et al. 2006; Selth, Lorch et al. 2009). Indeed, suggestive of a function in transcription elongation, Nap1 knock out strains in yeast show sensitivity to transcription elongation inhibitors (Del Rosario and Pemberton 2008).

Two mechanisms for a transcribing polymerase contending with the nucleosomal barrier *in vivo* have been proposed (Kristjuhan and Svejstrup 2004): either removal of histone-DNA contacts allowing passage of the polymerase through dissociation of histones, or retention of histones, but loosening of histone-DNA contacts through acetylation mediated by the acetyl transferases Elongator and Gcn5. Interestingly, a recent study has shown that the original H3-H4 released from nucleosomes ahead of the transcribing polymerase, and not histones from the soluble pool, are redeposited after polymerase passage (Jamai, Puglisi et al. 2009), contrasting with promoter regions (Schermer, Korber et al. 2005). This work agrees well with studies looking at histone turnover on genome-wide scales in yeast that have shown turnover within open reading frames is much reduced compared to that of gene promoters (Lee, Shibata et al. 2004; Dion, Kaplan et al. 2007; Jamai, Imoberdorf et al. 2007; Rufiange, Jacques et al. 2007; Kaplan, Liu et al. 2008; Williams, Truong et al. 2008). It could therefore be possible that Nap1 and Vps75 associate with the elongating RNA polymerase II complex and function in conserving the original histones by acting as platforms to retain the nucleosomal conformation of histones during their transient passage around the polymerase.

Indeed, Kaplan *et al.* (2008) provide a direct comparison of the effects of Asf1 and Vps75 knock outs on histone turnover. Deletion of Asf1 or Rtt109 resulted in a decrease in turnover of 'hot' nucleosomes (nucleosomal territories with a high turnover of histones), suggesting that Asf1 functions in nucleosome disassembly. In contrast, deletion of Vps75 resulted in an increase in turnover of hot nucleosomes, suggesting Vps75 functions to assemble nucleosomes, thereby conserving the chromatin state.

Current evidence would suggest a role for the FACT complex in mediating histone mobilisation during transcription elongation. However, it is perfectly possible that multiple classes of chaperones associate with the elongating polymerase synergising their activities in different aspects of histone mobilisation and deposition. Indeed, FACT co-purifies with Nap1 from yeast cells (Krogan, Cagney et al. 2006). Characterisation of the FACT complex both *in vitro* and *in vivo* suggests it has the

ability to alter histone-DNA contacts in a manner that promotes nucleosome disassembly (Rhoades, Ruone et al. 2004; VanDemark, Xin et al. 2008; Xin, Takahata et al. 2009). Therefore, FACT may be responsible for loosening and removal of nucleosomes ahead of the transcribing polymerase, whereas Nap1 and Vps75 act as platforms, retaining the original histones in their soluble state and redepositing them after the polymerase has passed. Further experimentation would be required to delineate the contributions of different chaperone complexes in transcription elongation, and provides an intriguing avenue for future investigations.

3.3.4 Symmetry as a requirement for $(H3\text{-}H4)_2$-tetramer interaction

It has not escaped our attention that Nap proteins, which are homodimeric, bind a tetramer of H3 and H4 consisting to two identical heterodimers. All Nap proteins crystallised to date contain a 2-fold rotational axis of symmetry along their dimerisation domain. Additionally, the $(H3\text{-}H4)_2$-tetramer within the nucleosome and histone octamer also contains a pseudo axis of symmetry that passes through the dyad interface of H3. On the other hand, Asf1 exists as an obligate monomer with no intrinsic symmetry. Therefore, symmetry within histone chaperones may reflect on their mode of interaction with H3-H4. For example, homodimers containing a two-fold symmetry may preferentially interact with a $(H3\text{-}H4)_2$-tetramer, such as the Nap proteins, whereas chaperones devoid of symmetry, such as Asf1, may interact with a dimer of H3-H4, although interaction with an H3-H4 dimer does not necessarily require splitting of the $(H3\text{-}H4)_2$-tetramer. Additionally, homodimerisation may not be the only mechanism for achieving symmetry, though as we see with Nap proteins, it is a possible outcome.

This begs the question, is homodimerisation prevalent within H3-H4 histone-chaperones? Among the chaperones studied to date, the answer seems to be no (Das, Tyler et al. 2010). In addition to proteins adopting the headphone fold of Nap1, the only other class of H3-H4 chaperone that has been definitively shown exist as a homodimer is nuclear autoantigenic sperm antigen (Nasp) (Richardson, Batova et al. 2000; Tagami, Ray-Gallet et al. 2004; Finn, Browne et al. 2008; Wang, Walsh et al. 2008). Nasp is processed as two splice isoforms, sNasp (somatic) and tNasp (testes), and is prevalent in metazoans, but lacking in budding yeast, although the chaperone Hif1 has been postulated as the yeast homologue (Ai and Parthun 2004). Interestingly, Nasp does not show homologies to Nap proteins based on their primary sequence, yet

it is able to bind both H3-H4 and H2A-H2B and also the linker histone H1, a property shared by yeast Nap1. The structure of Nasp and how it interacts with histones is not yet known.

In addition to Nasp, homodimerisation has also been implicated, but not definitively proven, in the CENP-A variant chaperone Hjurp (Shuaib, Ouararhni et al. 1349). Hjurp is responsible for recognising CENP-A-H4 and depositing them at the centromere, ensuring epigenetic memory of centromere location (Dunleavy, Roche et al. 2009; Foltz, Jansen et al. 2009). In the model proposed, dimerisation of Hjurp was proposed to occur through a predicted coiled coil domain at the N-terminus of the protein, allowing it to specifically recognise and deposit the $(CENPA\text{-}H4)_2$-tetramer (Shuaib, Ouararhni et al. 1349). Interestingly, the functional homologue of Hjurp in yeast, Scm3, also contains a predicted coiled coil domain at its N-terminus (data not shown, secondary structure prediction made using Jpred3, http://www.compbio.dundee.ac.uk/www-jpred/). The fission yeast Scm3 homologue Sim3, has been shown to be related to the Nasp family of chaperones (Dunleavy, Pidoux et al. 2007), and indeed, both Nasp and Hif1 contain predicted N-terminal coiled coil domains (data not shown). Interaction via an N-terminal alpha helical domain draws parallels with the Nap proteins, although in the case of Nap1 and its homologues interaction is via non-coiled coil alpha helices. It will be interesting to see if these proposed dimeric chaperones can bind H3-H4/CENPA-H4 in their tetrameric conformation, and offers an avenue for future investigation.

4. Probing the structure of the $(H3\text{-}H4)_2$-tetramer using SDSL and pulsed EPR

4.1 Introduction

Nucleosome are not static entities, but are subject to dynamic alterations in both their histone-DNA contacts and histone composition. Indeed, there is growing evidence that non-canonical nucleosome structures exist in nature and have an important biological role. Such non-canonical structures that have so far been reported include hexasomes (Baer and Rhodes 1983; Kireeva, Walter et al. 2002; Bruno, Flaus et al. 2003; Kulaeva, Gaykalova et al. 2009), tetrasomes (Vicent, Zaurin et al.; Bina-Stein and Simpson 1977; Ruiz-Carrillo and Jorcano 1979; Spangenberg, Eisfeld et al. 1998; Vicent, Nacht et al. 2004), hemisomes (Dalal, Wang et al. 2007) and dinucleosomes (Engeholm, de Jager et al. 2009). In addition to an altered composition, there is evidence that in the absence of H2A and H2B dimers H3 and H4 can undergo dramatic structural rearrangement (Hamiche, Carot et al. 1996; Bancaud, Wagner et al. 2007), raising the need for a more detailed investigation into $(H3\text{-}H4)_2$-tetramer structure.

In vivo it has been suggested that H3 and H4 exist predominantly as dimers, as ectopically expressed tagged H3 does not pull down native H3 (Tagami, Ray-Gallet et al. 2004), with dimerisation sustained through the interaction with the ubiquitous histone chaperone Asf1 (English, Maluf et al. 2005; English, Adkins et al. 2006; Natsume, Eitoku et al. 2007). However, the majority of soluble H3-H4 associating with Asf1 may mask interactions with other classes of chaperone, especially if they are transient or in lower abundance. Therefore it remains possible that the interaction with other classes of chaperones permit a non chromatin associated tetramer. Indeed, we have argued a strong case in the previous chapter that the Nap family of histone chaperones interact with H3 and H4 in their tetrameric form. The wide variety of protein folds displaying histone chaperoning ability suggests multiple modes of histone interaction are likely.

Previous studies that have aimed to characterise the structure of the histone tetramer utilised methods including crystallography (Lattman, Burlingame et al. 1982)

and deuterium exchange mass spectrometry (Black, Foliz et al. 2004). Crystallography resulted in limited success, whereas the study utilising deuterium exchange mass spectrometry focused primarily on tetramers containing the H3 variant CENP-A. Nuclear magnetic resonance spectroscopy has been used to investigate histones H2A/B in complex with a chaperone peptide (Zhou, Feng et al. 2008), however, the $(H3\text{-}H4)_2$-tetramer is typically too large to be investigated by this method. Forster resonance energy transfer has also met with some success in the study of the intrinsic dynamic nature of DNA within the nucleosome (Li, Levitus et al. 2005) and more recently in the investigation of ATP-dependent chromatin remodelers (Blosser, Yang et al. 2009; Racki, Yang et al. 2009). However, attaching a single acceptor and donor fluorophore is difficult to achieve in a multiply dimeric system such as the histone tetramer, thus FRET has not been able to relay detailed structural information from the underlying histone component of the nucleosome.

Here we employ the method of site directed spin labelling (SDSL) with pulsed electron paramagnetic resonance (EPR) to probe the conformation of the $(H3\text{-}H4)_2$-tetramer. By using the histone octamer as a platform for comparison we are able to gain a detailed picture of the tetramer particle. Regions of H3 and H4 that deviate when probed in their tetrameric conformation give an insight into the dynamic nature of the histone tetramer in solution and have implications for its interactions outside of chromatin. Furthermore, an approach for increasing the sensitivity of pulsed EPR experiments is described, along with ground work laid down for the study of the tetrasome particle by this method.

4.2 Results

4.2.1 Experimental rational

The core histone octamer and tetramer are especially amenable to investigation by SDSL and pulsed EPR as they contain only a single non-conserved cysteine residue and are comprised of multiple dimers. This means that introduction of a labelling site into the primary sequence of a histone results in the two spin labels required for pulsed EPR in the octamer/tetramer complex. Thus, the multiply dimeric nature of the histone octamer, that complicates analysis by FRET, aids in the analysis by EPR.

Distance distributions from pulsed EPR provide information regarding the modal distance between the two spin labels, which is generally robust, and also a

measurement of the breadth of the distribution, reporting on the dynamic aspect of the label's environment, which is more open to interpretation. Thus, pulsed EPR data provides a wealth of information on both the local region of the spin label and the geometry of the underlysing protein complex. Using the crystal structure of the histone octamer solved at atomic resolution possible conformations of the spin label at each labelling site can be modelled using molecular dynamics, increasing the resolution of the data by giving a measure of both modal distance and dynamics. Distance distributions extracted from the same site on the octamer and tetramer can be compared directly, allowing detection of even minor conformational changes. In this way, by extracting distance distributions from multiple sites and using the octamer as a direct comparison, we aimed to generate a global picture of the structure of the free tetramer complex using SDSL and pulsed EPR.

4.2.2 Selection of sites used for spin labelling

The crystal structure of the histone octamer was used as a guide for selecting potential labelling sites on H3 and H4. Labelling sites were chosen based on four criteria. Firstly, an even spread of labelling sites that would report on all the major secondary structural elements within the octamer/tetramer were chosen. Secondly, these sites

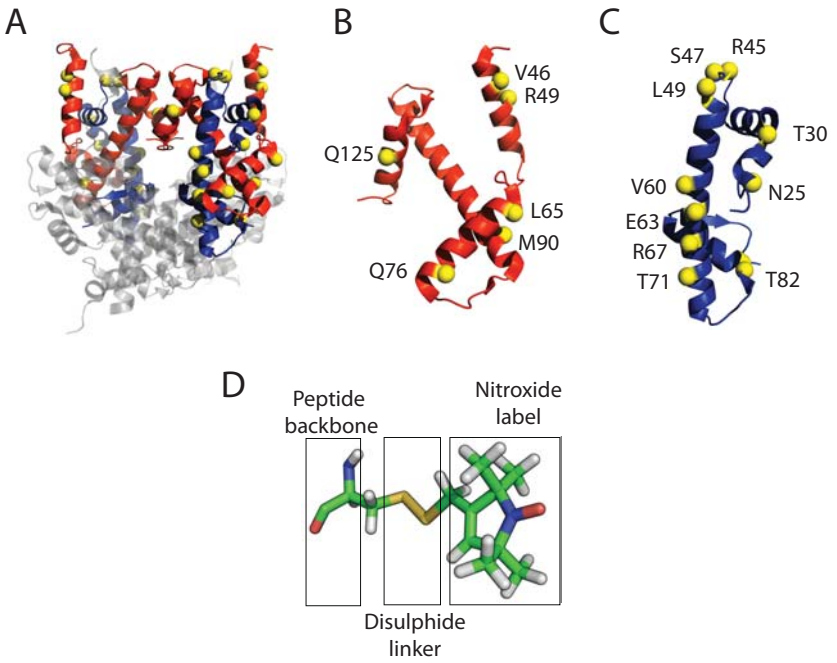

Figure 4.1. Sites used for the labelling of H3 and H4. (A) H3 (red) and H4 (blue) shown in the octameric conformation (PBD code 1TZY). The Cα of each labelling site is shown as a yellow sphere. (B) Positions of the labelling sites on H3. (C) Positions of the labelling sites of H4. (D) The structure of a spin labelled sidechain, R1 (taken from Bowman et al., 2010).

had to minimally perturb the structure of the tetramer and not be involved in its interaction with H2A and H2B in the octamer. Thirdly, the sites had to be solvent accessible to allow efficient spin labelling. Finally, the sites had to reside within 2-8 nm of each other, the window for distance extraction by pulsed EPR. Some labelling sites that fulfilled these criteria were developed during previous studies. These were supplemented by addition sites chosen based on the above criteria, generating 16 unique labelling sites spanning the globular domains of H3 and H4 (figure 4.1A, B and C). These sites were labelled with MTSL resulting in the spin-labelled sidechain denoted as R1 (figure 4.1D).

4.2.3 Distance extraction by EPR: considerations for data processing and interpretation

Analysis of pulsed EPR data from PELDOR experiments was carried out using the software DEERanalysis2006, which has been well documented (Jeschke, Chechik et al. 2006). The experimentally obtained time domain trace (figure 4.2A) is processed to remove intermolecular components that contribute to the background decay resulting in the corrected dipolar evolution (figure 4.2B). The trace is then fitted using Tikhonov regularisation with the appropriate regularisation factor alpha. Fitting is a compromise between goodness of fit to the experimental data and suppression of artefacts. A plot of alpha term verses quality of fit (mean squared deviation of experimental vs simulation) gives a characteristic L-curve, the inflection of which provides correct regularisation factor to use (figure 4.3C). Transformation of the dipolar evolution results in the distance distribution, a plot of distance verses the P(r) value (figure 4.2D). For accurate distance information PELDOR data should contain a full oscillation within the time domain trace and decay to baseline. Such data usually provides a dominant distribution that can be defined by a P(r) value and distribution breadth. Caution is required where oscillations aren't observed within the time domain trace as this can result in misleading distributions, defined by their low P(r) and extended distribution breadth. Positions resulting in such data are often defined as being 'mobile' or 'structurally heterogeneous'.

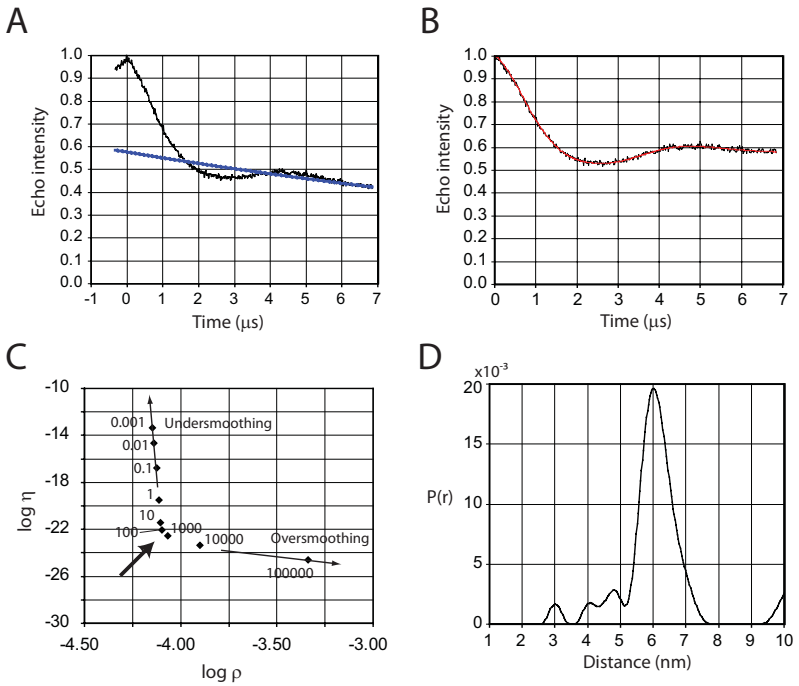

Figure 4.2. Distance extraction by pulsed EPR, considerations for data processing. (A) The time domain trace (black line) for site H3 V46 from the histone octamer. The baseline correction is shown as a blue line. (B) The corrected dipolar evolution (black trace) and simulated fit (red trace) corresponding to a Tikhonov regularisation with an alpha factor of 100. (C) A plot of the alpha factor against the quality of fit (mean square deviation between experimental data and simulation). Oversmoothing results in broadening of distribution, whereas undersmoothing results in sharpening and splitting of distribution into multiple peaks. In this case an alpha factor of 100 was most approriate. (D) The distance distribution, P(r), as determined by Tikhonov regularisation of the fitted time domain trace.

4.2.4 The histone octamer adopts a largely homogeneous structure

In the following section, and proceeding sections 4.2.5/6/8, pulsed EPR experiments, data processing and molecular dynamic simulations were carried out by Dr Richard Ward and Dr David Norman, College of Life Sciences, 5 Dow Street, University of Dundee, Dundee, DD3 5EH, United Kingdom.

In general the PELDOR data from the octamer suggest a stable, homogeneous particle, with clear oscillations in the time domain trace from nearly all positions probed. The structure of the histone octamer has previously been solved by crystallography to a resolution of 1.9 Å (Wood, Nicholson et al. 2005), suggesting that under these conditions the histone octamer is a structurally homogeneous particle. Simulating the position of the spin label using molecular dynamics on the octamer crystal structure, a good fit with the modal distances measured experimentally was found, with only three exceptions (figure 4.3). Indeed, plotting the modal distance

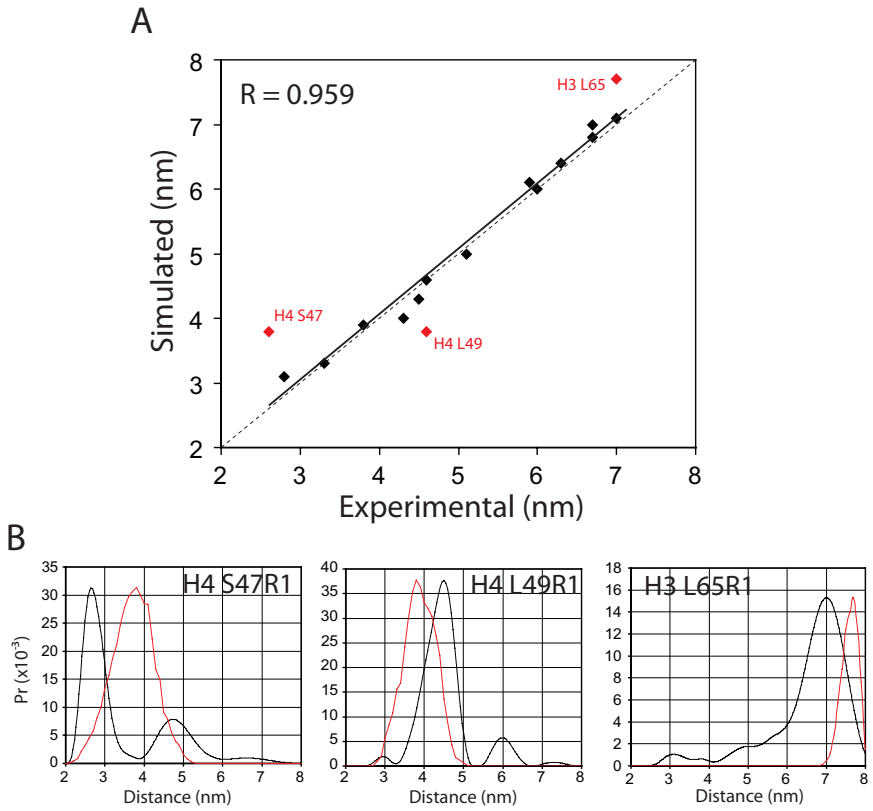

Figure 4.3. The histone octamer is a stable and structurally homogenous complex. (A) The modal distances from PELDOR data (experimental) were plotted against the modal distances from molecular dynamics simulations (simulation) for all labelling sites tested. The regression (solide black line) shows a very close fit to a perfect correlation (dotted black line) with an R value of 0.959. Data points with a discrepancy of greater than 0.5 nm are labelled in red. (B) Distance distributions of the sites that displayed greater than 0.5 nm discrepancy. Experimental (black trace) and simulated (red trace) distance distribution are plotted on the same axis for comparison.

from the PELDOR experiments against the modal distance derived from molecular dynamic simulations we see a correlation coefficient of 0.959 (figure 4.3A). Positions H4S47, H4L49 and H3L65 displayed appreciable difference between experimental and simulated distance (figure 4.3B). Although this may report on movements of the underlying backbone compared to that of the crystal structure the differences of 1.2, -0.8 and 0.7 nm, respectively, are within the span of the nitroxide moiety to the alpha backbone carbon for two spin labelled sidechains. Therefore, it is also possible that the discrepancy is due to favorable rotomers being under represented in the simulated distribution.

4.2.5 Structural heterogeneity within the histone tetramer particle

In the following section circular dichroism experiments were performed by Dr Sharon Kelly, Joseph Black Building, University of Glasgow, G12 8QQ, United Kingdom.

The stability of the histone octamer under conditions used for EPR, and its resemblance to that of the histone octamer crystal structure, allowed direct comparison to the histone tetramer. Thus, the structure of the histone tetramer was probed using the same 16 labelling sites as for the histone octamer. A scatter plot of distances from sites on the tetramer verses the same sites on the octamer reveals the conformation of H3 and H4 in the tetramer is very similar to that in the octamer (figure 4.4A) with only a single site, H4E63, showing a serious discrepancy. Site H4E63 deviates significantly in both is distribution and its modal distance in the tetramer particle. To determine if this was due to the mutation causing gross structural changes in the tetramer we analysed the WT and mutant tetramers (both containing the H3C110A mutation) by circular dichrosim (CD) spectroscopy. CD spectroscopy reports on the secondary structural composition of a protein, and thus if the mutation caused structural rearrangements within the tetramer one would expect to see a change in the CD spectrum. However, we did not observe any change in the secondary structural content compared to the WT tetramer, thus we concluded that the mutation did not introduce any major structural defects within the tetramer itself (figure 4.4C). Indeed, tetramers containing this mutation refolded and eluted as normal during gel filtration chromatography (data not shown). Another possibility could be that the addition of the spin labelled sidechain induces a structural rearrangement.

The PELDOR experiment contains information on both the modal distance between the two spin populations and their distribution. It was observed that although the modal distances in the tetramer are retained, oscillations within the time domain trace were often dampened, or in some cases not observable, when compared with their octamer counterparts. This suggests that such regions, although giving a modal distribution that agrees well with the corresponding site in the octamer, are not as structurally well defined in the tetramer resulting in extended distance distributions. In order to meaningfully compare the octamer and tetramer datasets with respects to the distribution of the spin population a measure of the discreteness of the distance distribution is required. The P(r) value can serve as such a measure as it is proportional to the amplitude of oscillation within the dipolar evolution. As oscillations within the dipolar evolution are dampened the distance distributions become broader, often consisting of multiple distinct peaks. Thus, the maximum P(r)

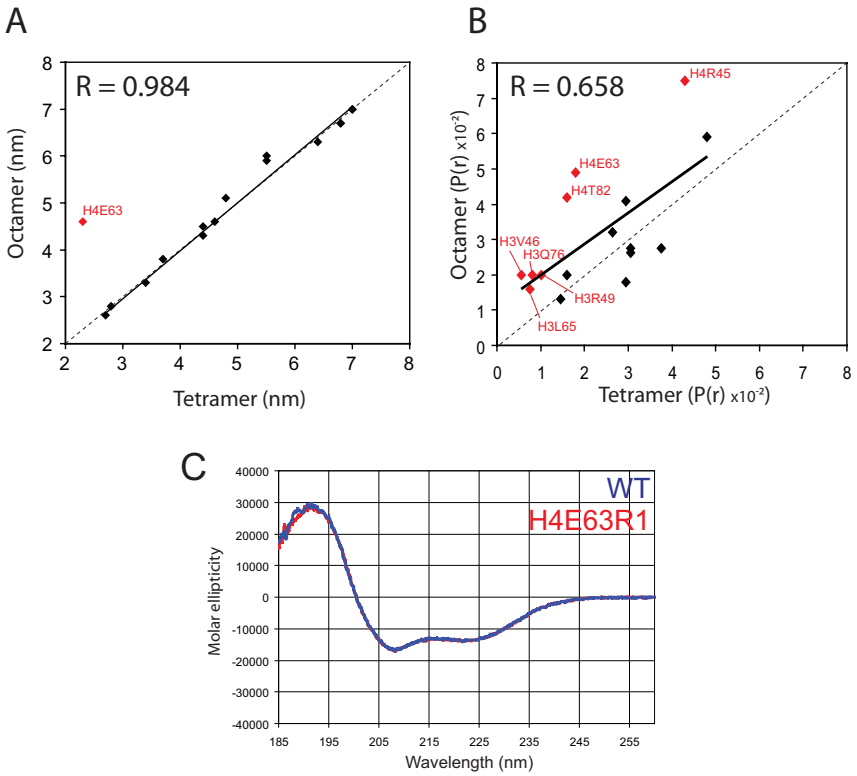

Figure 4.4. Structural heterogeneity within the histone tetramer. (A) Modal distances from PELDOR data derived from the octamer were plotted against the same sites derived from the tetramer. H4E63 is highlighted in red. The data (excluding position H4E63) fits very closely to a perfect correlation (dotted line) with an R value of 0.984. (B) The maximum P(r) value for the octamer plotted against the maximum P(r) value for the tetramer for each position probed. Again the ideal correlation is shown as a dotted black line and the actual regression shown as a solid black line giving an R value of 0.658. Positions of interest are labelled in red. (C) Circular dichroism of WT histone tetramer (blue) verses a tetramer carrying the mutation H4E63C (red). The spectra are virtually superimposable, suggesting no gross structural pertubation.

is also a more measurable parameter than the distribution breadth, leading to a better representation of the dynamism for comparison between multiple positions.

When the maximum P(r) values for each position from the tetramer were plotted against the same sites within the octamer the correlation was less defined than for their modal distances (figure 4.4B). This may be due to the distribution being more affected by data processing parameters than the modal distance. However, one can see that the majority of the data points reside above the line of y=1(x) that one would expect from a perfect correlation, i.e. the P(r) value of these sites in the tetramer is lower than that in the octamer (figure 4.4B). This would suggest that H3 and H4 in the tetramer, in general, are more structurally heterogeneous than in the octamer. Sites of particular interest, which deviate significantly from the perfect correlation, are labelled in red and shall be discussed in more detail below.

Structural heterogeneity within the histone tetramer occurred predominantly within two locations: the H4 α2/α3 and the H3 αN/α1 helices. Position H4E63 resides in the centre of the H4 α2 helix (figure 4.5B) and exhibits both a gross change in modal distance (figure 4.4A, figure 4.5A) and significant decrease in its P(r) value (figure 4.5A, top), suggesting a drastic structural rearrangement in this region bringing the two residues closer together. Such a rearrangement is hard to imagine as PELDOR data from positions H4V60 and H4R67, one turn of the helix each side of E63, show a good correlation between octamer and tetramer in both modal distance and distribution breadth (data not shown, Bowman et al., 2010). Yet, there is evidence in the literature that would support structural heterogeneity within this region (Black, Foliz et al. 2004). Black and colleagues used deuterium exchange mass spectrometry to probe the stability of the canonical H3 and CENP-A variant containing histone tetramers. They identified a peptide spanning resides 60-67 in H4 which has a marked increase in stability when in complex with the H3 variant, suggesting this region contains an inherent dynamism. Further work would be required to resolve these discrepancies, possibly making use of Asf1 as a stable platform for probing this region in more detail (see section 4.2.6). Position H4T82 also showed a discrepancy in the breadth of its distribution between octamer and tetramer (figure 4.5A, bottom right), appearing to be more mobile in the tetramer. T82 is positioned on the α3 helix of H4 (figure 4.5B). Interestingly, in the octamer this region makes contacts with H2B forming a four-helix-bundle interaction analogous to the H3-H3' interface. This suggests a stabilising effect of H2B in the octamer, whereas in the tetramer loss of this interaction may cause the mobility we see in this region.

Another region of the tetramer that shows structural heterogeneity is the H3 αN and α1 helices. In total four of the labelling sites probed reside on the αN and α1 helices (figure 4.6C). In each case removal of H2A/H2B dimers resulted in an essentially oscillation free dipolar evolution and a correspondingly broad distance distribution (Figure 4.6A, sites H3L65, top panel, and H3R49, middle panel, are representative samples from the α1 and αN, respectively). In addition H4R45, which is in close proximity to the αN helix of H3 and C-terminal extension of H2A (figure 4.6B), displayed an increase in mobility in the tetramer characterised by its drop in P(r) and increase in distribution breadth (figure 4.6A). The αN helix of H3

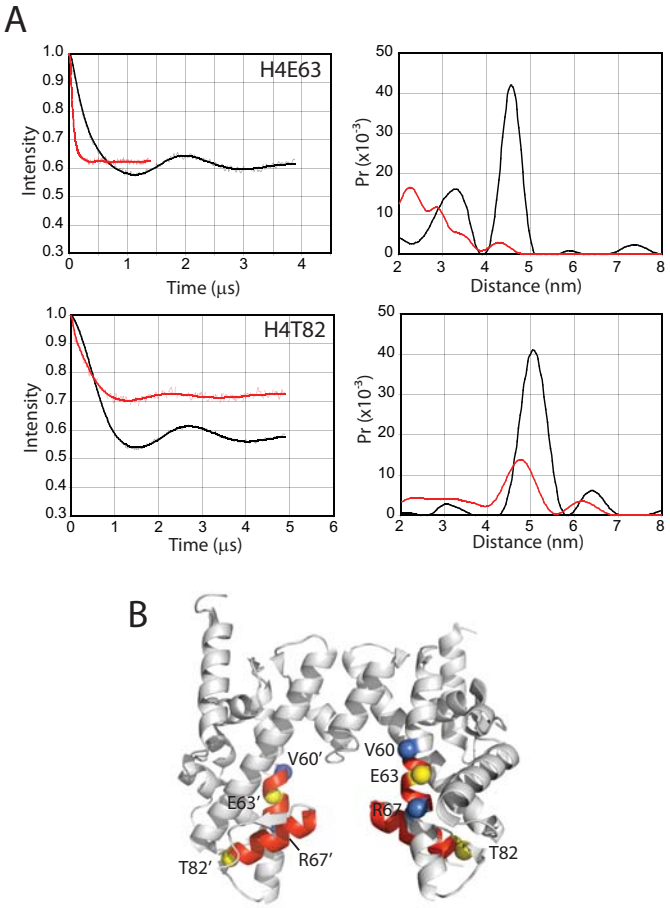

Figure 4.5. Structural heterogeneity within H4. (A) The dipolar evolution and distance distribution for sites H4E63 and H4T82. Black traces are data from the octamer, red traces are data from the tetramer. (B) Positions of E63 and T82 within the histone tetramer (Cα atoms of each residue shown as a yellow sphere). The secondary strucural element on which they report is shown in red. Positions H4 V60 and R67 also probed in this study are shown in blue.

makes multiple contacts with the H2A C-terminal extension in the octamer crystal structure. Thus, it seems that these contacts are crucial for stability of the αN and α1within the histone octamer. Indeed, it has been previously demonstrated that mutation of residues with the H3 αN helix can affect the binding of H2A/H2B dimers to the tetramer inhibiting the formation of a stable octamer (Ferreira, Somers et al. 2007). Mobility within the αN helix of H3 may propagate through to the α1 accounting for the structural heterogeneity we also see in this helix.

4.2.6 The use of Asf1 as a more sensitive probe of H3-H4

For labelling sites within the stable histone octamer a plot of P(r) verses modal distance reveals an interesting trend (figure 4.7A). Assuming a linear regression, a strong negative correlation is seen with a correlation coefficient of -0.706, suggesting that longer distances are prone to broader distributions (figure 4.7A). This is

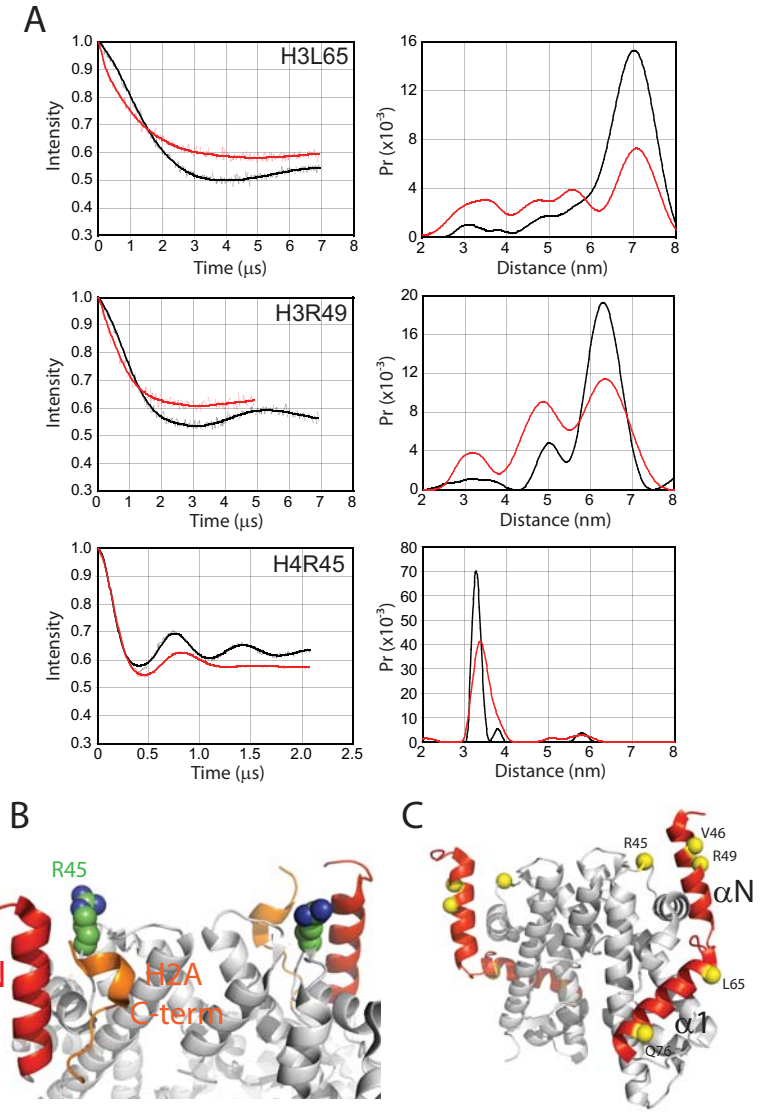

Figure 4.6. Structural heterogeneity within the H3 aN and a1 helices. (A) Dipolar evolution (left) and distance distributions (right) from representative sites within the aN and a1 helices of H3 and H4R45. Octamer data is shown in black, tetramer data is shown in red. (B) The local environment of H4 R45 in the histone octamer. The positions of the H3 aN helix (red), H2A C-terminal extension (orange) and position R45 on H4 (green/blue spheres) are shown. (C) Positions of the H3 aN and a1 helix (red) in the histone tetramer. Labelling sites are denoted with their Cα atoms highlighted as yellow spheres.

somewhat expected as molecular motions within the intervening protein act to disperse the labels within the two coupled populations. Therefore, subtle differences in the distributions at long range are more difficult to detect, with only substantial changes in protein conformation likely to be observed (Jeschke and Polyhach 2007). Thus, the structural heterogeneity we see within the H3 αN and α1 helices may be caused by a loss of secondary structure, yet they may also be due to multiple discrete conformations, the convolution of which results in an analogous oscillation-free spectrum. What is required to a gain a better understanding of the structural heterogeneity in such regions is a discrete labelling site at a more proximal position.

However, being multiply dimeric the ability to probe such regions from a proximal position in the tetramer, whilst retaining a two spin system, is very difficult.

We have shown in section 3.3.5 that the tetramer can be efficiently split by Asf1 under conditions used for EPR. This provides an avenue for effectively isolating a single H3-H4 dimer so that a two-spin system can be employed to probe αN and α1 of H3. The cocrystal structure of Asf1 with H3-H4 was used as a guide to identify possible labelling sites on Asf1 which ideally resided within ~3-4 nm of the αN and α1 helices of H3. It should be noted that in both co crystal structures of Asf1-H3-H4 the αN helix of H3 is not resolved, but is present in the expressed constructs (English, Adkins et al. 2006; Natsume, Eitoku et al. 2007). This in itself is suggestive, but not definitive evidence, that this region is disordered outside of the octamer/nucleosome. To overcome this absence, the H3-H4 dimer coordinates were extracted from the histone octamer crystal structure and aligned to the H3-H4 dimer coordinates in the Asf1 co crystal structure, giving an idea of where the helix should reside (figure 4.7B). Position K41 on Asf1 was identified as a possible labelling site and was probed using the stable labelling position of H4 R45 (data not shown). Indeed, this position on Asf1 yielded multiple deep oscillations in the time domain trace, suggesting its position within the β-sheet face of Asf1 is structurally well-defined. Asf1 labelled at K41 was then used to probe positions H3L65 and H3R49, labelling sites representative of the α1 and αN helices, respectively.

Probing of H3R49 on the αN helix from Asf1 gave a shorter distance than when probed in the tetramer (figure 4.7C, top) as would be expected due to Asf1 K41 being a lot closer to R49 than R49 is to itself within the tetramer. However, the background corrected spectrum did not show any observable oscillations resulting in a comparably broad, albeit shorter, distance distribution (figure 4.7C). Probing of H3L65 on the α1 helix again gave a shorter distance as would be expected when compared to the tetramer data (figure 4.7C, bottom), but in contrast to H3R49, the background corrected spectrum contained a slight, yet observable, oscillation. Upon regularisation a distance distribution with a markedly increased P(r) value (0.024), compared to that of the tetramer (0.007), was obtained (figure 4.7C, bottom).

By probing from a proximal, structurally well-defined position we can see that the αN helix is comparatively more dynamic than the juxtaposed α1 helix. We can

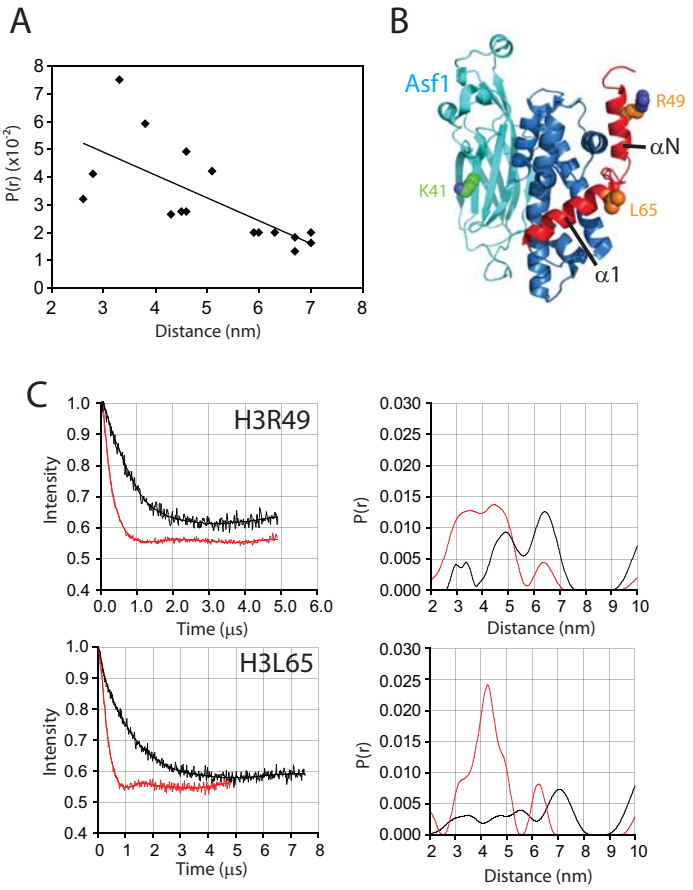

Figure 4.7. Asf1 as a stable platform for probing of the αN and α1 regions of H3. (A) The modal distance of the 16 sites probed in the octamer plotted agaisnt the P(r) value. The r and r values for linear correlation are -0.706 and 0.499, respectively. (B) The co-crystal structure of Asf1, H3 and H4 (PDB code 2HUE). The αN and α1 regions of H3 are coloured red, the H3H4 dimer in blue and Asf1 in cyan. Labelling sites used in this study are shown as spheres. (C) Dipolar evolutions (left) and distance distributions (right) for H3 R49 and H3 L65 probed from Asf1 K41. Data probed from Asf1 is shown in red, whereas data from the tetramer alone is shown in black.

also see that from the oscillation free spectrum the structurally heterogeneity of the αN most likely results from a disordered conformation rather than the existence of multiple meta-stable states, as multiple defined populations of spins should be able to be deconvoluted using the discrete labelling site on Asf1. This data agrees well with the domains of H3 resolved within the co crystal structure of Asf1 with H3-H4 (English, Adkins et al. 2006; Natsume, Eitoku et al. 2007). Asf1 is unlikely to mediate structural rearrangements with the H3 αN or α1 as it does not make any direct contacts within the crystal structure. This being said, the precise function of it C-terminal acidic domain, which is not present in the structure, is not known. Therefore, we conclude that outside of chromatin the αN helix of H3 adopts a largely disordered conformation effectively extending the N-terminal tail of H3 up to start of the α1 helix when in complex with Asf1, and most likely within the tetramer as well.

4.2.7 Optimisation and cloning of a tetrasomal DNA template

The histone tetramer forms the core of the nucleosome and as such plays an important role in nucleosome dynamics (Hamiche, Carot et al. 1996; Spangenberg, Eisfeld et al. 1998; Sivolob, De Lucia et al. 2000; Sivolob and Prunell 2000; Sivolob and Prunell 2004; Vicent, Nacht et al. 2004; Bancaud, Wagner et al. 2007). Deposition of an $(H3\text{-}H4)_2$-tetramer onto DNA results in the formation of a tetrasome (figure 1.2A), yet structural characterisation of this particle to date has been very limited. From the crystal structure of the nucleosome (Luger, Ma?der et al. 1997) we can see that the αN helix adopts a unique position making contacts with the entry/exit site of DNA, with a portion of DNA close to the dyad and with the H2A C-terminal extension (figure 1.3). Additionally, from biochemical characterisation (Ferreira, Somers et al. 2007) it was shown that the αN helix of H3 is important in regulating access to DNA at the periphery of the nucleosome, having implications in the dynamics of site exposure within the nucleosome (Li, Levitus et al. 2005). It would therefore be interesting to see how this helix, which we have shown to be predominantly disordered in its non chromatin bound state, yet well resolved in the octamer and nucleosome crystal structure, behaves in the tetrasome particle. Although an extensive study into the structure of the tetrasome was beyond the scope of this investigation, initial steps of optimisation for the production of tetrasomes, at quantities applicable for EPR, were carried out.

First, the sequence and length of the DNA template had to be optimised. Previous studies from other laboratories have identified DNA sequence preferences that favour wrapping in the nucleosome[5] (Lowary and Widom 1998; Thastrom, Lowary et al. 1999; Anderson and Widom 2000; Thastrom, Lowary et al. 2004). These sequences, include characteristic 10 base pair AT dinucleotide periodicity, and are likely also to be efficient for reconstitution of tetrasome particles. Of these unnatural sequences the 601 sequence was chosen for its unusually high affinity for histones (Lowary and Widom 1998; Thastrom, Lowary et al. 1999). Although sequence preference has been studied in detail, at least for the nucleosome, less is known about the length of DNA that is required to efficiently wrap the $(H3\text{-}H4)_2$-tetramer. In order to form mono-tetrasomes a template must contain enough base pairs of DNA to wrap a tetramer, but not too many as to allow a di-tetrasome to form. From

[5] Refer to Chapter 1, sub-section 1.1.4

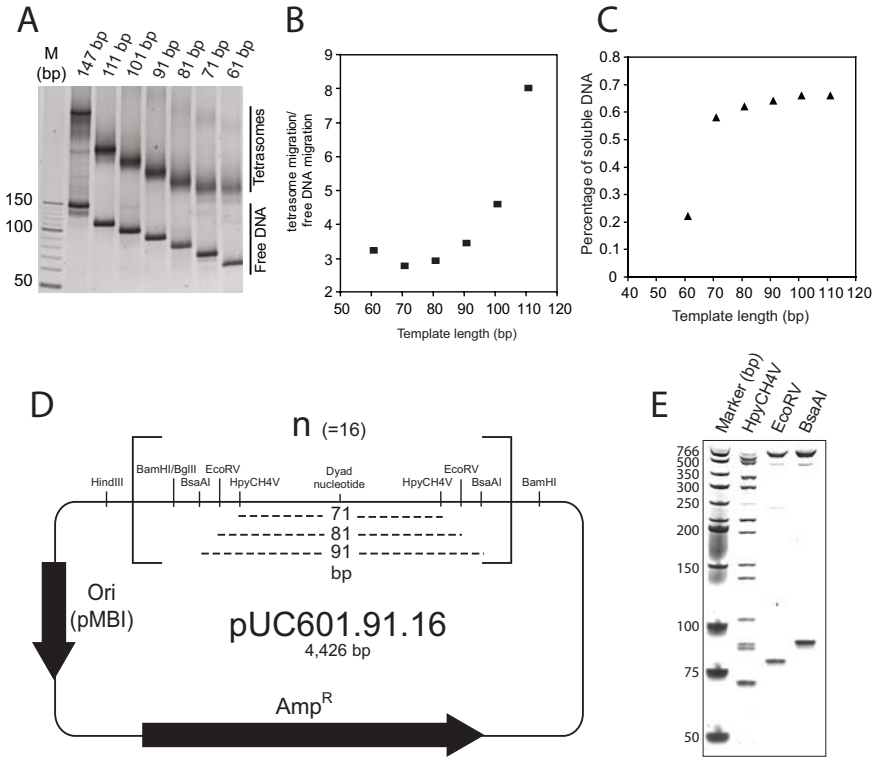

Figure 4.8. Optimisation and cloning of tetrasomal DNA templates. (A) Native PAGE analysis of the migration of tetrasomes reconstituted onto various length DNA templates. (B) Graphical representation of the migration of tetrasomal constructs shown in A normalised to the migration of free DNA. (C) DNA solubility as a function of template length. Total soluble DNA after reconstitution was quantified by it absorption at 260 nm. (D) Cloning of the 71/81/91 bp 16 repeat construct intp pUC19. (E) Restriction digest of the pUC601.91.16 plasmid using HpyCH4V (lane 1), EcoRV (lane 2) and BsaAI (lane 3), corresponding to the release of a 71, 81 or 91 base pair fragment, respectively.

the nucleosome crystal structure it can be seen that H3 and H4 make contacts with DNA up to superhelical location +3/-3, suggesting 61 base pairs is sufficient to wrap an $(H3\text{-}H4)_2$-tetramer (figure 1.2A). Biochemical analyses have reported particles of both 70 and 96 base pairs of DNA are protected from H2A/B depleted nucleosomes when subject to nuclease treatment (Read, Baldwin et al. 1985; Vicent, Nacht et al. 2004). In order resolve these ambiguities it was decided a more systematic investigation into optimal length of DNA required for efficient mono-tetrasomal reconstitution was needed.

Multiple truncated 601 sequence fragments were generated by preparative PCR and tested for their efficiency in forming tetrasomes via the salt diaysis method of reconstitution (Thastrom, Lowary et al. 2004). Reconstitution efficiency was analysed by quantifying the amount of soluble DNA by UV absorption before and after dialysis and by separation of free DNA from tetrasomes by native gel electrophoresis (figure 4.8A, B & C). Fragments spanning 61 to 111 base pairs at 10

base pair intervals were made consisting of an equal length either side of the central dyad nucleotide within the 601 sequence. It was found that reconstitution on fragments 71 to 111 base pairs resulted in little precipitation, with the majority of DNA being soluble after dialysis (figure 4.8C). Contrary to this, reconstitution on the 61 base pair fragment repeatedly resulted in precipitation, with the majority of the DNA being insoluble (figure 4.8C). Native gel electrophoresis shows that the intensity of the tetrasome band compared to free DNA band remains comparable for fragments 71 to 111 base pairs, but is markedly decreased for the 61 base pair fragment (figure 4.8A).

The migration of the tetrasome bands with respect the template length also showed an interesting trend (figure 4.8A & B). Quantifying the migration of the tetrasomal band with respects to the migration of the free DNA, and plotting this value against template length, appeared to follow a hyperbolic function, the apex of which occurring between 70-80 base pairs (figure 4.8B). Migration during native gel electrophoresis is dependent on the shape, size and charge of the particle. It is known that the migration of nucleosomes and subnucleosomal particles are predominantly dependent on their shape, with the extensive negative charge of the DNA predominating over the basic nature of the histones. This is demonstrated by the slower migration of a mono tetrasome compared to a nucleosome reconstituted onto the same fragment of DNA (Spangenberg, Eisfeld et al. 1998). The tetrasome is not as compact a particle as the nucleosome and is not as large, so although the basic charge and the mass are reduced in a tetrasome, the migration is slowed due to its extended shape. Migration of the tetrasomes reconstituted onto the 61-111 base pair fragments can thus be interpreted by the shape of the particle.

One can imagine that as the length of the DNA increases, it extends past the point of histone interaction producing various lengths of flanking DNA depending on the length of the template. Such flanking DNA would result in a less compact particle, and would thus migrate more slowly. From the experimental data we can see that the 61 and 71 base pair tetrasomes migrate at the same speed, whereas the migration of 71 compared to 81 base pairs, and 81 compared to 91 base pairs (and so on), results in a retarded migration of the larger template particle (figure 4.8A). Assuming the predominance of shape in determining the migration characteristics, we interpret the increase in migration from 111 to 71 base pairs as a reduction in the flanking DNA. As the DNA approaches the edge of the core tetrasome the particle retains a similar

compactness, and thus migrates at a similar speed, accounting for the similar migration of the 71 and 61 base pair fragments. When compared to the migration of free DNA this corresponds to the apex of the hyperbola shown in figure 4.8B. Extrapolating from the curve in figure 4.8B we can see the apex resides between data point 71 and 81, suggesting a tetrasomal DNA length of ~70-80 base pairs, in close agreement with findings by Read *et al*. (1985).

Reconstituting on a fragment smaller than that required to wrap the $(H3\text{-}H4)_2$-tetramer most likely results in inter-tetrasomal interactions as exposed basic regions of histones interact with DNA inter-tetrasomally . This could account for the extensive precipitation when reconstituting with the 61 base pair fragment, and the big step in solubility at 71 base pairs (figure 4.8C). Charge compensation of the histones is complete from ~71 base pairs of DNA, resulting in marginal increases in solubility with increasing fragment length (figure 4.8C).

Preparative PCR yields DNA quantities applicable for biochemical analysis, but becomes an expensive and time consuming approach for generating quantities applicable for pulsed EPR. Synthesis of oligonucleotides on a preparative scale was also investigated, but the number of reactions failing to reach greater than 71 nucleotides meant that yields were substantially affected, thus this approach too became uneconomical and time consuming in purifying away failed sequences (data not shown). Therefore, tetrasomal DNA was generated from a plasmid source isolated from bacteria, a similar approach to that used in generating DNA in quantities applicable for crystallography (Luger, Ma?der et al. 1997).

The doubling mechanism described in Richmond *et al.* (1988) was used to generate 16 copies of a tetrasomal fragment of modified 601 sequence (figure 4.8D). The repeat was designed so that 71, 81 and 91 base pair fragments could be released depending on the restriction enzyme used, thus making the construct a little more versatile with regards to its applicability in future experiments. The repeat is identical to the 601 sequence up until 34 nucleotides either side of the dyad, where modifications to the sequence had to be made to introduce restriction sites. It is believed these alterations will have minor effects on the reconstitution of tetrasome particles derived from these templates. Digestion of this construct with HpyCH4V, EcoRI or BsaAI yielded 71, 81 and 91 base pair fragments as expected (figure 4.8E). Unfortunately, due to the small recognition site of HpyCH4V multiple fragments were released from the plasmid backbone upon digestion. Purification from some of the

smaller fragments may be difficult, however, it would be possible to remove the whole 16n repeat sequence using the flanking restriction sites of HindIII and BamHI and ligate into a vector devoid of HpyCH4V sites if a 71 base pair fragment is required.

4.2.8 Protein deuteration as a method for increasing sensitivity and extending distance extractions in pulsed EPR

This study has shown that pulsed EPR is a powerful tool for probing the conformation of proteins and protein complexes. Yet the technique suffers from two major drawbacks: poor sensitivity and limited distance extraction of 8 nm (Jeschke and Polyhach 2007; Schiemann and Prisner 2007). These drawbacks are due, in part, to the short relaxation Tm. Tm is affected by hyperfine coupling to protons in the surrounding environment and the consequent spin-diffusion. Use of deuterated solvents, deuterium having a reduced magnetic moment compared to protons of a factor of ~6.5, is now common place in pulsed EPR spectroscopy, extending the window of distance extraction to ~8 nm and reducing sample concentrations to ~50 μM of spin pairs (Borbat and Freed 2007; Jeschke and Polyhach 2007). Yet, these concentrations and distance limitations still restrict the study of many biological macromolecules, especially large complexes, which suffer from molecular crowding, and limited solubility. In addition to protons derived from the solvent, protons within the macromolecule itself, and especially the protons of methyl groups (Zecevic, Eaton et al. 1998), are likely to contribute to modulation within the hyperfine field. Thus, exchange of these protons to deuterium would further reduce the hyperfine coupling and associated spin diffusion, effectively extending the Tm and further increasing both sensitivity and the limit of distance extraction.

Although deuteration levels in extent of 30 % are toxic to multicellular organisms, single cell organisms, especially prokaryotic cells, can survive in completely deuterated environments with only minimal effects of cell growth and division. Thus, expression of recombinant proteins in bacteria growing in a fully deuterated environment results in the production of deuterated proteins, and is a well characterised method for isotope labelling of proteins for study by NMR spectroscopy (Leiting, Marsilio et al. 1998; Marley, Lu et al. 2001; Meilleur, Weiss et al. 2009). The histone octamer was used as a model system for probing the effect of protein deuteration on sensitivity and distance gains for pulsed EPR. The site H3 Q76 was

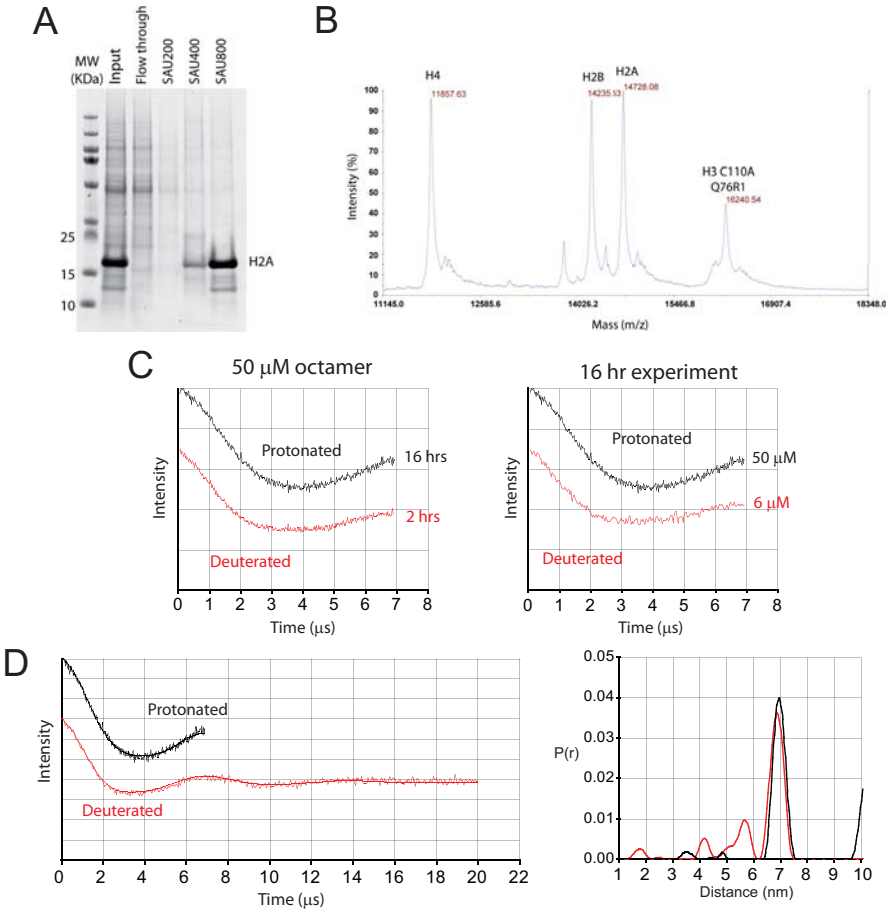

Figure 4.9. Deuteration of proteins as a method for increasing sensitivity and extending distance extraction from pulsed EPR. (A) Purification of deuterated histones, histone H2A shown as an example. Cation exchange purification was scaled down using 0.5 mL of cation exchange resin in 10 mL disposable chromatography columns. Deuterated histone bound in 200 mM sodium chloride (Input) was washed with 200 mM (SAU200), 400 mM (SAU400) and eluted with 800 mM (SAU800) sodium chloride. (B) MALDI-TOF analysis of the deuterated histone octamer. (C) The sensitivity increase of deuterated octamer compared to protonated octamer. Deuterated (red) and protonated (black) octamer from time (left panel) and concentration (right panel) experiments (D) The increase in sensitivity allows data to be collected over a longer time frame. Left: an experiment spaning 20 ms (red trace) compared to the 7 ms experiment possible for the protonated octamer (black trace). Right: the corresponding distance distributions for protonated (black line) and deuterated octamer (red line).

used as a position which gives a well defined distance at the limit of detection by current technology.

Histones expressed from *E. coli* grown in fully deuterated media (see section 2.1.2) resulted in virtually complete exchange of protons for deuterium (figure 4.9A, B and Table 4.1) when analysed by mass spectrometry. A PELDOR experiment was carried out on 50 µM of fully deuterated octamer and 50 µM of protonated octamer as a control, using identical experimental set ups. In order to achieve a signal to noise ratio comparable to that of the protonated data collected over a period of 16 hours, the PELDOR experiment had to be run for just 2 hours (figure 4.9C, left). Correspondingly, to achieve comparable signal to noise in a 16 hour PELDOR experiment the deuterated sample could be diluted from 50 to 6 µM (figure 4.9C,

right). This data demonstrates that deuteration of the spin-labelled protein can result in a sensitivity increase of close to 10 fold.

	Sequence	Non-deuterated mass	Expected mass	Deuterated mass (MS)	Percentage deuteration
H3Q76R1 C110A	ARTKQTARKSTGGKAPRKQ LATKAARKSAPATGGVKKP HRYRPGTVALREIRRYQKS TELLIRKLPFQRLVREIAC DFKTDLRFQSSAVMALQEA SEAYLVALFEDTNLAAIHA KRVTIMPKDIQLARRIRGERA	15398.09	16247.09	16240.54	99.2
H4	SGRGKGGKGLGKGGAKRHR KVLRDNIQGITKPAIRRLA RRGGVKRISGLIYEETRGV LKVFLENVIRDAVTYTEHA KRKTVTAMDVVYALKRQGR TLYGFGG	11236.1	11858.1	11857.63	99.9
H2A	SGRGKQGGKTRAKAKTRSSR AGLQFPVGRVHRLLRKGNYA ERVGAGAPVYLAAVLEYLTA EILELAGNAARDNKKTRIIP RHLQLAVRNDEELNKLLGRV TIAQGGVLPNIQSVLLPKKT ESSKSAKSK	13950.2	14734.2	14728.08	99.2
H2B	AKSAPAPKKGSKKAVTKTQK KDGKKRRKTRKESYAIYVYK VLKQVHPDTGISSKAMSIMN SFVNDVFERIAGEASRLAHY NKRSTITSREIQTAVRLLLP GELAKHAVSEGTKAVTKYTSAK	13493.6	14237.6	14235.5	99.7

Table 4.1. Quantifying the extent of deuteration for recombinantly expressed histones in Spectra9 medium (Cambridge Isotope Laboratories, Inc). Table showing amino-acid sequence, calculated mass of non-deuterated protein, calculated mass of deuterated protein (assuming exchange of all available positions), measured mass of deuterated proteins, and percentage deuterium incorporation.

In addition to the increase in sensitivity, we also found that data could be collected over a much longer time period (figure 4.9D, left). Indeed, oscillations within the time domain trace could be observed out to ~20 μs, theoretically allowing for probing of distance in excess of 10 nm. Acquisition over such extended time frames also allows for more accurate determination of distances, previously on the limit of detection, as more than a single oscillation can be recorded. In the case of the histone octamer this resulted in a more accurate measurement of the background decay, and worked to validate the longer distances previously probed in the protonated octamer (figure 4.9D, right).

4.3 Discussion

4.3.1 Summary

The core histone component of the nucleosome is comprised of a tetramer of H3 and H4. Deposition of the histone tetramer represents the initial step in nucleosome assembly and the final step in nucleosome disassembly, important processes in chromatin fluidity. Detailed knowledge of the structure of the tetramer is likely to provide insights into these processes, yet to date there has been little structural characterisation of H3 and H4 outside of the nucleosome or histone octamer.

In this study we employed the use of pulsed EPR to characterise the histone tetramer, making use of crystal structures of the histone octamer and nucleosome to serve as valuable platforms for comparison. We find that the structure of the $(H3\text{-}H4)_2$-tetramer alone contains subtle differences compared to its structure when sequestered in the octamer. The core crescent shape of the tetramer coordinated around the H3-H3' interface is retained, with discrepancies localised to specific regions of the H3 and H4. The importance of such structural heterogeneity within the histone tetramer with respects to its central role in chromatin biology is discussed below.

4.3.2 Structural heterogeneity within H4

Two sites within the H4 were found to become more structurally heterogeneous upon loss of H2A and H2B. One of these sites resides on the H4 α3 helix, which is involved in a four helix bundle interaction with H2B in the histone octamer (figure 4.5). Thus, it is not surprising that upon loss of this interaction these regions because more dynamic. The other labelling site that showed an interesting discrepancy between octamer and tetramer was H4 E63. Both the modal distance and distribution breadth were changed quite dramatically upon the removal of the H2A-H2B dimers (figure 4.5), suggesting a significant rearrangement is the underlying protein structure. Yet sites one turn of the helix above and below this position show no such discrepancy upon loss of the dimers, raising the possibility that the discrepancy may be due to alterations within the protein structure caused by the mutation and labelling. This seems unlikely as E63 does not appear to make any important interactions with other amino acids in the octamer. There is also evidence in the literature that suggests this region is dynamic within the soluble histone tetramer (Black, Foliz et al. 2004). Using deuterium exchange mass spectrometry Black *et al.* (2004) found that the

peptide spanning residues 60-67 of H4 adopted a more rigid conformation upon binding of the H3 variant CENP-A compared to H3.1. Although not direct evidence that this region is more structural heterogeneous in solution, it suggests that its secondary structure may contain a certain dynamism which can be modulated by histone variants. This region is resolved in the Asf1-H3-H4 co-crystal structure, which suggests it adopts a stable position. One possible avenue for future experimentation to try and consolidate these discrepancies would be to probe this region from the stable labelling site of Asf1. However, one must bear in mind when using Asf1 in this manner that the chaperone itself may confer stability to the region under interest.

4.3.3 The H3 αN helix

Previous research in our laboratory has identified the αN helix of H3 as having key roles in regulating nucleosome dynamics (Ferreira, Somers et al. 2007). Its position at the entry/exit site of DNA within the nucleosome defines its role in regulating access to nucleosome bound DNA both by transient unwrapping of DNA form the surface of the octamer and also during ATP-dependent and thermal remodelling activities (Li, Levitus et al. 2005; Ferreira, Somers et al. 2007; Somers and Owen-Hughes 2009). Indeed, it has been shown that posttranslational modification of this helix can alter inherent nucleosome dynamics (Neumann, Hancock et al. 2009). Thus, it is interesting that structural alterations in this region are observed in the soluble histone tetramer.

In the octamer the H3 αN makes contacts with the H2A C-terminal extension. The loss of these contacts in the tetramer, and the structural heterogeneity that results in the H3 αN, suggests that these contacts are required for stability of this region. In the nucleosome the H3 αN also contacts DNA at the entry/exit site and at the dyad (figure 1.3), which may also contribute to its stability. Therefore, it would be interesting to see how the αN helix behaves when it is in complex with DNA in the tetrasome. It could be that it retains its dynamic nature, only becoming structured upon addition of H2A-H2B dimers. Or it could be that it becomes structured upon deposition of the tetramer, forming a high affinity platform for the two dimers and thereby driving assembly of the nucleosome. Structural investigation into the tetrasome particle was abandoned during the early stages of this study as sufficient concentrations of mono-tetrasomes applicable for EPR could not be generated.

Optimisation of the template length for mono-tetrasome reconstitution, and the application of deuteration for increasing the sensitivity of pulsed EPR, provides an opportunity for future investigation into this interesting intermediate in nucleosome assembly.

4.3.4 Structural heterogeneity within the histone tetramer: implications in histone chaperone binding

From crystal structures of the nucleosome and histone octamer we have a good understanding of the structure of histones within chromatin. Less is known regarding the structure of histones outside of chromatin. It is known that factors interacting with soluble histones, such as the histone chaperones, are important in most, if not all, pathways for chromatin assembly and reorganisation. Thus, structural information regarding the conformation of histones outside of chromatin, both on their own and in complex with histone binding proteins, may provide insight into the mechanisms of chromatin assembly and reorganisation.

Our finding that certain regions of H3 and H4 can undergo rearrangements upon removal of H2A and H2B provides a new basis for the interaction of the soluble histone tetramer with its chaperones. For instance, the crystal structures of the small subunit of the ubiquitous histone chaperone complex CAF1 from *Drosophila* p55, and the related human protein RbAp46, contain a groove that binds the α1 helix of H4 (Murzina, Pei et al. 2008; Song, Garlick et al. 2008). In the crystal structure of the histone octamer, the α1 helix of H4 is partially buried within the histone fold, being occluded by the αN helix of H3. Our finding that the αN helix of H3 is highly mobile in the histone tetramer suggests that in solution the α1 helix of H4 may be more exposed to the solvent allowing sequestration of this helix by RbAp46/p55. As p55 and RbAp46 are responsible for directing histone deposition during DNA replication, the way in which it interacts with histones is likely to give key insights into the mechanism of nucleosome assembly by this chaperone, and provides a possible avenue for further research.

As we have demonstrated in the previous chapter, the histone chaperones Nap1 and Vps75 interact with H3 and H4 in their tetrameric form. We also showed that the interaction is predominantly ionic in nature (figure 3.1 & 3.2). Vps75 & Nap1 display a common surface charge distribution (Park and Luger 2006; Berndsen, Tsubota et al. 2008; Park, Sudhoff et al. 2008; Tang, Meeth et al. 2008),

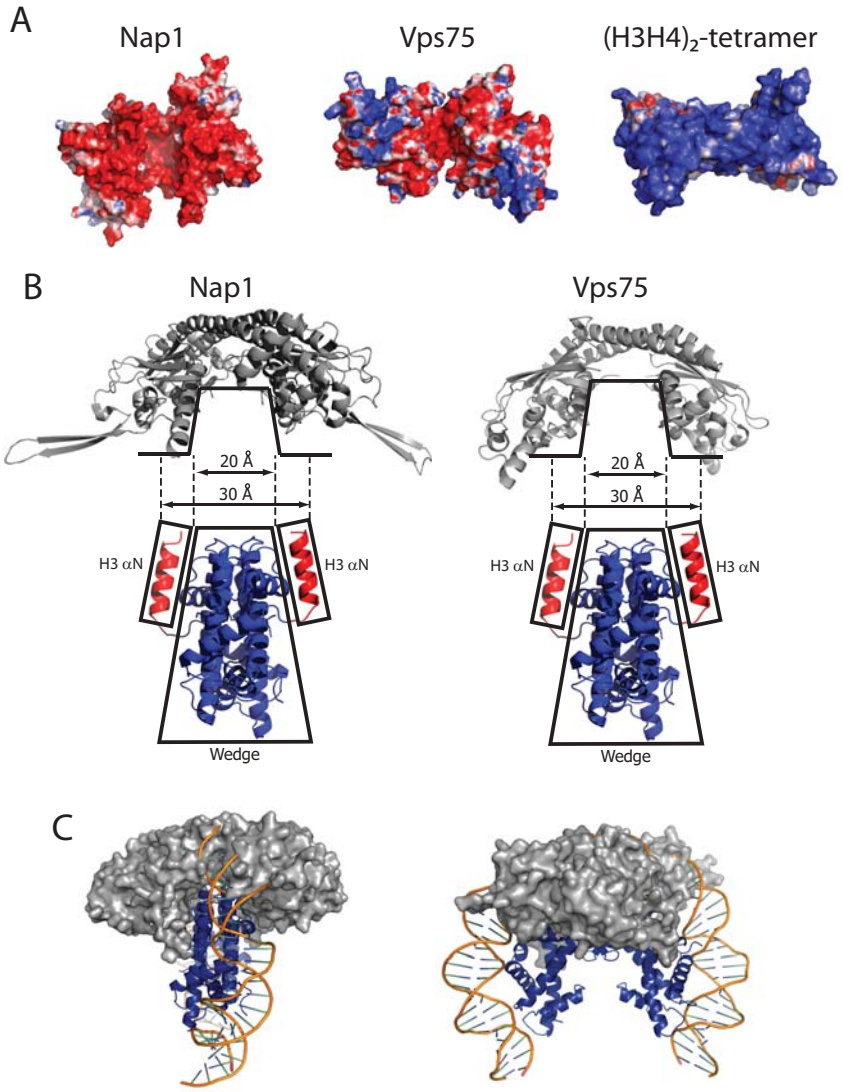

Figure 4.10. Possible mode of interaction between Nap proteins from yeast and (H3H4)2-tetramer. (A) Surface charge distribution of Nap1 (PDB code 2Z2R), Vps75 (PDB code 3C9D) and (H3-H4)2-tetramer (taken from PDB code 1KX5) (Electrostatic surface potentials generated by the APBS in PyMol, http://www.pymol.org). (B) Basic geometries of the acidic cavities of Nap1 and Vps75 and the (H3-H4)2- tetramer. (C) Conceptual model of Nap1's interaction with an (H3H4)2-tetramer. Manual alignment of the compact tetramer (missing the H3 aN helix) in the acidic cavity of Nap1 (using PyMol), suggesting a competition between Nap1 (grey) and DNA (orange) for binding H3-H4 (blue).

with the cavity formed between the two earmuff domains being predominantly acidic in nature (figure 4.10A). The tetramer, on the other hand, contains a highly basic patch in the form of a ramp around which the DNA wraps in the nucleosome (figure 4.10A). This suggests a possible mode of interaction where the helical ramp of the $(H3\text{-}H4)_2$-tetramer binds within the acidic cavity of Nap1/Vps75. Looking at the geometries of the two complexes it can be seen that the tetramer in its nucleosomal form is too large to fit without causing substantial steric hindrance (figure 4.10B). However, taking into consideration the structural heterogeneity we observe in the H3 aN helix, and treating it as a random coil, we can see that the core histone fold dimers of the $(H3\text{-}H4)_2$-tetramer adopt a geometry comparable to the cavity provided by

Nap1 and Vps75 (figure 4.10B). Indeed, it is interesting that although Nap1 and Vps75 are quite divergent in sequence the basic geometry of the cavity has been retained suggesting an evolutionary pressure to conform to a certain size, possibly provided by the requirement to bind H3 and H4 in their tetrameric form.

Binding of the histone tetramer at the dyad would result in a direct competition between Nap1/Vps75 and DNA (figure 4.10C). A mechanism of nucleosome assembly by Nap1 has been recently proposed that postulates Nap1 drives nucleosome assembly by eliminating non-nucleosomal interactions between histones and DNA (Andrews, Chen et al. 2010). A direct competition between DNA and Nap1 for the basic ramp of the $(H3\text{-}H4)_2$-tetramer would be compatible with this model. However, addition of a histone tetramer to the 91 base pair tetrasomal template at physiological ionic strength did not result in 'non-tetrasomal' interactions when analysed by native gel electrophoresis, only the reconstitution efficiency was reduced compared to deposition by Nap1 (figure 3.6C). This suggests that binding of a tetramer by Nap1 may actively direct histone deposition, possibly by subtle alterations in the regions of structural heterogeneity that we observed with EPR.

4.3.5 Structural heterogeneity within the histone tetramer: implications in post translational modification of soluble histones

After their synthesis and assembly, soluble histone fold dimers are subjected to post translationation modifications, predominantly in the form of lysine acetylation, before they are incorporated into chromatin. With regards to H3 and H4, this occurs generally on sites within the disordered N-terminal tails, such as H3 K9 and H4 K5/K12 (Sobel, Cook et al. 1995; Fillingham, Recht et al. 2008). Acetylation of histones seems to be necessary for their efficient incorporation into chromatin, with inhibition of acetylation compromising genomic stability (Recht, Tsubota et al. 2006; Han, Zhou et al. 2007; Chen, Carson et al. 2008; Fillingham, Recht et al. 2008; Li, Zhou et al. 2008). One of the acetyl transferases in yeast that is responsible for establishing such marks is Rtt109. Rtt109 is interesting as it acetylates sites both on the H3 N-terminal tail (K9) and also of the globular histone fold (K56) (Han, Zhou et al. 2007; Han, Zhou et al. 2007; Tsubota, Berndsen et al. 2007; Berndsen and Denu 2008; Fillingham, Recht et al. 2008). H3 K56 resides on the αN helix of H3, thus how does the acetyl transferase accommodate both random coil and alpha helix within its active site? An attempt at addressing this question was put forward upon solving the

high resolution crystal structure of Rtt109 (Lin and Yuan 2008). However, in our model of the soluble histone tetramer we propose that the disordered N-terminal tail of H3 extends through the αN helix in up to the α1 helix of the core histone fold, thus accommodation of α-helical structure is not necessary.

H3 K56 makes a water mediated contact with a backbone phosphate of DNA in the nucleosome crystal structure (Davey, Sargent et al. 2002), with its acetylation having subtle effects on nucleosome stability *in vitro* (Neumann, Hancock et al. 2009). It has also been implicated in increasing the affinity of certain histone chaperones (Li, Zhou et al. 2008), thermodynamically aiding the in the shuffling of histones between chaperone complexes, which eventually leads to histone deposition (Das, Tyler et al. 2010). Additionally, it has been shown using, CD spectroscopy, that the alpha-helical content of histones H3 and H4 is increased upon acetylation of their N-terminal tails (Prevelige and Fasman 1987; Wang, Moore et al. 2000). This suggests that acetylation of lysine residues increases the propensity of these peptides to form alpha helices, which is indeed the case for acetylated peptides (Xu, Cooper et al. 1995; Wang, Moore et al. 2000), and may be related to the 3-4 residue spacing of lysines within the histone tails (Sung and Dixon 1970; Strahl and Allis 2000). This is interesting in light of our findings that the αN helix of H3 looses, to some extent, its secondary structure in the soluble tetramer in its non acetylated form.Thus, acetylation within the αN helix of H3 by Rtt109 may function to stabilize its secondary structure, which in turn may play a role in deposition of H3 and H4 onto DNA or in the hand off to other chaperones (Li, Zhou et al. 2008; Das, Tyler et al. 2010). The positive charge at K56, being the C-terminal residue on the H3 αN, may function to stabiles the helix dipole. If so, removal of the positive charge by acetylation may have the opposite effect on the αN's stability. Further experimentation would be required to asses the effect of post translation modification on the stability of the αN helix of H3, and its role in chromatin assembly, providing an avenue for further investigation.

5. References

Adkins, M. W., J. J. Carson, et al. (2007). "The histone chaperone anti-silencing function 1 stimulates the acetylation of newly synthesized histone H3 in S-phase." J Biol Chem **282**(2): 1334-40.

Ai, X. and M. R. Parthun (2004). "The nuclear Hat1p/Hat2p complex: a molecular link between type B histone acetyltransferases and chromatin assembly." Mol Cell **14**(2): 195-205.

Allan, J., N. Harborne, et al. (1982). "Participation of core histone "tails" in the stabilization of the chromatin solenoid." J Cell Biol **93**(2): 285-97.

Allfrey, V. G., R. Faulkner, et al. (1964). "ACETYLATION AND METHYLATION OF HISTONES AND THEIR POSSIBLE ROLE IN THE REGULATION OF RNA SYNTHESIS." Proc Natl Acad Sci U S A **51**: 786-94.

Allshire, R. C. and G. H. Karpen (2008). "Epigenetic regulation of centromeric chromatin: old dogs, new tricks?" Nat Rev Genet **9**(12): 923-37.

Anderson, H. E., J. Wardle, et al. (2009). "The fission yeast HIRA histone chaperone is required for promoter silencing and the suppression of cryptic antisense transcripts." Mol Cell Biol **29**(18): 5158-67.

Anderson, J. D. and J. Widom (2000). "Sequence and position-dependence of the equilibrium accessibility of nucleosomal DNA target sites." Journal of Molecular Biology **296**(4): 979-987.

Andrews, A. J., X. Chen, et al. (2010). "The Histone Chaperone Nap1 Promotes Nucleosome Assembly by Eliminating Nonnucleosomal Histone DNA Interactions." Molecular Cell **37**(6): 834-842.

Andrews, A. J., G. Downing, et al. (2008). "A thermodynamic model for Nap1-histone interactions." Journal of Biological Chemistry **283**(47): 32412-32418.

Annunziato, A. T. (2005). "Split decision: What happens to nucleosomes during DNA replication?" Journal of Biological Chemistry **280**(13): 12065-12068.

Arents, G., R. W. Burlingame, et al. (1991). "The nucleosomal core histone octamer at 3.1 A resolution: a tripartite protein assembly and a left-handed superhelix." Proc Natl Acad Sci U S A **88**(22): 10148-52.

Asahara, H., S. Tartare-Deckert, et al. (2002). "Dual roles of p300 in chromatin assembly and transcriptional activation in cooperation with nucleosome assembly protein 1 in vitro." Mol Cell Biol **22**(9): 2974-83.

Axel, R. (1975). "Cleavage of DNA in nuclei and chromatin with staphylococcal nuclease." Biochemistry **14**(13): 2921-5.

Baer, B. W. and D. Rhodes (1983). "Eukaryotic RNA polymerase II binds to nucleosome cores from transcribed genes." Nature **301**(5900): 482-8.

Bancaud, A., G. Wagner, et al. (2007). "Nucleosome Chiral Transition under Positive Torsional Stress in Single Chromatin Fibers." Molecular Cell **27**(1): 135-147.

Bannister, A. J. and T. Kouzarides (2005). "Reversing histone methylation." Nature **436**(7054): 1103-6.

Bannister, A. J., P. Zegerman, et al. (2001). "Selective recognition of methylated lysine 9 on histone H3 by the HP1 chromo domain." Nature **410**(6824): 120-4.

Baxevanis, A. D., J. E. Godfrey, et al. (1991). "Associative behavior of the histone (H3-H4)2 Tetramer: Dependence on ionic environment." Biochemistry **30**(36): 8817-8823.

Bednar, J., R. A. Horowitz, et al. (1998). "Nucleosomes, linker DNA, and linker histone form a unique structural motif that directs the higher-order folding and compaction of chromatin." Proc Natl Acad Sci U S A **95**(24): 14173-8.

Belotserkovskaya, R., S. Oh, et al. (2003). "FACT facilitates transcription-dependent nucleosome alteration." Science **301**(5636): 1090-3.

Ben-Shahar, T. R., A. G. Castillo, et al. (2009). "Two fundamentally distinct PCNA interaction peptides contribute to chromatin assembly factor 1 function." Molecular and Cellular Biology **29**(24): 6353-6365.

Berndsen, C. E. and J. M. Denu (2008). "Catalysis and substrate selection by histone/protein lysine acetyltransferases." Curr Opin Struct Biol **18**(6): 682-9.

Berndsen, C. E. and J. M. Denu (2008). "Catalysis and substrate selection by histone/protein lysine acetyltransferases." Current Opinion in Structural Biology **18**(6): 682-689.

Berndsen, C. E., T. Tsubota, et al. (2008). "Molecular functions of the histone acetyltransferase chaperone complex Rtt109-Vps75." Nature Structural and Molecular Biology **15**(9): 948-956.

Bernstein, B. E., M. Kamal, et al. (2005). "Genomic maps and comparative analysis of histone modifications in human and mouse." Cell **120**(2): 169-81.

Bina-Stein, M. and R. T. Simpson (1977). "Specific folding and contraction of DNA by histones H3 and H4." Cell **11**(3): 609-18.

Birch, J. L., B. C. Tan, et al. (2009). "FACT facilitates chromatin transcription by RNA polymerases I and III." Embo J **28**(7): 854-65.

Biswas, D., Y. Yu, et al. (2005). "The yeast FACT complex has a role in transcriptional initiation." Mol Cell Biol **25**(14): 5812-22.

Black, B. E. and E. A. Bassett (2008). "The histone variant CENP-A and centromere specification." Curr Opin Cell Biol **20**(1): 91-100.

Black, B. E., D. R. Foliz, et al. (2004). "Structural determinants for generating centromeric chromatin." Nature **430**(6999): 578-582.

Blosser, T. R., J. G. Yang, et al. (2009). "Dynamics of nucleosome remodelling by individual ACF complexes." Nature **462**(7276): 1022-7.

Borbat, P. P. and J. H. Freed (2007). Measuring Distances by Pulsed Dipolar ESR Spectroscopy: Spin-Labeled Histidine Kinases. Methods in Enzymology. **423:** 52-116.

Bowman, A., R. Ward, et al. (2010). "Probing the (H3-H4)2 histone tetramer structure using pulsed EPR spectroscopy combined with site-directed spin labelling." Nucleic Acids Research **38**(2): 695-707.

Bowman, G. D. (2010). "Mechanisms of ATP-dependent nucleosome sliding." Curr Opin Struct Biol **20**(1): 73-81.

Bruno, M., A. Flaus, et al. (2003). "Histone H2A/H2B Dimer Exchange by ATP-Dependent Chromatin Remodeling Activities." Molecular Cell **12**(6): 1599-1606.

Burgess, R. J., H. Zhou, et al. "A role for Gcn5 in replication-coupled nucleosome assembly." Mol Cell **37**(4): 469-80.

Cao, H., H. R. Widlund, et al. (1998). "TGGA repeats impair nucleosome formation." J Mol Biol **281**(2): 253-60.

Cao, R., L. Wang, et al. (2002). "Role of histone H3 lysine 27 methylation in Polycomb-group silencing." Science **298**(5595): 1039-43.

Carruthers, L. M., J. Bednar, et al. (1998). "Linker histones stabilize the intrinsic salt-dependent folding of nucleosomal arrays: mechanistic ramifications for higher-order chromatin folding." Biochemistry **37**(42): 14776-87.

Caruthers, J. M. and D. B. McKay (2002). "Helicase structure and mechanism." Curr Opin Struct Biol **12**(1): 123-33.

Chaban, Y., C. Ezeokonkwo, et al. (2008). "Structure of a RSC-nucleosome complex and insights into chromatin remodeling." Nat Struct Mol Biol **15**(12): 1272-7.

Chen, C. C., J. J. Carson, et al. (2008). "Acetylated Lysine 56 on Histone H3 Drives Chromatin Assembly after Repair and Signals for the Completion of Repair." Cell **134**(2): 231-243.

Cremisi, C., A. Chestier, et al. (1978). "Assembly of SV40 and polyoma minichromosomes during replication." Cold Spring Harb Symp Quant Biol **42 Pt 1**: 409-16.

Culhane, J. C. and P. A. Cole (2007). "LSD1 and the chemistry of histone demethylation." Curr Opin Chem Biol **11**(5): 561-8.

Daganzo, S. M., J. P. Erzberger, et al. (2003). "Structure and Function of the Conserved Core of Histone Deposition Protein Asf1." Current Biology **13**(24): 2148-2158.

Dalal, Y., H. Wang, et al. (2007). "Tetrameric structure of centromeric nucleosomes in interphase Drosophila cells." PLoS Biology **5**(8): 1798-1809.

Das, C., J. K. Tyler, et al. (2010). "The histone shuffle: histone chaperones in an energetic dance." Trends in Biochemical Sciences.

Davey, C. A., D. F. Sargent, et al. (2002). "Solvent mediated interactions in the structure of the nucleosome core particle at 1.9 a resolution." J Mol Biol **319**(5): 1097-113.

De Koning, L., A. Corpet, et al. (2007). "Histone chaperones: An escort network regulating histone traffic." Nature Structural and Molecular Biology **14**(11): 997-1007.

Del Rosario, B. C. and L. F. Pemberton (2008). "Nap1 links transcription elongation, chromatin assembly, and messenger RNP complex biogenesis." Mol Cell Biol **28**(7): 2113-24.

Dhalluin, C., J. E. Carlson, et al. (1999). "Structure and ligand of a histone acetyltransferase bromodomain." Nature **399**(6735): 491-6.

Dilworth, S. M., S. J. Black, et al. (1987). "Two complexes that contain histones are required for nucleosome assembly in vitro: role of nucleoplasmin and N1 in Xenopus egg extracts." Cell **51**(6): 1009-18.

Dion, M. F., T. Kaplan, et al. (2007). "Dynamics of replication-independent histone turnover in budding yeast." Science **315**(5817): 1405-8.

Dorigo, B., T. Schalch, et al. (2004). "Nucleosome arrays reveal the two-start organization of the chromatin fiber." Science **306**(5701): 1571-3.

Downs, J. A. (2008). "Histone H3 K56 acetylation, chromatin assembly, and the DNA damage checkpoint." DNA Repair (Amst) **7**(12): 2020-4.

Drane, P., K. Ouararhni, et al. (2010). "The death-associated protein DAXX is a novel histone chaperone involved in the replication-independent deposition of H3.3." Genes Dev **24**(12): 1253-65.

Dunleavy, E. M., A. L. Pidoux, et al. (2007). "A NASP (N1/N2)-Related Protein, Sim3, Binds CENP-A and Is Required for Its Deposition at Fission Yeast Centromeres." Molecular Cell **28**(6): 1029-1044.

Dunleavy, E. M., D. Roche, et al. (2009). "HJURP is a cell-cycle-dependent maintenance and deposition factor of CENP-A at centromeres." Cell **137**(3): 485-97.

Durr, H., C. Korner, et al. (2005). "X-ray structures of the Sulfolobus solfataricus SWI2/SNF2 ATPase core and its complex with DNA." Cell **121**(3): 363-73.

Dutta, S., I. V. Akey, et al. (2001). "The crystal structure of nucleoplasmin-core: Implications for histone binding and nucleosome assembly." Molecular Cell **8**(4): 841-853.

Eisen, J. A., K. S. Sweder, et al. (1995). "Evolution of the SNF2 family of proteins: subfamilies with distinct sequences and functions." Nucleic Acids Res **23**(14): 2715-23.

Eisfeld, K., R. Candau, et al. (1997). "Binding of NF1 to the MMTV promoter in nucleosomes: influence of rotational phasing, translational positioning and histone H1." Nucleic Acids Res **25**(18): 3733-42.

Engeholm, M., M. de Jager, et al. (2009). "Nucleosomes can invade DNA territories occupied by their neighbors." Nat Struct Mol Biol **16**(2): 151-8.

English, C. M., M. W. Adkins, et al. (2006). "Structural Basis for the Histone Chaperone Activity of Asf1." Cell **127**(3): 495-508.

English, C. M., N. K. Maluf, et al. (2005). "ASF1 binds to a heterodimer of histones H3 and H4: A two-step mechanism for the assembly of the H3-H4 heterotetramer on DNA." Biochemistry **44**(42): 13673-13682.

Erkmann, J. A. and P. D. Kaufman (2009). "A negatively charged residue in place of histone H3K56 supports chromatin assembly factor association but not genotoxic stress resistance." DNA Repair (Amst) **8**(12): 1371-9.

Fan, J. Y., F. Gordon, et al. (2002). "The essential histone variant H2A.Z regulates the equilibrium between different chromatin conformational states." Nat Struct Biol **9**(3): 172-6.

Fan, J. Y., D. Rangasamy, et al. (2004). "H2A.Z alters the nucleosome surface to promote HP1alpha-mediated chromatin fiber folding." Mol Cell **16**(4): 655-61.

Ferreira, H., J. Somers, et al. (2007). "Histone tails and the H3 alphaN helix regulate nucleosome mobility and stability." Molecular and Cellular Biology **27**(11): 4037-4048.

Fillingham, J. and J. F. Greenblatt (2008). "A Histone Code for Chromatin Assembly." Cell **134**(2): 206-208.

Fillingham, J., P. Kainth, et al. (2009). "Two-color cell array screen reveals interdependent roles for histone chaperones and a chromatin boundary regulator in histone gene repression." Mol Cell **35**(3): 340-51.

Fillingham, J., J. Recht, et al. (2008). "Chaperone control of the activity and specificity of the histone H3 acetyltransferase Rtt109." Molecular and Cellular Biology **28**(13): 4342-4353.

Finch, J. T. and A. Klug (1976). "Solenoidal model for superstructure in chromatin." Proc Natl Acad Sci U S A **73**(6): 1897-901.

Finn, R. M., K. Browne, et al. (2008). "sNASP, a histone H1-specific eukaryotic chaperone dimer that facilitates chromatin assembly." Biophys J **95**(3): 1314-25.

Flaus, A., D. M. Martin, et al. (2006). "Identification of multiple distinct Snf2 subfamilies with conserved structural motifs." Nucleic Acids Res **34**(10): 2887-905.

Flaus, A. and T. Owen-Hughes (2003). "Dynamic Properties of Nucleosomes during Thermal and ATP-Driven Mobilization." Molecular and Cellular Biology **23**(21): 7767-7779.

Foltz, D. R., L. E. Jansen, et al. (2009). "Centromere-specific assembly of CENP-a nucleosomes is mediated by HJURP." Cell **137**(3): 472-84.

Formosa, T. (2008). "FACT and the reorganized nucleosome." Mol Biosyst **4**(11): 1085-93.

Franco, A. A., W. M. Lam, et al. (2005). "Histone deposition protein Asf1 maintains DNA replisome integrity and interacts with replication factor C." Genes Dev **19**(11): 1365-75.

Frehlick, L. J., J. M. Eirin-Lopez, et al. (2007). "New insights into the nucleophosmin/nucleoplasmin family of nuclear chaperones." Bioessays **29**(1): 49-59.

Fujii-Nakata, T., Y. Ishimi, et al. (1992). "Functional analysis of nucleosome assembly protein, NAP-1. The negatively charged COOH-terminal region is not necessary for the intrinsic assembly activity." J Biol Chem **267**(29): 20980-6.

Furuyama, T. and S. Henikoff (2009). "Centromeric nucleosomes induce positive DNA supercoils." Cell **138**(1): 104-13.

Garcia-Ramirez, M., F. Dong, et al. (1992). "Role of the histone "tails" in the folding of oligonucleosomes depleted of histone H1." J Biol Chem **267**(27): 19587-95.

Gerard, A., S. Koundrioukoff, et al. (2006). "The replication kinase Cdc7-Dbf4 promotes the interaction of the p150 subunit of chromatin assembly factor 1 with proliferating cell nuclear antigen." EMBO Rep **7**(8): 817-23.

Gill, J., A. Kumar, et al. (2010). "Structure, localization and histone binding properties of nuclear-associated nucleosome assembly protein from Plasmodium falciparum." Malar J **9**: 90.

Gill, J., M. Yogavel, et al. (2009). "Crystal structure of malaria parasite nucleosome assembly protein: Distinct modes of protein localization and histone recognition." Journal of Biological Chemistry **284**(15): 10076-10087.

Gkikopoulos, T., K. M. Havas, et al. (2009). "SWI/SNF and Asf1p cooperate to displace histones during induction of the saccharomyces cerevisiae HO promoter." Mol Cell Biol **29**(15): 4057-66.

Goldberg, A. D., L. A. Banaszynski, et al. (2010). "Distinct factors control histone variant H3.3 localization at specific genomic regions." Cell **140**(5): 678-91.

Goll, M. G. and T. H. Bestor (2002). "Histone modification and replacement in chromatin activation." Genes Dev **16**(14): 1739-42.

Groth, A., A. Corpet, et al. (2007). "Regulation of replication fork progression through histone supply and demand." Science **318**(5858): 1928-31.

Groth, A., D. Ray-Gallet, et al. (2005). "Human Asf1 regulates the flow of S phase histones during replicational stress." Mol Cell **17**(2): 301-11.

Hamiche, A., V. Carot, et al. (1996). "Interaction of the histone (H3-H4)2 tetramer of the nucleosome with positively supercoiled DNA minicircles: Potential flipping of the protein from a left- to a right-handed superhelical form." Proceedings of the National Academy of Sciences of the United States of America **93**(15): 7588-7593.

Han, J., H. Zhou, et al. (2007). "Acetylation of lysine 56 of histone H3 catalyzed by RTT109 and regulated by ASF1 is required for replisome integrity." Journal of Biological Chemistry **282**(39): 28587-28596.

Han, J., H. Zhou, et al. (2007). "The Rtt109-Vps75 histone acetyltransferase complex acetylates non-nucleosomal histone H3." Journal of Biological Chemistry **282**(19): 14158-14164.

Hansen, J. C., J. K. Nyborg, et al. (2010). "Histone chaperones, histone acetylation, and the fluidity of the chromogenome." J Cell Physiol **224**(2): 289-99.

Hartley, P. D. and H. D. Madhani (2009). "Mechanisms that specify promoter nucleosome location and identity." Cell **137**(3): 445-58.

Havas, K., A. Flaus, et al. (2000). "Generation of superhelical torsion by ATP-dependent chromatin remodeling activities." Cell **103**(7): 1133-42.

Hjelm, R. P., G. G. Kneale, et al. (1977). "Small angle neutron scattering studies of chromatin subunits in solution." Cell **10**(1): 139-51.

Huang, S., H. Zhou, et al. (2005). "Rtt106p is a histone chaperone involved in heterochromatin-mediated silencing." Proc Natl Acad Sci U S A **102**(38): 13410-5.

Huang, S., H. Zhou, et al. (2007). "A novel role for histone chaperones CAF-1 and Rtt106p in heterochromatin silencing." Embo J **26**(9): 2274-83.

Huisinga, K. L. and B. F. Pugh (2004). "A genome-wide housekeeping role for TFIID and a highly regulated stress-related role for SAGA in Saccharomyces cerevisiae." Mol Cell **13**(4): 573-85.

Huynh, V. A., P. J. Robinson, et al. (2005). "A method for the in vitro reconstitution of a defined "30 nm" chromatin fibre containing stoichiometric amounts of the linker histone." J Mol Biol **345**(5): 957-68.

Ishimi, Y. and A. Kikuchi (1991). "Identification and molecular cloning of yeast homolog of nucleosome assembly protein I which facilitates nucleosome assembly in vitro." J Biol Chem **266**(11): 7025-9.

Ito, T., M. Bulger, et al. (1996). "Drosophila NAP-1 is a core histone chaperone that functions in ATP-facilitated assembly of regularly spaced nucleosomal arrays." Molecular and Cellular Biology **16**(6): 3112-3124.

Iwase, S., F. Lan, et al. (2007). "The X-linked mental retardation gene SMCX/JARID1C defines a family of histone H3 lysine 4 demethylases." Cell **128**(6): 1077-88.

Jackson, V. (1990). "In vivo studies on the dynamics of histone-DNA interaction: evidence for nucleosome dissolution during replication and transcription and a low level of dissolution independent of both." Biochemistry **29**(3): 719-31.

Jacobson, R. H., A. G. Ladurner, et al. (2000). "Structure and function of a human TAFII250 double bromodomain module." Science **288**(5470): 1422-5.

Jamai, A., R. M. Imoberdorf, et al. (2007). "Continuous histone H2B and transcription-dependent histone H3 exchange in yeast cells outside of replication." Mol Cell **25**(3): 345-55.

Jamai, A., A. Puglisi, et al. (2009). "Histone chaperone spt16 promotes redeposition of the original h3-h4 histones evicted by elongating RNA polymerase." Mol Cell **35**(3): 377-83.

Jasencakova, Z., A. N. Scharf, et al. (2010). "Replication stress interferes with histone recycling and predeposition marking of new histones." Mol Cell **37**(5): 736-43.

Jenuwein, T. and C. D. Allis (2001). "Translating the histone code." Science **293**(5532): 1074-80.

Jeschke, G., V. Chechik, et al. (2006). "DeerAnalysis2006 - A comprehensive software package for analyzing pulsed ELDOR data." Applied Magnetic Resonance **30**(3-4): 473-498.

Jeschke, G. and Y. Polyhach (2007). "Distance measurements on spin-labelled biomacromolecules by pulsed electron paramagnetic resonance." Phys Chem Chem Phys **9**(16): 1895-910.

Johansen, K. M. and J. Johansen (2006). "Regulation of chromatin structure by histone H3S10 phosphorylation." Chromosome Res **14**(4): 393-404.

Jorcano, J. L. and A. Ruiz-Carrillo (1979). "H3·H4 tetramer directs DNA and core histone octamer assembly in the nucleosome core particle." Biochemistry **18**(5): 768-774.

Kagalwala, M. N., B. J. Glaus, et al. (2004). "Topography of the ISW2-nucleosome complex: insights into nucleosome spacing and chromatin remodeling." EMBO J **23**(10): 2092-104.

Kaplan, N., I. K. Moore, et al. (2009). "The DNA-encoded nucleosome organization of a eukaryotic genome." Nature **458**(7236): 362-6.

Kaplan, T., C. L. Liu, et al. (2008). "Cell cycle- and chaperone-mediated regulation of H3K56ac incorporation in yeast." PLoS Genetics **4**(11).

Kimura, H. and P. R. Cook (2001). "Kinetics of core histones in living human cells: little exchange of H3 and H4 and some rapid exchange of H2B." J Cell Biol **153**(7): 1341-53.

Kireeva, M. L., W. Walter, et al. (2002). "Nucleosome remodeling induced by RNA polymerase II: Loss of the H2A/H2B dimer during transcription." Molecular Cell **9**(3): 541-552.

Kleinschmidt, J. A., A. Seiter, et al. (1990). "Nucleosome assembly in vitro: separate histone transfer and synergistic interaction of native histone complexes purified from nuclei of Xenopus laevis oocytes." EMBO J **9**(4): 1309-18.

Klose, R. J., E. M. Kallin, et al. (2006). "JmjC-domain-containing proteins and histone demethylation." Nat Rev Genet **7**(9): 715-27.

Klose, R. J., K. Yamane, et al. (2006). "The transcriptional repressor JHDM3A demethylates trimethyl histone H3 lysine 9 and lysine 36." Nature **442**(7100): 312-6.

Kobor, M. S., S. Venkatasubrahmanyam, et al. (2004). "A protein complex containing the conserved Swi2/Snf2-related ATPase Swr1p deposits histone variant H2A.Z into euchromatin." PLoS Biol **2**(5): E131.

Kong, S. E., M. S. Kobor, et al. (2005). "Interaction of Fcp1 phosphatase with elongating RNA polymerase II holoenzyme, enzymatic mechanism of action, and genetic interaction with elongator." J Biol Chem **280**(6): 4299-306.

Kornberg, R. D. (1974). "Chromatin structure: a repeating unit of histones and DNA." Science **184**(139): 868-71.

Kornberg, R. D. and J. O. Thomas (1974). "Chromatin structure; oligomers of the histones." Science **184**(139): 865-8.

Kouzarides, T. (2007). "Chromatin modifications and their function." Cell **128**(4): 693-705.

Kristjuhan, A. and J. Q. Svejstrup (2004). "Evidence for distinct mechanisms facilitating transcript elongation through chromatin in vivo." EMBO J **23**(21): 4243-52.

Krogan, N. J., G. Cagney, et al. (2006). "Global landscape of protein complexes in the yeast Saccharomyces cerevisiae." Nature **440**(7084): 637-643.

Krogan, N. J., M. C. Keogh, et al. (2003). "A Snf2 family ATPase complex required for recruitment of the histone H2A variant Htz1." Mol Cell **12**(6): 1565-76.

Krogan, N. J., M. Kim, et al. (2003). "Methylation of histone H3 by Set2 in Saccharomyces cerevisiae is linked to transcriptional elongation by RNA polymerase II." Mol Cell Biol **23**(12): 4207-18.

Kruithof, M., F. T. Chien, et al. (2009). "Single-molecule force spectroscopy reveals a highly compliant helical folding for the 30-nm chromatin fiber." Nat Struct Mol Biol **16**(5): 534-40.

Kulaeva, O. I., D. A. Gaykalova, et al. (2009). "Mechanism of chromatin remodeling and recovery during passage of RNA polymerase II." Nat Struct Mol Biol **16**(12): 1272-8.

Kulaeva, O. I., D. A. Gaykalova, et al. (2007). "Transcription through chromatin by RNA polymerase II: histone displacement and exchange." Mutat Res **618**(1-2): 116-29.

Kulic, I. M. and H. Schiessel (2003). "Chromatin dynamics: nucleosomes go mobile through twist defects." Phys Rev Lett **91**(14): 148103.

Kulic, I. M. and H. Schiessel (2003). "Nucleosome repositioning via loop formation." Biophys J **84**(5): 3197-211.

Kuo, M. H., J. E. Brownell, et al. (1996). "Transcription-linked acetylation by Gcn5p of histones H3 and H4 at specific lysines." Nature **383**(6597): 269-72.

Lachner, M., D. O'Carroll, et al. (2001). "Methylation of histone H3 lysine 9 creates a binding site for HP1 proteins." Nature **410**(6824): 116-20.

Langst, G. and P. B. Becker (2004). "Nucleosome remodeling: one mechanism, many phenomena?" Biochim Biophys Acta **1677**(1-3): 58-63.

Laskey, R. A., B. M. Honda, et al. (1978). "Nucleosomes are assembled by an acidic protein which binds histones and transfers them to DNA." Nature **275**(5679): 416-420.

Lattman, E., R. Burlingame, et al. (1982). "Crystallization of the tetramer of histones H3 and H4." Science **216**(4549): 1016-1018.

Le Masson, I., D. Y. Yu, et al. (2003). "Yaf9, a novel NuA4 histone acetyltransferase subunit, is required for the cellular response to spindle stress in yeast." Mol Cell Biol **23**(17): 6086-102.

Lee, C. K., Y. Shibata, et al. (2004). "Evidence for nucleosome depletion at active regulatory regions genome-wide." Nat Genet **36**(8): 900-5.

Lee, W., D. Tillo, et al. (2007). "A high-resolution atlas of nucleosome occupancy in yeast." Nat Genet **39**(10): 1235-44.

Leiting, B., F. Marsilio, et al. (1998). "Predictable deuteration of recombinant proteins expressed in Escherichia coli." Analytical Biochemistry **265**(2): 351-355.

Leschziner, A. E., A. Saha, et al. (2007). "Conformational flexibility in the chromatin remodeler RSC observed by electron microscopy and the orthogonal tilt reconstruction method." Proc Natl Acad Sci U S A **104**(12): 4913-8.

Levchenko, V., B. Jackson, et al. (2005). "Histone release during transcription: Displacement of the two H2A-H2B dimers in the nucleosome is dependent on different levels of transcription-induced positive stress." Biochemistry **44**(14): 5357-5372.

Lewis, P. W., S. J. Elsaesser, et al. (2010). "Daxx is an H3.3-specific histone chaperone and cooperates with ATRX in replication-independent chromatin assembly at telomeres." Proc Natl Acad Sci U S A **107**(32): 14075-80.

Li, B., M. Carey, et al. (2007). "The role of chromatin during transcription." Cell **128**(4): 707-19.

Li, G., M. Levitus, et al. (2005). "Rapid spontaneous accessibility of nucleosomal DNA." Nature Structural and Molecular Biology **12**(1): 46-53.

Li, G. and J. Widom (2004). "Nucleosomes facilitate their own invasion." Nat Struct Mol Biol **11**(8): 763-9.

Li, Q., H. Zhou, et al. (2008). "Acetylation of Histone H3 Lysine 56 Regulates Replication-Coupled Nucleosome Assembly." Cell **134**(2): 244-255.

Lia, G., E. Praly, et al. (2006). "Direct observation of DNA distortion by the RSC complex." Mol Cell **21**(3): 417-25.

Lin, C. and Y. A. Yuan (2008). "Structural Insights into Histone H3 Lysine 56 Acetylation by Rtt109." Structure **16**(10): 1503-1510.

Liu, C. L., T. Kaplan, et al. (2005). "Single-nucleosome mapping of histone modifications in S. cerevisiae." PLoS Biol **3**(10): e328.

Liu, Y., H. Huang, et al. (2010). "Structural analysis of Rtt106p reveals a DNA binding role required for heterochromatin silencing." J Biol Chem **285**(6): 4251-62.

Lohr, D., J. Corden, et al. (1977). "Comparative subunit structure of HeLa, yeast, and chicken erythrocyte chromatin." Proc Natl Acad Sci U S A **74**(1): 79-83.

Lohr, D., R. T. Kovacic, et al. (1977). "Quantitative analysis of the digestion of yeast chromatin by staphylococcal nuclease." Biochemistry **16**(3): 463-71.

Lorch, Y., B. Maier-Davis, et al. (2006). "Chromatin remodeling by nucleosome disassembly in vitro." Proceedings of the National Academy of Sciences of the United States of America **103**(9): 3090-3093.

Lorch, Y., B. Maier-Davis, et al. (2010). "Mechanism of chromatin remodeling." Proc Natl Acad Sci U S A **107**(8): 3458-62.

Lorch, Y., M. Zhang, et al. (1999). "Histone octamer transfer by a chromatin-remodeling complex." Cell **96**(3): 389-92.

Lowary, P. T. and J. Widom (1997). "Nucleosome packaging and nucleosome positioning of genomic DNA." Proc Natl Acad Sci U S A **94**(4): 1183-8.

Lowary, P. T. and J. Widom (1998). "New DNA sequence rules for high affinity binding to histone octamer and sequence-directed nucleosome positioning." Journal of Molecular Biology **276**(1): 19-42.

Lowary, P. T. and J. Widom (1998). "New DNA sequence rules for high affinity binding to histone octamer and sequence-directed nucleosome positioning." J Mol Biol **276**(1): 19-42.

Lu, X., M. D. Simon, et al. (2008). "The effect of H3K79 dimethylation and H4K20 trimethylation on nucleosome and chromatin structure." Nat Struct Mol Biol **15**(10): 1122-4.

Lucchini, R., R. E. Wellinger, et al. (2001). "Nucleosome positioning at the replication fork." EMBO J **20**(24): 7294-302.

Luger, K., A. W. Ma?der, et al. (1997). "Crystal structure of the nucleosome core particle at 2.8 A resolution." Nature **389**(6648): 251-260.

Luger, K., T. J. Rechsteiner, et al. (1997). "Characterization of nucleosome core particles containing histone proteins made in bacteria." J Mol Biol **272**(3): 301-11.

Luk, E., N. D. Vu, et al. (2007). "Chz1, a nuclear chaperone for histone H2AZ." Mol Cell **25**(3): 357-68.

Malik, H. S. and S. Henikoff (2003). "Phylogenomics of the nucleosome." Nat Struct Biol **10**(11): 882-91.

Marley, J., M. Lu, et al. (2001). "A method for efficient isotopic labeling of recombinant proteins." Journal of Biomolecular NMR **20**(1): 71-75.

Meersseman, G., S. Pennings, et al. (1991). "Chromatosome positioning on assembled long chromatin. Linker histones affect nucleosome placement on 5 S rDNA." J Mol Biol **220**(1): 89-100.

Meersseman, G., S. Pennings, et al. (1992). "Mobile nucleosomes--a general behavior." EMBO J **11**(8): 2951-9.

Meilleur, F., K. L. Weiss, et al. (2009). "Deuterium labeling for neutron structure-function-dynamics analysis." Methods in molecular biology (Clifton, N.J.) **544**: 281-292.

Mello, J. A., H. H. Sillje, et al. (2002). "Human Asf1 and CAF-1 interact and synergize in a repair-coupled nucleosome assembly pathway." EMBO Rep **3**(4): 329-34.

Mersfelder, E. L. and M. R. Parthun (2006). "The tale beyond the tail: histone core domain modifications and the regulation of chromatin structure." Nucleic Acids Res **34**(9): 2653-62.

Mizuguchi, G., X. Shen, et al. (2004). "ATP-Driven Exchange of Histone H2AZ Variant Catalyzed by SWR1 Chromatin Remodeling Complex." Science **303**(5656): 343-348.

Moriniere, J., S. Rousseaux, et al. (2009). "Cooperative binding of two acetylation marks on a histone tail by a single bromodomain." Nature **461**(7264): 664-8.

Morrison, A. J. and X. Shen (2009). "Chromatin remodelling beyond transcription: the INO80 and SWR1 complexes." Nat Rev Mol Cell Biol **10**(6): 373-84.

Mosammaparast, N., C. S. Ewart, et al. (2002). "A role for nucleosome assembly protein 1 in the nuclear transport of histones H2A and H2B." Embo J **21**(23): 6527-38.

Mousson, F., A. Lautrette, et al. (2005). "Structural basis for the interaction of Asf1 with histone H3 and its functional implications." Proceedings of the National Academy of Sciences of the United States of America **102**(17): 5975-5980.

Murzina, N. V., X. Y. Pei, et al. (2008). "Structural basis for the recognition of histone H4 by the histone-chaperone RbAp46." Structure **16**(7): 1077-85.

Muto, S., M. Senda, et al. (2007). "Relationship between the structure of SET/TAF-II-beta/INHAT and its histone chaperone activity." Proceedings of the National Academy of Sciences of the United States of America **104**(11): 4285-4290.

Namboodiri, V. M., I. V. Akey, et al. (2004). "The structure and function of Xenopus NO38-core, a histone chaperone in the nucleolus." Structure **12**(12): 2149-60.

Natsume, R., M. Eitoku, et al. (2007). "Structure and function of the histone chaperone CIA/ASF1 complexed with histones H3 and H4." Nature **446**(7133): 338-341.

Neumann, H., S. M. Hancock, et al. (2009). "A method for genetically installing site-specific acetylation in recombinant histones defines the effects of H3 K56 acetylation." Mol Cell **36**(1): 153-63.

Ng, H. H., F. Robert, et al. (2003). "Targeted recruitment of Set1 histone methylase by elongating Pol II provides a localized mark and memory of recent transcriptional activity." Mol Cell **11**(3): 709-19.

Nielsen, P. R., D. Nietlispach, et al. (2002). "Structure of the HP1 chromodomain bound to histone H3 methylated at lysine 9." Nature **416**(6876): 103-7.

Nowak, S. J. and V. G. Corces (2004). "Phosphorylation of histone H3: a balancing act between chromosome condensation and transcriptional activation." Trends Genet **20**(4): 214-20.

Ohkuni, K., K. Shirahige, et al. (2003). "Genome-wide expression analysis of NAP1 in Saccharomyces cerevisiae." Biochem Biophys Res Commun **306**(1): 5-9.

Okuhara, K., K. Ohta, et al. (1999). "A DNA unwinding factor involved in DNA replication in cell-free extracts of Xenopus eggs." Curr Biol **9**(7): 341-50.

Orphanides, G., G. LeRoy, et al. (1998). "FACT, a factor that facilitates transcript elongation through nucleosomes." Cell **92**(1): 105-16.

Oudet, P., M. Gross-Bellard, et al. (1975). "Electron microscopic and biochemical evidence that chromatin structure is a repeating unit." Cell **4**(4): 281-300.

Owen, D. J., P. Ornaghi, et al. (2000). "The structural basis for the recognition of acetylated histone H4 by the bromodomain of histone acetyltransferase gcn5p." EMBO J **19**(22): 6141-9.

Ozdemir, A., S. Spicuglia, et al. (2005). "Characterization of lysine 56 of histone H3 as an acetylation site in Saccharomyces cerevisiae." J Biol Chem **280**(28): 25949-52.

Park, Y. J. and K. Luger (2006). "Structure and function of nucleosome assembly proteins." Biochemistry and Cell Biology **84**(4): 549-558.

Park, Y. J. and K. Luger (2006). "The structure of nucleosome assembly protein 1." Proceedings of the National Academy of Sciences of the United States of America **103**(5): 1248-1253.

Park, Y. J. and K. Luger (2008). "Histone chaperones in nucleosome eviction and histone exchange." Current Opinion in Structural Biology **18**(3): 282-289.

Park, Y. J., S. J. McBryant, et al. (2008). "A beta-hairpin Comprising the Nuclear Localization Sequence Sustains the Self-associated States of Nucleosome Assembly Protein 1." Journal of Molecular Biology **375**(4): 1076-1085.

Park, Y. J., K. B. Sudhoff, et al. (2008). "Histone chaperone specificity in Rtt109 activation." Nature Structural and Molecular Biology **15**(9): 957-964.

Parthun, M. R., J. Widom, et al. (1996). "The major cytoplasmic histone acetyltransferase in yeast: links to chromatin replication and histone metabolism." Cell **87**(1): 85-94.

Pennings, S., G. Meersseman, et al. (1991). "Mobility of positioned nucleosomes on 5 S rDNA." J Mol Biol **220**(1): 101-10.

Pinto, D. M. and A. Flaus (2010). "Structure and function of histone H2AX." Subcell Biochem **50**: 55-78.

Pokholok, D. K., C. T. Harbison, et al. (2005). "Genome-wide map of nucleosome acetylation and methylation in yeast." Cell **122**(4): 517-27.

Polach, K. J. and J. Widom (1995). "Mechanism of protein access to specific DNA sequences in chromatin: a dynamic equilibrium model for gene regulation." J Mol Biol **254**(2): 130-49.

Prevelige, P. E., Jr. and G. D. Fasman (1987). "Structural studies of acetylated and control inner core histones." Biochemistry **26**(10): 2944-55.

Prior, C. P., C. R. Cantor, et al. (1980). "Incorporation of exogenous pyrene-labeled histone into Physarum chromatin: a system for studying changes in nucleosomes assembled in vivo." Cell **20**(3): 597-608.

Prochasson, P., L. Florens, et al. (2005). "The HIR corepressor complex binds to nucleosomes generating a distinct protein/DNA complex resistant to remodeling by SWI/SNF." Genes Dev **19**(21): 2534-9.

Racki, L. R. and G. J. Narlikar (2008). "ATP-dependent chromatin remodeling enzymes: two heads are not better, just different." Curr Opin Genet Dev **18**(2): 137-44.

Racki, L. R., J. G. Yang, et al. (2009). "The chromatin remodeller ACF acts as a dimeric motor to space nucleosomes." Nature **462**(7276): 1016-21.

Rando, O. J. (2007). "Global patterns of histone modifications." Curr Opin Genet Dev **17**(2): 94-9.

Ransom, M., B. K. Dennehey, et al. (2010). "Chaperoning histones during DNA replication and repair." Cell **140**(2): 183-95.

Ray-Gallet, D., J. P. Quivy, et al. (2007). "The histone chaperone Asf1 is dispensable for direct de novo histone deposition in Xenopus egg extracts." Chromosoma **116**(5): 487-96.

Read, C. M., J. P. Baldwin, et al. (1985). "Structure of subnucleosomal particles. Tetrameric (H3/H4)2 146 base pair DNA and hexameric (H3/H4)2(H2A/H2B)1 146 base pair DNA complexes." Biochemistry **24**(16): 4435-4450.

Recht, J., T. Tsubota, et al. (2006). "Histone chaperone Asf1 is required for histone H3 lysine 56 acetylation, a modification associated with S phase in mitosis and meiosis." Proc Natl Acad Sci U S A **103**(18): 6988-93.

Rhoades, A. R., S. Ruone, et al. (2004). "Structural features of nucleosomes reorganized by yeast FACT and its HMG box component, Nhp6." Mol Cell Biol **24**(9): 3907-17.

Richardson, R. T., I. N. Batova, et al. (2000). "Characterization of the histone H1-binding protein, NASP, as a cell cycle-regulated somatic protein." J Biol Chem **275**(39): 30378-86.

Richmond, T. J. and C. A. Davey (2003). "The structure of DNA in the nucleosome core." Nature **423**(6936): 145-150.

Richmond, T. J., J. T. Finch, et al. (1984). "Structure of the nucleosome core particle at 7 A resolution." Nature **311**(5986): 532-7.

Richmond, T. J., M. A. Searles, et al. (1988). "Crystals of a nucleosome core particle containing defined sequence DNA." J Mol Biol **199**(1): 161-70.

Robinson, P. J., W. An, et al. (2008). "30 nm chromatin fibre decompaction requires both H4-K16 acetylation and linker histone eviction." J Mol Biol **381**(4): 816-25.

Robinson, P. J., L. Fairall, et al. (2006). "EM measurements define the dimensions of the "30-nm" chromatin fiber: evidence for a compact, interdigitated structure." Proc Natl Acad Sci U S A **103**(17): 6506-11.

Robinson, P. J. and D. Rhodes (2006). "Structure of the '30 nm' chromatin fibre: a key role for the linker histone." Curr Opin Struct Biol **16**(3): 336-43.

Rufiange, A., P. E. Jacques, et al. (2007). "Genome-wide replication-independent histone H3 exchange occurs predominantly at promoters and implicates H3 K56 acetylation and Asf1." Mol Cell **27**(3): 393-405.

Ruiz-Carrillo, A. and J. L. Jorcano (1979). "An octamer of core histones in solution: central role of the H3-H4 tetramer in the self-assembly." Biochemistry **18**(5): 760-8.

Satchwell, S. C., H. R. Drew, et al. (1986). "Sequence periodicities in chicken nucleosome core DNA." J Mol Biol **191**(4): 659-75.

Schalch, T., S. Duda, et al. (2005). "X-ray structure of a tetranucleosome and its implications for the chromatin fibre." Nature **436**(7047): 138-141.

Schermer, U. J., P. Korber, et al. (2005). "Histones are incorporated in trans during reassembly of the yeast PHO5 promoter." Mol Cell **19**(2): 279-85.

Schiemann, O. and T. F. Prisner (2007). "Long-range distance determinations in biomacromolecules by EPR spectroscopy." Quarterly Reviews of Biophysics **40**(1): 1-53.

Schulze, J. M., A. Y. Wang, et al. (2009). "YEATS domain proteins: a diverse family with many links to chromatin modification and transcription." Biochem Cell Biol **87**(1): 65-75.

Schwabish, M. A. and K. Struhl (2004). "Evidence for eviction and rapid deposition of histones upon transcriptional elongation by RNA polymerase II." Mol Cell Biol **24**(23): 10111-7.

Schwanbeck, R., H. Xiao, et al. (2004). "Spatial contacts and nucleosome step movements induced by the NURF chromatin remodeling complex." J Biol Chem **279**(38): 39933-41.

Schwarz, P. M., A. Felthauser, et al. (1996). "Reversible oligonucleosome self-association: dependence on divalent cations and core histone tail domains." Biochemistry **35**(13): 4009-15.

Seale, R. L. (1976). "Studies on the mode of segregation of histone nu bodies during replication in HeLa cells." Cell **9**(3): 423-9.

Segal, E., Y. Fondufe-Mittendorf, et al. (2006). "A genomic code for nucleosome positioning." Nature **442**(7104): 772-8.

Segal, E. and J. Widom (2009). "What controls nucleosome positions?" Trends Genet **25**(8): 335-43.

Selth, L. and J. Q. Svejstrup (2007). "Vps75, a new yeast member of the NAP histone chaperone." Journal of Biological Chemistry **282**(17): 12358-12362.

Selth, L. A., Y. Lorch, et al. (2009). "An rtt109-independent role for vps75 in transcription-associated nucleosome dynamics." Mol Cell Biol **29**(15): 4220-34.

Sharma, N. and J. K. Nyborg (2008). "The coactivators CBP/p300 and the histone chaperone NAP1 promote transcription-independent nucleosome eviction at the HTLV-1 promoter." Proc Natl Acad Sci U S A **105**(23): 7959-63.

Shi, Y., F. Lan, et al. (2004). "Histone demethylation mediated by the nuclear amine oxidase homolog LSD1." Cell **119**(7): 941-53.

Shikama, N., H. M. Chan, et al. (2000). "Functional interaction between nucleosome assembly proteins and p300/CREB-binding protein family coactivators." Mol Cell Biol **20**(23): 8933-43.

Shogren-Knaak, M., H. Ishii, et al. (2006). "Histone H4-K16 acetylation controls chromatin structure and protein interactions." Science **311**(5762): 844-7.

Shuaib, M., K. Ouararhni, et al. (1349). "HJURP binds CENP-A via a highly conserved N-terminal domain and mediates its deposition at centromeres." Proc Natl Acad Sci U S A **107**(4): 1349-54.

Simpson, R. T., F. Thoma, et al. (1985). "Chromatin reconstituted from tandemly repeated cloned DNA fragments and core histones: a model system for study of higher order structure." Cell **42**(3): 799-808.

Singer, M. S., A. Kahana, et al. (1998). "Identification of high-copy disruptors of telomeric silencing in Saccharomyces cerevisiae." Genetics **150**(2): 613-32.

Sivolob, A., F. De Lucia, et al. (2000). "Nucleosome dynamics. VI. Histone tail regulation of tetrasome chiral transition. A relaxation study of tetrasomes on DNA minicircles." Journal of Molecular Biology **295**(1): 55-69.

Sivolob, A. and A. Prunell (2000). "Nucleosome dynamics. V. Ethidium bromide versus histone tails in modulating ethidium bromide-driven tetrasome chiral

transition. A fluorescence study of tetrasomes on DNA minicircles." Journal of Molecular Biology **295**(1): 41-53.

Sivolob, A. and A. Prunell (2004). "Nucleosome conformational flexibility and implications for chromatin dynamics." Philosophical Transactions of the Royal Society A: Mathematical, Physical and Engineering Sciences **362**(1820): 1519-1547.

Smith, B. C. and J. M. Denu (2009). "Chemical mechanisms of histone lysine and arginine modifications." Biochim Biophys Acta **1789**(1): 45-57.

Smith, S. and B. Stillman (1989). "Purification and characterization of CAF-I, a human cell factor required for chromatin assembly during DNA replication in vitro." Cell **58**(1): 15-25.

Sobel, R. E., R. G. Cook, et al. (1995). "Conservation of deposition-related acetylation sites in newly synthesized histones H3 and H4." Proceedings of the National Academy of Sciences of the United States of America **92**(4): 1237-1241.

Sogo, J. M., H. Stahl, et al. (1986). "Structure of replicating simian virus 40 minichromosomes. The replication fork, core histone segregation and terminal structures." J Mol Biol **189**(1): 189-204.

Somers, J. and T. Owen-Hughes (2009). "Mutations to the histone H3 alpha N region selectively alter the outcome of ATP-dependent nucleosome-remodelling reactions." Nucleic Acids Res **37**(8): 2504-13.

Song, J. J., J. D. Garlick, et al. (2008). "Structural basis of histone H4 recognition by p55." Genes Dev **22**(10): 1313-8.

Spangenberg, C., K. Eisfeld, et al. (1998). "The mouse mammary tumour virus promoter positioned on a tetramer of histones H3 and H4 binds nuclear factor 1 and OTF1." Journal of Molecular Biology **278**(4): 725-739.

Spangenberg, C., K. Eisfeld, et al. (1998). "The mouse mammary tumour virus promoter positioned on a tetramer of histones H3 and H4 binds nuclear factor 1 and OTF1." J Mol Biol **278**(4): 725-39.

Spector, M. S., A. Raff, et al. (1997). "Hir1p and Hir2p function as transcriptional corepressors to regulate histone gene transcription in the Saccharomyces cerevisiae cell cycle." Mol Cell Biol **17**(2): 545-52.

Stillman, B. (1986). "Chromatin assembly during SV40 DNA replication in vitro." Cell **45**(4): 555-65.

Strahl, B. D. and C. D. Allis (2000). "The language of covalent histone modifications." Nature **403**(6765): 41-5.

Straube, K., J. S. Blackwell, Jr., et al. (2010). "Nap1 and Chz1 have separate Htz1 nuclear import and assembly functions." Traffic **11**(2): 185-97.

Strohner, R., M. Wachsmuth, et al. (2005). "A 'loop recapture' mechanism for ACF-dependent nucleosome remodeling." Nat Struct Mol Biol **12**(8): 683-90.

Studitsky, V. M., D. J. Clark, et al. (1995). "Overcoming a nucleosomal barrier to transcription." Cell **83**(1): 19-27.

Studitsky, V. M., G. A. Kassavetis, et al. (1997). "Mechanism of transcription through the nucleosome by eukaryotic RNA polymerase." Science **278**(5345): 1960-3.

Stuwe, T., M. Hothorn, et al. (2008). "The FACT Spt16 "peptidase" domain is a histone H3-H4 binding module." Proc Natl Acad Sci U S A **105**(26): 8884-9.

Suau, P., G. G. Kneale, et al. (1977). "A low resolution model for the chromatin core particle by neutron scattering." Nucleic Acids Res **4**(11): 3769-86.

Subramanya, H. S., L. E. Bird, et al. (1996). "Crystal structure of a DExx box DNA helicase." Nature **384**(6607): 379-83.

Sung, M. T. and G. H. Dixon (1970). "Modification of histones during spermiogenesis in trout: a molecular mechanism for altering histone binding to DNA." Proc Natl Acad Sci U S A **67**(3): 1616-23.

Suto, R. K., M. J. Clarkson, et al. (2000). "Crystal structure of a nucleosome core particle containing the variant histone H2A.Z." Nat Struct Biol **7**(12): 1121-4.

Tagami, H., D. Ray-Gallet, et al. (2004). "Histone H3.1 and H3.3 Complexes Mediate Nucleosome Assembly Pathways Dependent or Independent of DNA Synthesis." Cell **116**(1): 51-61.

Takahata, S., Y. Yu, et al. (2009). "FACT and Asf1 regulate nucleosome dynamics and coactivator binding at the HO promoter." Mol Cell **34**(4): 405-15.

Talbert, P. B. and S. Henikoff (2010). "Histone variants--ancient wrap artists of the epigenome." Nat Rev Mol Cell Biol **11**(4): 264-75.

Tan, B. C., C. T. Chien, et al. (2006). "Functional cooperation between FACT and MCM helicase facilitates initiation of chromatin DNA replication." Embo J **25**(17): 3975-85.

Taneva, S. G., S. Banuelos, et al. (2009). "A mechanism for histone chaperoning activity of nucleoplasmin: thermodynamic and structural models." J Mol Biol **393**(2): 448-63.

Tang, Y., M. A. Holbert, et al. (2008). "Fungal Rtt109 histone acetyltransferase is an unexpected structural homolog of metazoan p300/CBP." Nature Structural and Molecular Biology **15**(7): 738-745.

Tang, Y., K. Meeth, et al. (2008). "Structure of Vps75 and implications for histone chaperone function." Proceedings of the National Academy of Sciences of the United States of America **105**(34): 12206-12211.

Taverna, S. D., H. Li, et al. (2007). "How chromatin-binding modules interpret histone modifications: lessons from professional pocket pickers." Nat Struct Mol Biol **14**(11): 1025-40.

Thastrom, A., P. T. Lowary, et al. (1999). "Sequence motifs and free energies of selected natural and non-natural nucleosome positioning DNA sequences." J Mol Biol **288**(2): 213-29.

Thastrom, A., P. T. Lowary, et al. (2004). "Measurement of histone-DNA interaction free energy in nucleosomes." Methods **33**(1): 33-44.

Thiriet, C. and J. J. Hayes (2005). "Replication-independent core histone dynamics at transcriptionally active loci in vivo." Genes Dev **19**(6): 677-82.

Toth, K. F., J. Mazurkiewicz, et al. (2005). "Association states of nucleosome assembly protein 1 and its complexes with histones." Journal of Biological Chemistry **280**(16): 15690-15699.

Tsubota, T., C. E. Berndsen, et al. (2007). "Histone H3-K56 Acetylation Is Catalyzed by Histone Chaperone-Dependent Complexes." Molecular Cell **25**(5): 703-712.

Tsukiyama, T., J. Palmer, et al. (1999). "Characterization of the imitation switch subfamily of ATP-dependent chromatin-remodeling factors in Saccharomyces cerevisiae." Genes Dev **13**(6): 686-97.

Turner, B. M. (2002). "Cellular memory and the histone code." Cell **111**(3): 285-91.

van Attikum, H. and S. M. Gasser (2009). "Crosstalk between histone modifications during the DNA damage response." Trends Cell Biol **19**(5): 207-17.

van Holde, K. and T. Yager (2003). "Models for chromatin remodeling: a critical comparison." Biochem Cell Biol **81**(3): 169-72.

VanDemark, A. P., M. Blanksma, et al. (2006). "The structure of the yFACT Pob3-M domain, its interaction with the DNA replication factor RPA, and a potential role in nucleosome deposition." Mol Cell **22**(3): 363-74.

VanDemark, A. P., H. Xin, et al. (2008). "Structural and functional analysis of the Spt16p N-terminal domain reveals overlapping roles of yFACT subunits." J Biol Chem **283**(8): 5058-68.

Venditti, P., L. Di Croce, et al. (1998). "Assembly of MMTV promoter minichromosomes with positioned nucleosomes precludes NF1 access but not restriction enzyme cleavage." Nucleic Acids Res **26**(16): 3657-66.

Verreault, A., P. D. Kaufman, et al. (1996). "Nucleosome assembly by a complex of CAF-1 and acetylated histones H3/H4." Cell **87**(1): 95-104.

Verreault, A., P. D. Kaufman, et al. (1998). "Nucleosomal DNA regulates the core-histone-binding subunit of the human Hat1 acetyltransferase." Curr Biol **8**(2): 96-108.

Vicent, G. P., A. S. Nacht, et al. (2004). "DNA instructed displacement of histones H2A and H2B at an inducible promoter." Mol Cell **16**(3): 439-52.

Vicent, G. P., A. S. Nacht, et al. (2004). "DNA instructed displacement of histones H2A and H2B at an inducible promoter." Molecular Cell **16**(3): 439-452.

Vicent, G. P., R. Zaurin, et al. "Nuclear factor 1 synergizes with progesterone receptor on the mouse mammary tumor virus promoter wrapped around a histone H3/H4 tetramer by facilitating access to the central hormone-responsive elements." J Biol Chem **285**(4): 2622-31.

Vicent, G. P., R. Zaurin, et al. (2010). "Nuclear factor 1 synergizes with progesterone receptor on the mouse mammary tumor virus promoter wrapped around a histone H3/H4 tetramer by facilitating access to the central hormone-responsive elements." J Biol Chem **285**(4): 2622-31.

Wang, A. Y., J. M. Schulze, et al. (2009). "Asf1-like structure of the conserved Yaf9 YEATS domain and role in H2A.Z deposition and acetylation." Proc Natl Acad Sci U S A **106**(51): 21573-8.

Wang, H., S. T. Walsh, et al. (2008). "Expanded binding specificity of the human histone chaperone NASP." Nucleic Acids Res **36**(18): 5763-72.

Wang, X., S. C. Moore, et al. (2000). "Acetylation increases the alpha-helical content of the histone tails of the nucleosome." J Biol Chem **275**(45): 35013-20.

Weake, V. M. and J. L. Workman (2008). "Histone ubiquitination: triggering gene activity." Mol Cell **29**(6): 653-63.

Weintraub, H. (1976). "Cooperative alignment of nu bodies during chromosome replication in the presence of cycloheximide." Cell **9**(3): 419-22.

Wellen, K. E., G. Hatzivassiliou, et al. (2009). "ATP-citrate lyase links cellular metabolism to histone acetylation." Science **324**(5930): 1076-80.

Whitehouse, I., A. Flaus, et al. (1999). "Nucleosome mobilization catalysed by the yeast SWI/SNF complex." Nature **400**(6746): 784-7.

Widlund, H. R., H. Cao, et al. (1997). "Identification and characterization of genomic nucleosome-positioning sequences." J Mol Biol **267**(4): 807-17.

Widom, J. and A. Klug (1985). "Structure of the 300A chromatin filament: X-ray diffraction from oriented samples." Cell **43**(1): 207-13.

Williams, S. K., D. Truong, et al. (2008). "Acetylation in the globular core of histone H3 on lysine-56 promotes chromatin disassembly during transcriptional activation." Proc Natl Acad Sci U S A **105**(26): 9000-5.

Williams, S. P., B. D. Athey, et al. (1986). "Chromatin fibers are left-handed double helices with diameter and mass per unit length that depend on linker length." Biophys J **49**(1): 233-48.

Wittmeyer, J. and T. Formosa (1997). "The Saccharomyces cerevisiae DNA polymerase alpha catalytic subunit interacts with Cdc68/Spt16 and with Pob3, a protein similar to an HMG1-like protein." Mol Cell Biol **17**(7): 4178-90.

Wittmeyer, J., L. Joss, et al. (1999). "Spt16 and Pob3 of Saccharomyces cerevisiae form an essential, abundant heterodimer that is nuclear, chromatin-associated, and copurifies with DNA polymerase alpha." Biochemistry **38**(28): 8961-8971.

Wood, C. M., J. M. Nicholson, et al. (2005). "High-resolution structure of the native histone octamer." Acta Crystallographica Section F: Structural Biology and Crystallization Communications **61**(6): 541-545.

Wunsch, A. and V. Jackson (2005). "Histone release during transcription: acetylation stabilizes the interaction of the H2A-H2B dimer with the H3-H4 tetramer in nucleosomes that are on highly positively coiled DNA." Biochemistry **44**(49): 16351-64.

Wysocka, J., T. Swigut, et al. (2006). "A PHD finger of NURF couples histone H3 lysine 4 trimethylation with chromatin remodelling." Nature **442**(7098): 86-90.

Xin, H., S. Takahata, et al. (2009). "yFACT induces global accessibility of nucleosomal DNA without H2A-H2B displacement." Mol Cell **35**(3): 365-76.

Xu, M., C. Long, et al. (2010). "Partitioning of histone H3-H4 tetramers during DNA replication-dependent chromatin assembly." Science **328**(5974): 94-8.

Xu, X., L. G. Cooper, et al. (1995). "Helix formation in model peptides based on nucleolin TPAKK motifs." Biopolymers **35**(1): 93-102.

Yang, M., C. B. Gocke, et al. (2006). "Structural basis for CoREST-dependent demethylation of nucleosomes by the human LSD1 histone demethylase." Mol Cell **23**(3): 377-87.

Ye, J., X. Ai, et al. (2005). "Histone H4 lysine 91 acetylation a core domain modification associated with chromatin assembly." Mol Cell **18**(1): 123-30.

Yuan, G. C., Y. J. Liu, et al. (2005). "Genome-scale identification of nucleosome positions in S. cerevisiae." Science **309**(5734): 626-30.

Zecevic, A., G. R. Eaton, et al. (1998). "Dephasing of electron spin echoes for nitroxyl radicals in glassy solvents by non-methyl and methyl protons." Molecular Physics **95**(6): 1255-1263.

Zeng, L., Q. Zhang, et al. (2010). "Mechanism and regulation of acetylated histone binding by the tandem PHD finger of DPF3b." Nature **466**(7303): 258-62.

Zeng, L. and M. M. Zhou (2002). "Bromodomain: an acetyl-lysine binding domain." FEBS Lett **513**(1): 124-8.

Zhang, H., D. O. Richardson, et al. (2004). "The Yaf9 component of the SWR1 and NuA4 complexes is required for proper gene expression, histone H4 acetylation, and Htz1 replacement near telomeres." Mol Cell Biol **24**(21): 9424-36.

Zhang, Y., Z. Moqtaderi, et al. (2009). "Intrinsic histone-DNA interactions are not the major determinant of nucleosome positions in vivo." Nat Struct Mol Biol **16**(8): 847-52.

Zhang, Y., H. H. Ng, et al. (1999). "Analysis of the NuRD subunits reveals a histone deacetylase core complex and a connection with DNA methylation." Genes Dev **13**(15): 1924-35.

Zhang, Y., C. L. Smith, et al. (2006). "DNA translocation and loop formation mechanism of chromatin remodeling by SWI/SNF and RSC." Mol Cell **24**(4): 559-68.

Zhou, W., X. Wang, et al. (2009). "Histone H2A ubiquitination in transcriptional regulation and DNA damage repair." Int J Biochem Cell Biol **41**(1): 12-5.

Zhou, Z., H. Feng, et al. (2008). "NMR structure of chaperone Chz1 complexed with histones H2A.Z-H2B." Nature Structural and Molecular Biology **15**(8): 868-869.

Zhou, Z., H. Feng, et al. (2008). "NMR structure of chaperone Chz1 complexed with histones H2A.Z-H2B." Nat Struct Mol Biol **15**(8): 868-9.

Zlatanova, J. and A. Thakar (2008). "H2A.Z: view from the top." Structure **16**(2): 166-79.

Zofall, M., J. Persinger, et al. (2006). "Chromatin remodeling by ISW2 and SWI/SNF requires DNA translocation inside the nucleosome." Nat Struct Mol Biol **13**(4): 339-46.

Acknowledgements

I would like to thank Richard Ward, David Norman and Hassane El-Mkami (who carried out the EPR measurements), Nicola Wiechens (who helped a lot with the acetylation assay), Karoline Luger and Paul Kaufman (for supplying protein expression vectors) and Sharon Kelly (for CD spectroscopy). A special thanks to my supervisor Tom, who has given me much freedom whilst subtly guiding my project (I think it worked out ok in the end!?), and of course a big thank-you to the rest of the TOH lab for interesting discussions.

Now with the serious bit out of the way, I suppose this is the point for me to reflect on my time as a PhD student. The problem is that I have spent so much of it having fun it all kind of blends in to a single hazy memory: late night poker sessions, early morning hill runs, ice climbing, rock climbing, paragliding, night runs in heavy downpours, attempting to surf, attempting to ski, food parties, sailing on Loch Tay and general craziness in the Union and Speedies all come to mind. I think it is safe to say that the majority of the TOH lab have been involved in one or more of the above, so first and foremost I would like to thank everyone in the lab for making it such a fun place to be for three years. I have to thank Tom for understanding that when it is -5 °C, 10 mph winds and blue skies outside the likelihood of finding me in the lab is very small. Also, I need thank my many other friends that I have made since arriving in Dundee, especially members of Team Hamburg (that helped me discover the true meaning behind TOH – you know who you are… and what it means), Peter and Helena (who keep me regularly fed with wholesome German food), Julin (for ordering the good stuff at Mandarin Gardens) and of course Sabine (for putting up with my nonsense, and being a pretty good climbing partner).